Process control of solid-state fermentation

Simultaneous control of temperature and moisture content

Promotor:

Prof. Dr. Ir. J. Tramper
Hoogleraar in de Bioprocestechnologie

Co-promotor:

Dr. Ir. A. Rinzema
Universitair docent bij de sectie Proceskunde

Promotiecommissie:

Prof. Dr. Ir. R.M. Boom *(Wageningen Universiteit)*
Dr. Ir. M.L.F. Giuseppin *(Avebe)*
Prof. Dr. D. Mitchell *(Universidade Federal do Parana)*
Dr. Ir. M.J.R. Nout *(Wageningen Universiteit)*

Franciscus Johannes Ignatius Nagel

Process control of solid-state fermentation

Simultaneous control of temperature and moisture content

Proefschrift
ter verkrijging van de graad van doctor
op gezag van de rector magnificus
van Wageningen Universiteit,
prof. dr. ir. L. Speelman,
in het openbaar te verdedigen
op vrijdag 1 februari 2002
des namiddags te half twee in de Aula.

ISBN 90-5808-513-9

Voor mijn ouders

Contents

Chapter 1

General Introduction

USE OF SOLID-STATE FERMENTATION

The main task of fungi in nature is to produce hydrolytic enzymes for the breakdown of organic waste materials, plant residues, vegetables and all sorts of waste into inorganic mineral compounds. Bacteria largely do the actual breakdown. To ensure that bacteria do not scavenge all the hydrolysis products, many fungi make antibiotics. These capabilities are the basis of the flourishing antibiotics and enzyme industries. Nowadays, micro-organisms are used in many industrial processes to produce enzymes and other molecules, which are used in peoples everyday life. For example, washing powder now contains enzymes that enable the process to be carried out at a relatively low temperature, and we cannot imagine a life without antibiotics.

In the Western world, the fermentation industry cultivates fungi – and other micro-organisms – in liquid nutrient broth, so-called submerged fermentation (SmF). In Asia, fermentation products are made by cultivating fungi in the absence of free-flowing water on a solid substrate such as cereal grains or beans, so-called solid-state fermentation (SSF). Fungi grow well in solid-state fermentation, because the conditions are similar to their natural habitats, such as organic waste materials, trees and soil. Fungi can withstand limited water availability in the solid substrate, whereas most bacteria cannot. SSF holds tremendous potential for the production of enzymes, which break down macromolecules to smaller molecules that can be further metabolised by bacteria, but also for high added-value pharmaceutical products.

The breakdown or conversion of molecules using enzymes is of interest to almost any industry. These enzymes give a very specific, natural conversion under mild conditions in contrast to chemical conversions, which usually require harsh process conditions that often give undesired side products. In addition to the production of enzymes, SSF can be used to produce a variety of complicated biomolecules, which are almost impossible to synthesize chemically. In the following paragraphs a short overview is given on how SSF is or can be applied in several industries.

Food industry

SSF can be used in the food industry for the production of enzymes, organic acids, aroma compounds and other substances of interest. For the manufacture of soy sauce, enzymes like proteinases are produced industrially by cultivation of *Aspergillus oryzae*

on a mixture of wheat bran and soy flakes. These proteinases convert the insoluble protein in the soy flakes into smaller soluble peptides and amino acids, which make up the soy sauce.
Citric acid is the most important organic acid for the food industry and is currently produced in tonnage by submerged fermentation. However, SSF has great potential to produce citric acid more economically using alternative feedstocks such as agro-industrial residues (VandenBerghe *et al.*, 1999).
Bacteria and fungi are able to synthesize different interesting aroma compounds in SSF. For example, *Ceratocystis fimbriata* cultivated in SSF on coffee husk produces strong pineapple aroma (Soares *et al.*, 2000). Also food additives like pyrazines, which possess a nutty and roasty flavour, can be produced using SSF (Seitz, 1994). L-glutamic acid, a flavour enhancer, is produced by SSF with a bacterial strain of *Brevibacterium* sp. on sugarcane bagasse impregnated with a defined media (Nampoothiri and Pandey, 1996).
Recently, a culture of *Xanthomonas campestris* was used in an SSF-based process for the production of xanthan gum that is used in the food industry as an emulsifier or thickener (Stredansky and Conti, 1999).

Pharmaceutical industry

A new era in medical therapy and the pharmaceutical industry started with the discovery of antibiotics. Penicillin and other secondary products of fungi, actinomycetes and bacteria have provided the most powerful tools to fight bacterial and fungal infections. Several patents (Merck, 1990; 1991) describe the use of SSF for the production of new antibiotics against for example *Cryptococcus* sp., *Candida* sp. and *Streptomyces* sp. Surfactin, a lipopeptide antibiotic, which inhibits fibrin clotting, was produced by cultivating a *Bacillus* sp. on okara, which is a solid waste product of Tofu (bean curd) production. The production in SSF was 4-5 times more effective than in SmF (Nakayama *et al.*, 1997; Ohno *et al.*, 1995).
In January 2001, a lovastatin production facility that uses SSF has been approved by the FDA (www.biocon.com). Statins belong to a group of cholesterol reducing drugs effective in preventing both first and second heart attacks in patients with hypercholesterolemia.

Agro-industry

Fungal biopesticides are an environmentally friendly alternative to chemical pesticides. In literature, a large number of fungi are described as promising candidates for biopesticides (Deshpande, 1999). For example, *Coniothyrium minitans* is a natural antagonist of the fungus *Sclerotinia sclerotiorum*, a widespread plant pathogen affecting more than 360 plant species. This biopesticide is commercially available and is produced by solid-state fermentation on cereal grains (www.prophyta.com). SSF is preferred for the production of this biopesticide as spore yields are higher compared to submerged fermentation (McQuilken *et al.*, 1997). This applies to many fungal biopesticides.

Biological detoxification

Certain agro-industrial residues contain toxic (anti-physiological and anti-nutritional) compounds such as hydrogen cyanide, caffeine, tannins, aflatoxins, etc. that pose difficulties in their effective utilisation. Their disposal is a problem for the processing industries as it leads to serious environmental burdens. SSF has been recently applied to detoxify residues such as cassava peels, rapeseed meal, canola meal, coffee husk, coffee pulp, etc. For example, SSF of cassava peels showed a 95% reduction in hydrogen cyanide level and a 42% reduction in soluble-tannin levels (Ofuya and Obilor, 1994).

COMMERCIALIZATION OF SSF

In recent years, research on SSF has led to a wide range of applications on lab scale, and comparative studies between SmF and SSF claim higher yields for products made by SSF (Pandey *et al.*, 2000; Pandey *et al.*, 1999). In spite of these examples the commercial application of SSF processes in Western countries remains unusual mainly due to problems associated with scale-up. In the Western world, SmF has become the standard process for microbial products. However, in South-East Asia, where SSF is more common, research attention was directed towards the industrialization of fermented foods like soy sauce, miso, natto, sufu, tempeh, and the like, to meet the growing demand of these products caused by a rapidly increasing population. These

products were all made using SSF and large bioreactors were developed from 1950 onwards (Steinkraus, 1989).

The main problem associated with scale-up of SSF is the removal of heat generated by the metabolic activity of the micro-organisms. Heat removal by conduction in static packed beds is limited due to: (1) the poor heat transfer through the bed (Saucedo-Casteneda *et al.*, 1990); and (2) the lack of heat-exchange surface on a large scale. Evaporative cooling has proven to be more efficient than convection and conduction (Sargantanis *et al.*, 1993). It results, however, in large moisture losses and drying of the solid substrate. Therefore, it is essential to combine temperature and moisture control in large-scale SSF systems. Moisture-content control is achieved by adding water during fermentation. The addition of water has major implications on the design of the bioreactor. Water has to be added homogeneously to the solid substrate, which requires a mixing device inside the bioreactor. Mixing during SSF sets additional requirements for the solid substrate and the fungus. First, the solid substrate should be able to withstand shear forces caused by mixing and should not have the tendency to aggregate to clumps as a result of mixing. Second, mixing could damage the fungus, which could decrease its growth and production rate. This effect could also depend on the bioreactor scale, because the scale affects forces acting on the solid mash.

Besides the question "How to add water?", it is also important how much water should be added for optimum growth of the fungus. For example, the production of enzymes and secondary metabolites like aromas and antibiotics, is influenced by the water activity of the solid substrate (Gervais, 1990; Liu and Tzeng, 1999; Narahara *et al.*, 1982). The water activity of the solid substrate changes as a result of SSF. For example, water is taken up by the fungus in order to synthesize new fungal hyphae. In addition, water evaporates from the solid substrate due to metabolic-heat production and solute concentrations increase as a result of enzymatic degradation. All these processes influence the water activity, which makes it very difficult to control. Besides that, information about the water balance and water activity during solid-state fermentation is scarce.

OUTLINE OF THIS THESIS

The aim of the project described in this thesis was to demonstrate the feasibility of solid-state fermentation with controlled temperature and moisture content on labscale.
At first a model system was chosen based on an agar matrix as solid support in which a defined medium was dissolved. *Rhizopus oligosporus*, having known physiology and kinetic parameters, was chosen as a model organism. Chapter 2 describes the improvements made to this model system with respect to pH control and growth.
It was expected that such a well-defined model system would facilitate research, as the results would be more reproducible. A second advantage of using an agar gel is that it allows direct determination of biomass dry matter and this is almost impossible when a solid substrate is used. However, this model system turned out to be not very practical for research on SSF. The main problem was that the effect of dehydration of agar beads is not comparable to the dehydration that occurs in the majority of SSF applications, due to the high moisture content of agar beads (95% water).
The use of *R. oligosporus* as model organism also had some disadvantages that would hinder the interpretation of data. *R. oligosporus* has the ability to convert sugars anaerobically when oxygen limitation occurs. This would hamper the prediction of biomass production and the relation between heat production and oxygen consumption would become less accurate.
Therefore, we decided to switch to a different SSF system in which *Aspergillus oryzae* was cultivated on moist wheat grains. Like *R. oligosporus*, *A. oryzae* is widely applied in industrial SSF for the production of enzymes and "koji", an intermediate which is used for the production of soy sauce and miso.
The use of mixed bioreactors for SSF was considered the first step in solving scale-up problems with respect to temperature and moisture-content control. Although mixing of the solid substrate offers many advantages, the question remained if these would outweigh possible disadvantages like effects of shear on growth. Chapter 3 shows that mixed SSF can be applied without seriously affecting fungal growth.
In Chapter 4 a model is decribed, which estimates the extracellular (nonfungal) and overall water content of wheat grains during SSF. Model parameters were determined using an experimental membrane-based model system, which mimicked the growth of *A. oryzae* on the wheat grains and permitted direct measurement of the fungal biomass

dry weight and wet weight. The model can be used to calculate the water addition that is required to control the extracellular water content in a mixed solid-state bioreactor.

Chapter 5 describes a control strategy for simultaneous control of the temperature and moisture content during cultivation of *A. oryzae* on wheat in a continuously mixed paddle bioreactor. Evaporative cooling with varying air flow rate was applied to control the temperature of the solid substrate (Chapter 3). The extracellular water content was controlled by adding a fine mist of water droplets to the mixed solid substrate, using a previously described model (Chapter 4) to calculate the required addition.

Chapter 6 describes the use of ^{1}H-NMR imaging as a powerful technique to study solid-state fermentation at the particle level. Gradients inside substrate particles cannot be prevented in solid-state fermentation. In this chapter we describe gradients in moisture and glucose content during cultivation of *A. oryzae* on membrane-covered wheat-dough slices; the gradients were calculated from ^{1}H-NMR images measured *in vivo*.

Finally, in the last chapter two commercial bioreactors are discussed that can facilitate the scale-up and process control of SSF. The koji bioreactor is discussed as a suitable alternative for the production of low to medium-added-value products in the food industry. Bioreactors based on the design of industrial solids mixers are discussed as alternative for the production of pharmaceuticals and other high-added-value products.

REFERENCES

Deshpande MV. 1999. Mycopesticide production by fermentation: potential and challenges. Crit Rev Microbiol 25: 229-243.

Gervais, P. 1990. Water activity: a fundamental parameter of aroma production by microorganisms. Appl Microbiol Biotechnol 33: 72-75.

Liu BL, Tzeng YM. 1999. Water content and water activity for the production of cyclodepsipeptides in solid-state fermentation by *Metarrhizium anisopliae*. Biotechnol Lett 21: 657-661.

McQuilken MP, Budge SP, Whipps JM. 1997. Production, survival and evaluation of liquid-culture produced inocula of *Coniothyrium minitans* against *Sclerotinia sclerotiorum*. Biocontr Sci Technol 7: 23-36.

Merck, 1990. New 2-nonatrienyl-pyran-3-yl glycine ester. US Patent number US-4952604, Merck, USA.

Merck, 1991. New fungicide antibiotic isolated from *Fusarium* sp. fermentation broth. US patent number US-5008187, Merck, USA.

Nakayama S, Takahashi S, Hirai M, Shoda M. 1997. Isolation of new variants of surfactin by a recombinant *Bacillus subtilis*. Appl Microbiol Biotechnol 48: 80-82.

Nampoothiri KM, Pandey A. 1996. Solid state fermentation for L-glutamic acid production using *Brevibacterium* sp. Biotechnol Lett 16: 199-204.

Narahara H, Koyama Y, Yoshida T, Pichangkura S, Ueda R, Taguchi H. 1982. Growth and enzyme production in a solid state culture of *Aspergillus oryzae*. J Ferment Technol 60: 311-319.

Ofuya CO, Obilor SN. 1994. The effects of solid state fermentation on the toxic components of cassava peel. Proc Biochem 29: 251-257.

Ohno A, Ano T, Shoda M. 1995. Production of a lipopeptide antibiotic, surfactin, by recombinant *Bacillus* in solid-state fermentation. Biotechnol Bioeng 80: 209-214.

Pandey A, Selvakumar P, Soccol CR, Nigam P. 1999. Solid state fermentation for the production of industrial enzymes. Current science 77: 149-162.

Pandey A, Soccol CR, Mitchell DA. 2000. New developments in solid state fermentation: I-bioprocesses and products. Proc Biochem 35: 1153-1169.

Sargantanis J, Karim MN, Murphy VG, Ryoo D, Tengerdy RP. 1993. Effect of operating conditions on solid-substrate fermentation. Biotechnol Bioeng 42: 149-158.

Saucedo-Castaneda G, Gutierrez-Rojas M, Bacquet G, Raimbault M, Viniegra-Gonzalez G. 1990. Heat transfer simulation in solid substrate fermentation. Biotechnol Bioeng 35: 802-808.

Seitz EW. 1994. Fermentation production of pyrazines and terpenoids for flavour and fragrances. In: Gabeliman A, editor. Bioprocess production of flavour, fragrance and colour. New York: Wiley, p. 95-134.

Soares M, Christen P, Pandey A, Soccol CR. 2000. Fruity flavour production by *Ceratocystis fimbriata* grown on coffee husk in solid state fermentation. Proc Biochem 35: 8.

Stedansky M, Conti E. 1999. Xanthan production by solid state fermentation. Proc Biochem 34: 581-587.

Steinkraus KH, editor. Industrialisation of fermented foods. 1989. Marcel Dekker Inc, New York.

Vandenberghe LPS, Soccol CR, Pandey A, Lebeault JM. 1999. Microbial production of citric acid. Braz Arch Biol Technol 42: 262-274.

Chapter 2

Improved model system for solid-substrate fermentation

F.J.I. Nagel, J. Oostra, J. Tramper, A. Rinzema.
Process Biochemistry (1999), 35: 69-75

ABSTRACT

In a model system for solid-substrate cultivation of *Rhizopus oligosporus*, it was observed that without pH control rapid acidification occurred, which inhibited the biomass production. With some degree of pH control, biomass production was improved significantly. Several buffering agents with different initial pH values were tested to find the optimum pH and the most suitable buffer for this model system. Between pH 4 and 6, the biomass-production rate was not significantly influenced by pH and citric acid was the most suitable buffer.

Addition of 5 g/L tryptone to a standard mineral medium increased both the maximum specific growth rate (μ_{max}) and the maximum CO_2-production rate, and strongly shortened the lag phase.

INTRODUCTION

Solid-substrate fermentation (SSF) is generally defined as the growth of micro-organisms - often fungi - on solid substrates in systems with a continuous gas phase and no free-flowing water. In order to develop bioreactors for large-scale SSF, a quantitative analysis of kinetics and stoichiometry of the reaction is needed. This analysis is hampered in most natural SSF systems by experimental difficulties, because the substrate/support is structurally and nutritionally heterogeneous and measurement of biomass dry matter is impossible. Several model systems have been developed to overcome these problems. For example, Raimbault and Alazard (1980) impregnated bagasse with a mineral glucose medium and Mitchell *et al.* (1986; 1988a; 1988b; 1989) used κ-carrageenan gel with a mineral starch medium. The advantage of using a gel over bagasse is that it allows direct determinations of biomass dry weight. Auria *et al.* (1990) used a synthetic resin (Amberlite IRA-900) impregnated with a defined mineral medium, which also allowed direct biomass determination.

In previous work (Rinzema *et al.*, 1997) a model system with agar and a defined glucose medium was used to cultivate *Rhizopus oligosporus*, which is quite similar to the system described by Mitchell *et al.* (1988b). However, glucose rather than starch was used as carbon source, in order to avoid a decrease in reaction rate attributed to diffusion limitation of glucoamylase into the matrix (Mitchell *et al.*, 1991). Two

drawbacks were observed with this model system : (1) the pH change was large and its effect on the growth rate was not clear; (2) the specific growth rate was low compared to that for the natural substrate (soy beans). The present paper describes two attempts to improve the model system: better pH control and enhanced growth rate.

Control of pH could be critical for certain SSF processes (Agosin *et al.*, 1989; Yang and Chiu, 1986), but is difficult in unmixed SSF. Some degree of pH control in both natural and model SSF systems is usually obtained by using different ratios of ammonium salts and urea in the substrate (Raimbault and Alazard, 1980; Yang, 1988; Saucedo-Castañeda *et al.*, 1992). Supplementation with urea is not completely effective in stabilising the pH, which in most cases results in a fluctuation of the pH by more than one pH unit (Prior *et al.*, 1992). Combining the above with the narrow optimal pH range (7-7.5) found for *R. oligosporus* in radial-growth-rate studies (Mitchell *et al.*, 1988b), better pH control is expected to be necessary.

The second improvement of the model system concerns the increase of the growth rate. A high growth rate is essential for studying one of the major scale-up problems in SSF: the removal of reaction enthalpy. Heat removal through the wall is expected to be minimal in large-scale bioreactors due to the relative decrease in wall area versus reactor volume. In research with down-scaled bioreactors aiming at scale-up studies, a high growth rate minimises the ratio between inevitable heat losses over heat production and will therefore help to approach the behaviour of a large-scale bioreactor. The maximum specific growth rate (μ_{max}) measured for *R. oligosporus* on soy beans at 30 °C was 0.46 h^{-1} (De Reu, 1995). In our initial model system (Rinzema *et al.*, 1997) the average value for μ_{max} was only 0.27 h^{-1} (unpublished). However, the purpose is to develop a model system which approaches the specific growth rate found on the natural substrate. For that, the effect of subsequent additions of soya peptone, tryptone or vitamins on μ_{max} is studied.

The first aim of this research was to improve pH control in the model system through optimal use of buffering agents. First, the effect of increasing phosphate-buffer concentrations on the pH decline was investigated. Second, the effect of pH on the maximum specific growth rate was studied. Third, four buffers were compared to find the most suitable buffer. The second aim of this research was to increase the growth rate by subsequent additions of soya peptone, tryptone or vitamins.

MATERIALS AND METHODS

Culture

Rhizopus oligosporus NRRL 5905 was grown for 7 days at 30 °C on malt-extract agar (Oxoid, CM 59, UK). To obtain the sporangiospore suspension, a solution of 1 g neutralised bacteriological peptone (Oxoid, L34, UK), 8.5 g NaCl and 10 ml Tween 80 per 1000 ml distilled water was made. Ten millilitres of this solution was added to the plates and a sporangiospore suspension was obtained by scraping the sporangia off the agar. This suspension was filtered through sterile glass wool to discard the remaining mycelium. This spore suspension was stored at -80 °C in cryo vials (Greiner, Germany) for up to 6-8 months. Each vial contained 800 µl suspension and 300 µl glycerol. The viable count of each cryo vial varied between $2 \cdot 10^5$ - $3 \cdot 10^5$ colony forming units (cfu) per ml.

Inoculum

The sporangiospore suspension in the cryo vial was allowed to defrost at 4°C for 2 hours. Inoculum was prepared by mixing the content of one cryo vial with 9 ml of a solution containing 1 g neutralised bacteriological peptone (Oxoid, L34) and 8.5 g NaCl per 1000 ml distilled water.

Media

All chemicals were obtained from Merck (Germany), unless otherwise stated. The standard medium consisted of 22 g $C_6H_{12}O_6 \cdot H_2O$, 10 g $(NH_4)_2SO_4$, 10 ml filter-sterilised stock solution of trace elements ($MnCl_2 \cdot 4H_2O$ 0.1 g/l, $CoCl_2 \cdot 6H_2O$ 0.03 g/l, $CuSO_4 \cdot 5H_2O$ 0.02 g/l, $Na_2MoO_4 \cdot 2H_2O$ 0.02 g/l, $FeSO_4 \cdot 7H_2O$ 0.5 g/l, $ZnSO_4 \cdot 7H_2O$ 0.2 g/l, EDTA 1 g/l), 1 g $CaCl_2$, 0.5 g $MgCl_2 \cdot 6H_2O$, 2 g K_2HPO_4, 15 g agar (Oxoid, L11) and a buffer per 990 ml distilled water. The phosphate buffer was prepared from equimolar quantities of K_2HPO_4 and NaH_2PO_4. Lactic-acid buffer was prepared by adding 30 g lactic acid (90% DL, Cat. no. 366) and 13.5 g KOH to 1 liter standard medium. Citric-acid buffer was prepared by adding 27.5 g citric acid (Cat. no. 244) and 20 g KOH to 1 liter standard medium. Succinic-acid buffer was prepared by adding 17.25 g succinic acid (Cat. no. 681) and 5.8 g KOH to 1 liter standard medium. All molar buffer concentrations are given in Table 1.

Several additions to the standard medium with 0.14 M citric-acid buffer were done in order to investigate their effect on the growth rate. Vitamins were added using 10 ml of Kao and Michayluk vitamin mixture (Cat. no. K3129, Sigma, USA) and 1 ml Provasoli's vitamin mixture (Cat. no. P9931, Sigma, USA) per 1000 ml medium. Filter-sterilised tryptone (L42, Oxoid, UK) was used in two different concentrations: 1 and 5 g/l. Filter-sterilised soya peptone (L44, Oxoid, UK) was used in a concentration of 1 g/l.

Experimental Set-up

For each series, 20 agar plates with 20 ml medium were inoculated with 100 µl inoculum. Two glass jars were used, equipped with a septum and each containing one agar plate, to ensure a closed environment in which the cumulative CO_2-production and O_2-consumption during growth could be determined in duplicate. Agar plates and jars were placed in an incubator (IKS, The Netherlands) at 30 °C.

Sampling procedure

Two agar plates were removed at regular time intervals. The mycelium could easily be pulled off the agar slab. This gave virtually complete recovery of biomass dry weight, whereas melting and filtration gave significant dry-weight losses. Although no membranes were used in these experiments (except for the experiment shown in figure 2), the agar did not adhere to the mycelium and no significant mycelium fragments could be measured by melting and filtration of the remaining agar. In the experiment shown in figure 2, sterile 0.45 µm membranes (Schleicher & Schuell, OE67, Germany) were used. The mycelium was dried for 2 days at 80 °C, placed in a desiccator with kieselgel to cool down to room temperature, and dry weight was measured on an analytical balance (Mettler, AE260-S, Switzerland).

The agar slab was cut in vertical direction into two equal pieces with a scalpel. One piece was liquefied in a micro-wave oven after which the pH was measured at approximately 50°C with a pH meter (WTW, ph323, Germany). The pH measurement in this way represents an average pH value of the agarslab, which may not be the pH the fungus actually encounters. The second piece of agar slab was weighed and frozen at -20 °C in a sample bottle for further analysis. Before analysis this sample was thawed and 10 ml of distilled water was added. The diluted sample was homogenised

through rotation of the sample bottle for 2 h with three small glass beads (∅ 1 cm). The homogenate was filtered through a 0.45 µm filter (Schleicher and Schuell, FP030/2, Germany) and stored at -20 °C for later assay.

Glucose analysis

Glucose was determined using a Peridochrom glucose kit (Cat. no. 676543, Boehhringer Mannheim, Germany).

Organic-acids analysis

Citric acid and succinic acid were analysed by HPLC using an Aminex HPX-87H stainless-steel column (Biorad) at 37 °C and a refractive-index detector (RM IV, Thermo Separation Products, The Netherlands). The acids were eluted with 5 mM H_2SO_4 (0.6 ml·min^{-1}).

Determination of specific growth rate and lag phase

The specific growth rate of *R. oligosporus* was determined from the accumulation of CO_2 in the head space of the jars. Several authors (Narahara *et al.*, 1982; Nishio et *al.*, 1979; Okazaki and Sugama, 1979; Okazaki *et al.*, 1980) have shown that CO_2 production can be used to determine the specific growth rate during SSF. At regular time intervals 100 µl gas samples were taken from the jars. Samples were analysed on a gas chromatograph (CP9001 TCT/PTI 4001, Chrompack, England) for CO_2 and O_2 concentrations. Maximum specific growth rates were estimated by fitting the logistic-growth equation, modified to allow for a lag phase, to the measured amount of CO_2.
The modified logistic-growth equation reads :

$$\begin{aligned} t \le \lambda: &\qquad P(t) = P_0 \\ t > \lambda: &\qquad P(t) = \frac{P_0 \cdot P_{\max}}{(P_{\max} - P_0) \cdot e^{-\mu_{\max}(t-\lambda)} + P_0} \end{aligned} \tag{1}$$

Where

P_0	=	initial amount of CO_2	[mol]
P_{max}	=	maximum amount of CO_2	[mol]
$P(t)$	=	amount of CO_2	[mol]
μ_{max}	=	maximum specific growth rate	[h^{-1}]
λ	=	lag phase	[h]

The values for μ_{max}, λ, P_0 and P_{max} were determined by using the curve-fitting program TableCurve™ 2D (v2.03, Jandel Scientific Software). Figure 1 shows an example of a curve fit. For this method to be used, the respiration coefficient should be constant and anaerobic fermentation should not occur. Anaerobic conditions were avoided in these experiments by using a low glucose concentration and a thin layer of agar in the petri-dish. Therefore the respiration coefficient remained constant during cultivation, which was verified with oxygen and carbon-dioxide measurements.

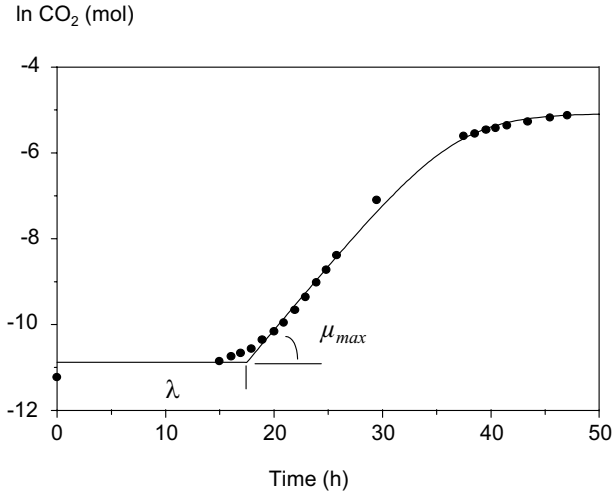

Figure 1. Natural logarithm of the amount of carbon dioxide produced and the fit by the modified logistic equation for growth of *Rhizopus oligosporus* in a model system to determine the maximum specific growth rate (μ_{max}). data ●; Modified logistic equation (——).

Calculation of required buffer concentration

In order to determine the effect of pH on the the specific growth rate, the pH changes should be minimal during cultivation. Different buffers have to be used for different initial pH values in such a way that equal pH changes can be expected. Therefore the buffer concentration was calculated for each buffer from an expected biomass production, a chosen initial pH (pH_0) and pH change (ΔpH). From previous experiments the maximum biomass dry weight for this model system was predicted. In this model system $(NH_4)_2SO_4$ is used as nitrogen source and this is responsible for the pH decrease during cultivation. Through the stoichiometric formula of *R. oligosporus* $CH_{1.88}O_{0.51}N_{0.17}$, the amount of used NH_4^+ (ΔNH_4) is calculated with the assumption that every NH_4^+ used by the fungus releases H^+ into the medium.

The following equation yields the necessary buffer concentration in mol/l to allow for a chosen pH decrease during cultivation:

$$HB_{tot} = \frac{\left[\Delta NH_4 + 10^{-pH_0} - 10^{-(pH_0-\Delta pH)}\right]\cdot\left[10^{-pH_0} + K_a\right]\cdot\left[10^{-(pH_0-\Delta pH)} + K_a\right]}{-\left[10^{-pH_0} - 10^{-(pH_0-\Delta pH)}\right]\cdot K_a} \qquad (2)$$

Where

HB_{tot}	=	total buffer concentration	[M]
pH_0	=	initial pH medium	[-]
ΔpH	=	maximum allowable pH drop	[-]
ΔNH_4	=	ammonium uptake for biomass production	[-]
K_a	=	dissociation constant	[M]

RESULTS & DISCUSSION

Effect of pH

In our model system it was observed that rapid acidification to pH 2.5 occurred with a 0.018 M phosphate buffer. An increase of the phosphate-buffer concentration to 0.12 M gave biomass yields that were more than twice as high (Figure 2).

The pH decline with the 0.12 M phosphate buffer was still rather large (2.6 pH units), and it was unclear from this experiment if the final amount of biomass could be further improved. A further increase of the phosphate-buffer concentration minimised the pH decline during cultivation, but the maximum amount of biomass was the same and heterogeneous biomass distribution over the agar plate was observed.

The fact that the pH dropped to 4 (0.12 M phosphate buffer) and that the biomass production rate did not change significantly (Figure 2), was not in agreement with the narrow optimal pH range found by Mitchell *et al.* (1988b), based on radial-growth rates. Thus the aim of the following experiment was to determine the effect of pH on the maximum specific growth rate and the biomass production rate. Different buffers were used to stabilise the pH at different initial pH values in order to avoid large differences in ionic strength. The concentrations of the various buffers were calculated to give equal buffering capacity.

Table 1. Effect of pH on specific growth rate and maximum biomass production of *Rhizopus oligosporus* on agar plates at 30 °C with the use of different buffering agents.

buffer	mol/l	initial pH	pKa	μ_{max} * (h^{-1})	r_{CO2} * ($\cdot 10^{-4}$ mol/h)	max. biomass dry weight (g)
Phosphate	0.18	6.29	7.21	0.29 (± 0.016)	2.87 (± 0.17)	0.22
Succinic acid	0.15	5.91	5.61	0.31 (± 0.028)	3.17 (± 0.26)	0.17
Citric acid	0.14	4.91	4.77	0.28 (± 0.027)	3.04 (± 0.09)	0.20
Lactic acid	0.14	4.01	3.86	0.23 (± 0.034)	2.33 (± 0.15)	0.11
Lactic acid	0.30	4.40	3.86	0.24 (± 0.007)	3.10 (± 0.36)	0.15

*The values between brackets indicate the ± 95 % confidence intervals

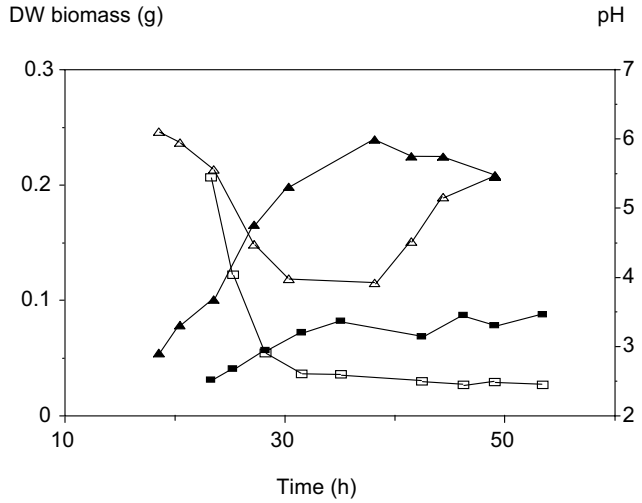

Figure 2. Effect of an increase in phosphate-buffer concentration on the pH profile and biomass development during growth of *Rhizopus oligosporus* using a model system. $[PO_4^{3-}]_{tot}$ = 0.018 M (DW ■, pH □); $[PO_4^{3-}]_{tot}$ = 0.12 M (DW ▲, pH △)

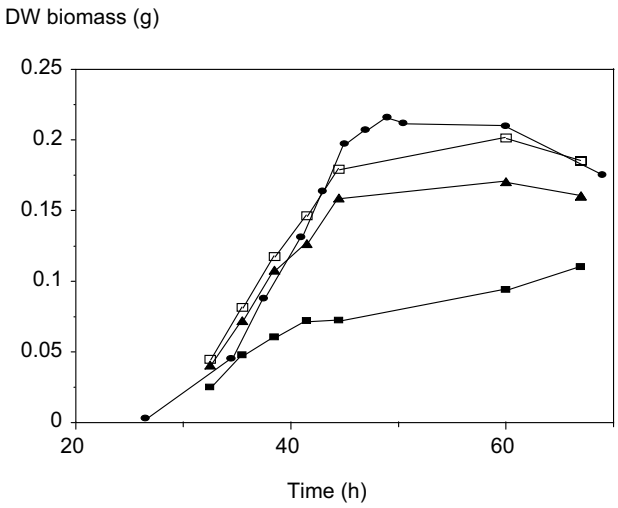

Figure 3. Biomass profiles during growth of *Rhizopus oligosporus* using a model system with different buffer solutions. Phosphate (0.18 M) ●; Succinic acid (0.15 M) □; Citric acid (0.14 M) ▲; Lactic acid (0.14 M) ■.

A broad optimal pH range from 4 - 6.5 was observed for the maximum specific growth rate (μ_{max}) of *Rhizopus oligosporus* in this model system (Table 1). A similar result was also found by Mitchell *et al.* (1991) where pH had little effect on the specific glucose uptake over a range between 5 and 7. These results are not in agreement with the narrow optimal pH range found by Mitchell *et al.* (1988b), for radial-growth rates. This may be due to an effect of pH on the width of the peripheral growth zone. The specific growth rate is only directly related to colony radial growth rate if the peripheral growth zone remains constant, which apparently is not the case for *R. oligosporus* when pH effects are studied.

Biomass profiles (Figure 3) were also considered because μ_{max} is only an indicator of the initial specific growth rate and does not reflect effects over the whole growth curve.

Results showed for the case of the lactic-acid buffer (pH = 4) that although μ_{max} was high (Table 1), the biomass production was lower due to pH values below 3.5 (Figures 3 and 4). This was confirmed with additional experiments using a stronger lactic-acid buffer (0.3 M, initial pH 4.4) which gave better biomass yields and a final pH of 3.9. These results indicated that problems can be expected for growth of *R. oligosporus* at pH values below 4.

At the end of the cultivation an increase in pH was observed of 1-1.5 pH units above the initial values with citric acid or succinic acid as buffer (Figure 4).

In preliminary experiments with these buffers in which glucose was omitted from the medium, it was found that these buffers could not be consumed as sole carbon sources. Nevertheless, it was found that citric acid and succinic acid were consumed when glucose became limiting (Figure 5), which explained the increase in pH towards the end of the cultivation period.

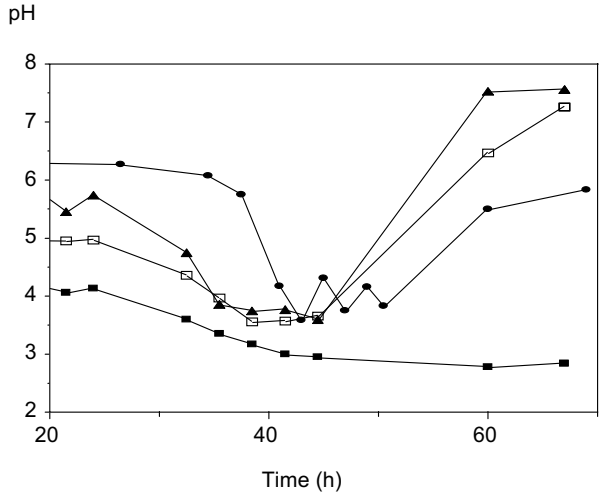

Figure 4. pH profiles during growth of *Rhizopus oligosporus* using a model system with different buffer solutions. Phosphate (0.18 M) ●; Succinic acid (0.15 M) □; Citric acid (0.14 M) ▲; Lactic acid (0.14 M) ■.

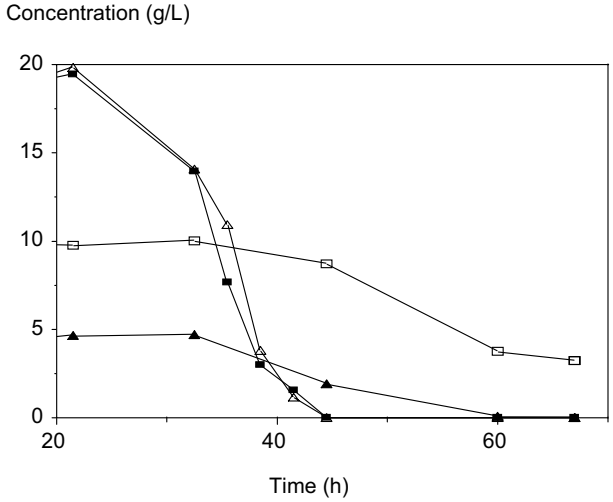

Figure 5. Glucose and buffer concentrations during cultivation of *Rhizopus oligosporus* on media with glucose(■) + citric acid (□) and glucose(△) + succinic acid (▲) respectively.

The increase in pH for the phosphate buffer towards the end of the cultivation period could not be explained directly. In order to find a non-utilised buffer in a slightly acidic environment, phthalate was also considered as buffer in this study. Growth did not occur with a 0.15 M phthalate buffer at pH 6, which made this buffer not suitable.
In summary, pH has little influence on growth between pH values of 4 and 6.3, which means that pH dependencies can be omitted from the kinetic description in this range. In order to avoid bacterial growth during fermentation a slightly acidic environment is preferred. Therefore, citric acid is chosen as the most suitable buffer for the model system. The fact that citric acid can be utilised as carbon source holds no complication because in bioreactor studies the period after the primary-carbon-source depletion is not of interest.

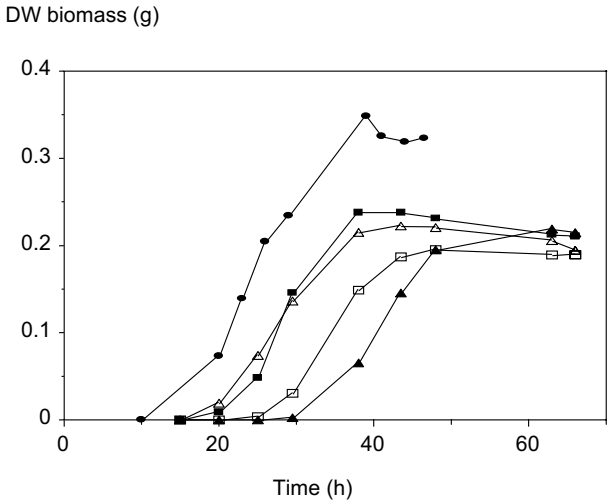

Figure 6. Biomass profiles during cultivation of *Rhizopus oligosporus* using a model system with additions of Tryptone 1 g/l (■), Tryptone 5 g/l (●) Soya peptone 1 g/l (△), Vitamins (□) and no addition (▲).

Effect of nutrient additions

The purpose of this study was to increase the growth rate of *R. oligosporus* for future studies, concerning the removal of metabolic heat in large-scale bioreactors. Vitamins, tryptone or soya peptone were added to the standard mineral medium to increase the growth rate. Since the exponential growth phase was rather short in these experiments (and in SSF in general) and because 65% of the total biomass was produced in the linear part of the growth curve (Figure 6), maximum CO_2-production rate (r_{CO2}) was considered a better indicator for metabolic heat production than μ_{max}.

Nonetheless both parameters were evaluated and the whole cumulative CO_2-production curve was taken to determine μ_{max}, r_{CO2} and the lag phase. μ_{max} and lag phase were calculated from the logistic equation (equation 1, Figure 1) and r_{CO2} was estimated from a linear part of the cumulative CO_2-production curve.

The addition of vitamins did not significantly change μ_{max} or r_{CO2} (Table 2). The addition of soya peptone (1 g/l) or tryptone (1 g/l) increased μ_{max}, but an adverse effect could be observed on r_{CO2}.

The biomass profiles of these two series showed no effect in the biomass production rate (Figure 6). However, the same amount of biomass was obtained more rapidly due to a much shorter lag phase. The short lag phase with these two series is advantageous for the model system, but still the main goal of increasing the heat production was not met.

A further increase in the tryptone concentration to 5 g/l showed a significant increase in both μ_{max} and r_{CO2} compared to all previous series (Table 2). The final amount of biomass was higher compared to the reference, which implies that tryptone was used for biomass production. This means that additional measurements on tryptone conversion are necessary in this model system to obtain correct stoichiometric coefficients during growth. The advantages of a high r_{CO2} and short lag phase were considered more beneficial than the disadvantage of additional measurements.

Table 2. Effect of different additions to a standard synthetic medium on growth of *Rhizopus oligosporus* on agar plates at 30 °C.

additions to standard medium	μ_{max} * (h^{-1})	r_{CO2} * ($\cdot 10^{-4}$ mol/h)	Lag-time * (h)	max. biomass dry weight (g)
none	0.27 (± 0.014)	3.03 (± 0.15)	21.6 (± 0.54)	0.22
Vitamins	0.30 (± 0.020)	3.12 (± 0.37)	17.5 (± 0.52)	0.20
Soya peptone (1 g/l)	0.35 (± 0.037)	2.56 (± 0.09)	10.7 (± 1.58)	0.22
Tryptone (1 g/l)	0.34 (± 0.036)	2.80 (± 0.08)	11.5 (± 0.52)	0.24
Tryptone (5 g/l)	0.42 (± 0.017)	4.31 (± 0.24)	10.8 (± 0.46)	0.35

* The values between brackets indicate the ± 95 % confidence intervals

CONCLUSIONS

Experiments showed that pH control was necessary in this model system when ammonium sulphate was used as nitrogen source. However, the growth rate did not vary much between pH values 4 and 6. Thus only some degree of pH control was necessary (depending on the initial pH) and citric acid was the most suitable buffer for this model system.

Addition of tryptone and soya peptone considerably shortened the lag phase for *Rhizopus oligosporus*. The maximum specific growth rate and maximum CO_2-production rate increased significantly with the addition of 5 g/l of tryptone to a standard mineral medium.

In summary, a model system for solid-substrate fermentation was improved through (1) better pH control by using a citric-acid buffer and (2) an overall shortening of the total fermentation time via the addition of 5 g/l tryptone.

ACKNOWLEDGEMENTS

The authors wish to thank M.S.N. Bakker and M. Stork for performing most of the experiments. Furthermore the financial support of the Dutch Graduate School on Process Technology is gratefully acknowledged.

REFERENCES

Agosin E, Jarpa S, Rojas E, Espejo E. 1989. Solid-state fermentation of pine sawdust by selected brown-rot fungi. Enz Microbiol Technol 11: 511-517.

Auria R, Hernandez S, Raimbault M, Revah S. 1990. Ion exchange resin: a model support for solid state growth fermentation of *Aspergillus niger*. Biotechnol Techn 4: 391-396.

De Reu JC. 1995. Solid-substrate fermentation of soya beans to tempeh: process innovations and product characteristics. PhD thesis, Wageningen Agricultural University, The Netherlands.

Mitchell DA, Greenfield PF, Doelle HW. 1986. A model substrate for solid-state fermentation. Biotechnol Lett 8: 827-832.

Mitchell DA, Greenfield PF, Doelle HW. 1988a. Development of a model solid-state fermentation system. Biotechnol Techn 2: 1-6.

Mitchell DA, Greenfield PF, Doelle HW. 1988b. Agar plate growth studies of *Rhizopus oligosporus* and *Aspergillus oryzae* to determine their suitability for solid-state fermentation. Appl Microbiol Biotechnol 28: 598-602.

Mitchell DA, Doelle HW, Greenfield PF. 1989. Suppression of penetrative hyphae of *Rhizopus oligosporus* by membrane filters in a model solid-state fermentation system. Biotechnol Tech 3: 45-50.

Mitchell DA, Do DD, Greenfield PF, Doelle HW. 1991. A semimechanistic mathematical model for growth of *Rhizopus oligosporus* in a model solid-state fermentation system. Biotechnol Bioeng 38: 353-362.

Narahara H, Koyama Y, Yoshida T, Pichangkura S, Ueda R, Taguchi H. 1982. Growth and enzyme production in a solid-state culture of *Aspergillus oryzae.* J Ferment Technol 60: 311-319.

Nishio N, Tai K, Nagai S. 1979. Hydrolase production by *Aspergillus niger* in solid-state cultivation. Eur J Appl Environmental Microbiol 8: 263-270.

Okazaki N, Sugama S. 1979. A new apparatus for automatic growth estimation of mold cultured on solid media. J Ferment Technol 57: 413-417.

Okazaki N, Sugama S, Tanaka T. 1980. Mathematical model for surface culture of Koji mold. J Ferment Technol 58: 471-476.

Prior BA, Du Preez JC, Rein PW. 1992. In: Doelle HW, Mitchell DA, Rolz CE, editors. Solid substrate cultivation. London: Elsevier Science Publishers, pp 77-80.

Raimbault M, Alazard D. 1980. Culture method to study fungal growth in solid fermentation. Eur J Appl Microbiol Biotechnol 9: 199-209.

Rinzema A, de Reu JC, Oostra J, Nagel FJI, Nijhuis GJA, Scheepers AA, Nout, MJR, Tramper J. 1997. Models for solid-state cultivation of *Rhizopus oligosporus*. In: Roussos S, Lonsane BK, Raimbault M, Viniegra-Gonzalez G, editors. Advances in solid state fermentation. Dordrecht: Kluwer Academic Publishers, pp 143-154.

Saucedo-Castañeda G, Lonsane BK, Navarro JM, Roussos S, Raimbault M. 1992. Importance of medium pH in solid state fermentation for growth of *Schwanniomyces castellii*. Lett Appl Microbiol 15: 164-167.

Yang SS, Chiu WF. 1986. Protease production with sweet potato residue by solid-state fermentation. Chin J Microbiol Immun 19: 276-288.

Yang SS. 1988. Protein enrichment of sweet potato residue with amylolytic yeasts by solid-state fermentation. Biotechnol Bioeng 32: 886-890.

Chapter 3

Temperature control in a continuously mixed bioreactor

F.J.I. Nagel, J. Tramper, M.S.N. Bakker, A. Rinzema.
Biotechnology and Bioengineering (2001), 72: 219-230

SUMMARY

A continuously mixed, aseptic paddle mixer was used succesfully for solid-state fermentation (SSF) with *Aspergillus oryzae* on whole wheat kernels. Continuous mixing improved temperature control and prevented inhomogeneities in the bed. Respiration rates found in this system were comparable to those in small, isothermal unmixed beds, which showed that continuous mixing did not cause serious damage to the fungus or the wheat kernels. Continuous mixing improves heat transport to the bioreactor wall, which reduces the need for evaporative cooling and thus may help to prevent the desiccation problems that hamper large-scale SSF. However, scale-up calculations for the paddle mixer indicated that wall cooling becomes insufficient at the 2 m^3 scale for a rapidly growing fungus like *A. oryzae*. Consequently, evaporative cooling will remain important in a large-scale mixed system. Experiments showed that water addition will be necessary when evaporative cooling is applied in order to maintain a sufficiently high water activity of the solid substrate. Mixing is necessary to ensure homogeneous water addition in SSF. Automated process control might be achieved using the enthalpy balance. The enthalpy balance for the case of evaporative cooling in the paddle mixer was validated. This work shows that continuous mixing provides promising possibilities for simultaneous control of temperature and moisture content in solid-state fermentation on a large scale.

INTRODUCTION

Solid-state fermentation (SSF), that is, cultivation of micro-organisms on moist solid substrates in the absence of free-flowing water, is an alternative for submerged fermentation (SmF) for the production of biotechnological products. In recent years, research on SSF has led to a wide range of applications on lab scale (Gupte and Madamwar, 1997; Gutierrez-Correa and Tengerdy, 1998; Hang and Woodams, 1998; Kotwal *et al.*, 1998; Sekar and Balaraman, 1998), and comparative studies between SmF and SSF have claimed superior product yields for the latter (Barrios-Gonzalez *et al.*, 1988; Lekha and Lonsane, 1994; Maldona and Strasser de Saad, 1998; Ohno *et al.*, 1992). In spite of these examples the commercial application of SSF processes in Western countries has been limited (Lonsane *et al.*, 1985; Mitchell and Lonsane,

1992), mainly due to problems associated with scale-up (Lonsane *et al.*, 1992; Pandey, 1991). The results presented here are part of a research project aiming to develop scale-up guidelines for SSF.

The main problem associated with scale-up is the removal of heat generated by the metabolic activity of the microorganisms (Saucedo-Castaneda *et al.*, 1990 and 1992). Heat removal by conduction in static packed beds is limited due to : (1) the poor heat transfer through the bed (Saucedo-Castaneda *et al.*, 1990); and (2) the lack of heat-exchange surface on a large scale. Evaporative cooling has proven to be more efficient than convection and conduction (Laukevics *et al.*, 1984, Sargantanis, 1993). It results, however, in large moisture losses and drying of the solid substrate (Narahara *et al.*, 1984, Trevelyan, 1974). Therefore, it is essential to combine temperature and moisture control in large-scale SSF systems (Lonsane *et al.*, 1992; Ryoo *et al.*, 1991; Saucedo-Castaneda, 1992). Evaporative cooling should be combined with spraying of water onto the solid substrate (Barstow *et al.*, 1988). The use of mixed bioreactors is necessary to ensure homogeneous water addition and evaporation. In addition, mixing of the solid substrate offers many advantages, which in many cases outweigh possible disadvantages such aseffects of shear on growth (Stuart *et al.*, 1999; Aidoo *et al.*, 1984). The main advantages of using a mixed SSF system include (1) reduction of inhomogeneity in the bed; (2) uniform distribution of additions during cultivation; and (3) potentially improved gas exchange, evaporation and heat transfer. This will result in better, more stable, reproducible bioreactor performance and process control. In several bioreactors at the pilot scale (100 to 1000 kg wet weight) (Durand and Chereau, 1988; Durand *et al.*, 1996, Fernández *et al.*, 1996) and large scale (25000 kg wet weight or more) (Xue *et al.*, 1992) mixing devices are used for control purposes.

In this article, an aseptic, continuously mixed bioreactor is presented which is suitable for scale-up with respect to heat-removal. A 35-L bioreactor was developed based on the well-known paddle mixer (Aidoo, 1984; Laukevics et al., 1984) in which *Aspergillus oryzae* was grown on whole wheat grains. A rapidly growing fungus *(A. oryzae)* was chosen to assure sufficient heat generation, so that scale-up guidelines would be based on a worst-case with regard to heat-removal problems. In addition, *A. oryzae* is commonly used in SSF for the industrial production of koji (for the production of soy sauce) and for lab-scale production of a variety of enzymes like α-

amylase (Torrado *et al.*, 1998), lipase (Ohnishi *et al.*, 1994) and proteinase (Narahara *et al.*, 1982).

Bioreactor performance of our mixed system was compared to that of nonmixed systems and a packed-bed bioreactor from the literature (Narahara *et al.*, 1984). Scale-up guidelines for temperature control in large-scale mixed bioreactors were developed. Two temperature-control strategies, wall cooling and evaporative cooling, were used separately in this bioreactor for automatic temperature control. Data from these fermentations were used in scale-up calculations to determine the scale at which the capacity of wall cooling would become insufficient for heat removal.

By comparing these two temperature-control strategies we were able to quantify when dehydration affects the growth for the case of evaporative cooling. It was demonstrated that water addition is necessary when evaporative cooling is applied. For large-scale bioreactor design this implies: (1) the necessity for simultaneous control of temperature and moisture content; and (2) the need for agitation devices in SSF systems. Automated control might be achieved using the enthalpy balance. The enthalpy balance during fermentation with evaporative cooling was verified in order to determine the reliability of all measurements in the system. We were able to prove that accurate on-line monitoring of evaporated water is possible, which is an important aspect for automatic moisture-content control.

MATERIALS AND METHODS

Micro-organism and inoculum preparation

Aspergillus oryzae CBS 570.65 was obtained from Centraal Bureau voor Schimmelcultures (Baarn, The Netherlands). A spore suspension was obtained by growing the fungus on malt-extract agar (Oxoid, CM 59) for 7 days at 30 °C and harvesting the spores with 20 mL solution containing 1 g neutralized bacteriological peptone (Oxoid, L34), 8.5 g NaCl and 10 mL Tween 80 per 1000 mL distilled water. This spore suspension was filtered through sterile glass wool to remove the remaining mycelium. Spore suspension (43.5 mL) and 16.5 g glycerol were added to 125 mL-plastic bottles (Nalgene 2105-0004, UK), which were stored at -20 °C for up to 3 months. The spore count of each plastic bottle was approximately $9.7 \cdot 10^6$ spores/mL,

measured by microscope using a Neubauer counting chamber. Inoculum was prepared in a laminar-flow cabinet by dividing the content of one 125-mL bottle spore suspension over two sterile 500-mL pressure tanks each containing 70 mL sterilized water. The inoculation level for the fermentations was $1.3 \cdot 10^5$ spores/g dry weight substrate.

Preparation of the solid substrate

A single batch of wheat grains of commercial origin (Blok, Woerden, The Netherlands), stored at 10°C, was used for all experiments. The initial moisture content of this batch was 0.12 kg water/ kg dry wheat. Five kg of this batch was soaked for 2.5 h in excess water (60°C) for a final moisture content of 0.85 kg water/kg dry wheat. After sieving, the soaked grains were divided over four 25-L bottles (Nalgene 2251-0050,UK) and autoclaved (1.5 h, 121°C).

Fermenter and agitator design

Several successful cultivations were done in the horizontal paddle mixer and, throughout the development phase, this bioreactor was slightly adapted and auxiliary equipment was optimized. The horizontal paddle mixer (Figure 1) had the following dimensions: internal diameter 30 cm, length 50 cm and internal volume 35.3 L. The bioreactor consisted of a glass cylinder (Schott, Germany) with two stainless-steel side plates. Along the central axis, six V-shaped paddles were placed at an equal distance and at a 90° angle relative to the adjacent paddle; two flat rectangular paddles were mounted at each end of the central axis. The central axis was driven by a Watson-Marlow drive (type 505DU, Cornwall, UK) fitted with a factor-10 gearwheels transmission for a sufficient torque on the axis. Air entered the bioreactor via the hollow central axis and came out at the end of each paddle to provide uniform air distribution throughout the bed. An air outlet was situated in the headspace of each side plate. A pressure control valve (Type 1525, Eriks, The Netherlands) was fitted on each side plate to maintain a constant pressure ($1.2 \cdot 10^5$ Pa) in the bioreactor, irrespective of the airflow.

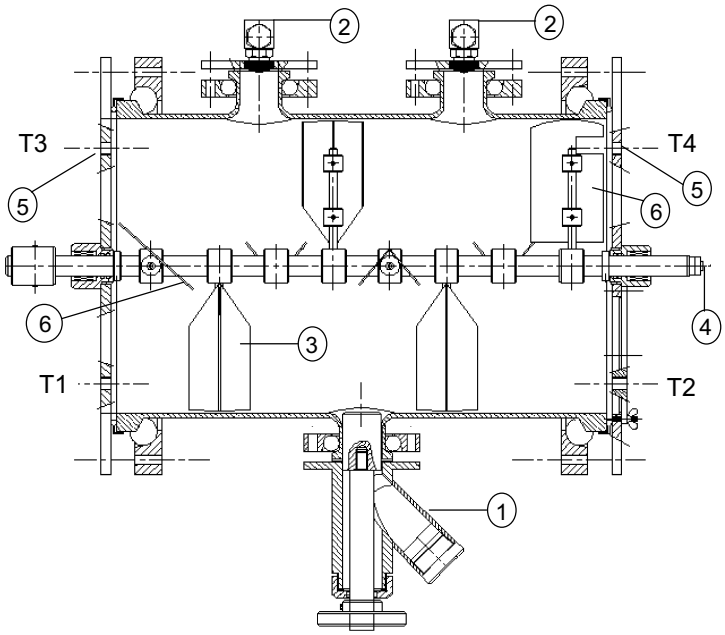

Figure 1. The 35-L horizontal paddle mixer: (1) sampling device; (2) spraying nozzle; (3) V-shaped paddle; (4) air inlet; (5) air outlet; (6) rectangular paddle; (T1 and T2) temperature sensors in the solid substrate bed; and (T3 and T4) temperature sensors in the headspace.

Two full-cone spraying nozzles of the air/water pressure type (Spraying systems, The Netherlands) were mounted onto the glass cylinder in order to spray the spore suspension evenly over the solid substrate. To control the temperature of the wall, a flat rubber tube (Tamson, The Netherlands) was twisted around the glass cylinder and connected to a water bath (Haake type F3, Germany, for the wall cooling experiments; Julabo type F25, Germany, for the evaporative cooling experiments). The temperature of the water bath was controlled based on an external setpoint. In addition, the bioreactor was placed in a temperature-controlled incubator to prevent the disturbing effects of ambient temperature variations.

Air-conditioning system

A controlled vapor delivery system (Bronckhorst Hitec, Veenendaal, The Netherlands) enabled accurate control of the relative humidity of the inlet air (Figure 2). This system was externally controlled and consisted of a mass-flow controller (0-100 L/min, type F202AC), a liquid-flow controller (0-250 g/h, type L2) and a temperature-controlled evaporator (type W303). The moisturised air was filter sterilized using a 0.2-µm hydrophobic membrane (Gellman, type CFF92HP 1700 cm^2, USA). The temperature of the incoming air was equal to the temperature of the cabinet (35°C in all experiments).

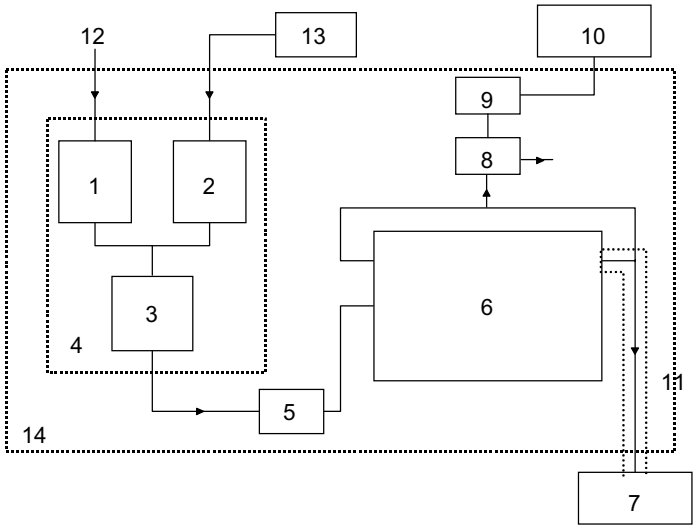

Figure 2. Schematic overview of the air-conditioning system used in the experiments: (1) mass-flow controller; (2) liquid-flow controller; (3) controller-mixed evaporator (CEM); (4) CEM-controlled vapor-delivery system; (5) sterilizing membrane filter; (6) horizontal paddle mixer; (7) cooled-mirror dewpoint-measuring system; (8) bioreactor pressure-control valve; (9) condenser; (10) O_2/CO_2 analyzer; (11) heated coil; (12) air pressure (6 bar); (13) pressure tank for water; and (14) temperature-controlled cabinet.

Fermentation process

The autoclaved and moisturized wheat grains were transferred to the previously autoclaved (1.5 h, 121 °C) and cooled horizontal paddle mixer. The filled reactor was again sterilized for 1.5 h at 121°C in an autoclave. The 500-mL pressure tanks were aseptically connected to the spraying nozzles on top of the bioreactor and the inoculum was sprayed over the continuously mixed (2.5 rpm) wheat grains. During the first 24 hours after inoculation, the wheat grains were discontinuously mixed (55 min with no agitation; 5 min with agitation at 1 rpm) to allow undisturbed germination and to minimize grain damage. During this period the temperature of the wall was set to 34.5 °C and the air flow to 20 L/min (273 K, $1.031 \cdot 10^5$ Pa). After this period continuous mixing (0.5 rpm) was applied. When the temperature of the bed reached 35°C, temperature control was started automatically as explained in what follows.

On-line measurements

Six temperature sensors (Pt-100 Ω Tempcontrol, Voorburg, The Netherlands) were used for on-line temperature readings. Two sensors were placed in the solid substrate and two in the headspace at the positions marked T1 to T4 in Figure 1. Two additional sensors were located outside the fermentor in contact with the glass wall on each side of the bioreactor.

The effluent gas was analyzed for O_2 and CO_2 in a paramagnetic O_2 analyzer (Servomex, Xentra 4100, Servomex Zoetermeer, The Netherlands) and an infrared CO_2 analyzer (Servomex Series 1400). Prior to these analysis, the effluent gas was cooled to 2°C in a condenser. The O_2 analyzer was fitted with a second channel to measure the O_2 concentration in the surrounding air in order to accurately determine O_2 consumption. Both oxygen sensors corrected the readings for pressure fluctuations. CO_2 production was calculated by subtracting a previously measured average of the CO_2 concentration in air from the effluent reading.

The dewpoint of the effluent gas was measured in a cooled-mirror dewpoint-measuring system (DEWMET SD, Michell Instruments Ltd., UK). The effluent gas line to the dewpoint meter was heated with a water-heated coil (50°C) to prevent condensation prior to the measurement. A fit relation, based on literature data (Lide, 1993), was used to convert dewpoint temperature (T in °C) readings to water-vapor pressures:

$$p_{w,sat} = \left(\frac{24.503 + 0.68363 \cdot T + 3.5349 \cdot 10^{-3} \cdot T^2}{1 - 9.935 \cdot 10^{-3} \cdot T + 4.1781 \cdot 10^{-5} \cdot T^2} \right)^2 \quad \text{[Pa]} \qquad (1)$$

To enable automatic process control, all sensors and equipment were linked to a computer-controlled data acquisition system consisting of hardware (RTI 820 boards with 5B modules, Analog Devices Inc., USA), software (VIEWDAC revision 2.10, Keithley Instruments Inc., USA) and a personal computer (80486 PC). The temperature-control strategy (see later) was implemented in a sequence in VIEWDAC and operated fully automatically.

Temperature control strategies

Two temperature control strategies were employed, consisting of wall cooling and evaporative cooling.

In the wall cooling strategy, the temperature of the cooling water circulating in the flat rubber tubes wrapped around the fermentor was lowered to maintain the desired bed temperature. This resulted in a lower wall temperature, which was recorded by a temperature sensor. The air flow rate was manually set at a level that kept the CO_2 concentration between the limits of the analyzer (0 to 24 h, 20 L/min; 24 to 51 h, 40 L/min; 51 h to end, 60 L/min). The humidity of the inlet air was kept constant at 0.0259 mole per mole of dry air, which corresponds to a relative humidity of 45.5% at 35°C and $1.013 \cdot 10^5$ Pa; complete saturation of the incoming air was not possible due to overpressure and subsequent condensation problems before the sterilizing filter. Due to the undersaturation of the incoming gas, evaporation could not be neglected in the enthalpy balance.

In the evaporative cooling strategy, the air flow rate to the fermenter was adjusted to maintain the desired bed temperature. The temperature of the wall was kept at 34.5°C throughout the fermentation to minimize heat transfer through the wall. A constant flow rate of water vapor (13 g/h) was mixed with the inlet air using the liquid-flow controller described above (air-conditioning system). As a consequence of the increasing air flow rate, the inlet relative humidity decreased.

Control algorithm

In both temperature-control strategies, on-line measurements were used to first estimate the control variable from the enthalpy balance over the bioreactor. Then, the estimated control variable was adjusted using a PI controller based on the bed temperature, to correct for setpoint deviations (Figure 3).

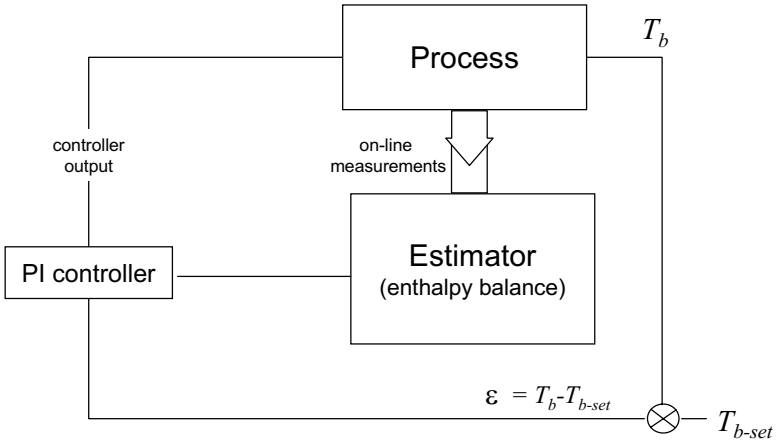

Figure 3. Schematic overview of the temperature-control strategy used during the fermentations to calculate the control variables T_{wall} (wall cooling) and F_{air} (evaporative cooling).

The enthalpy balance used to estimate the control variable is made up of several terms:

$$\frac{dT_b}{dt}\sum_i M_i \cdot C_{p,i} = r_{met} + J_{wall} + J_{evap} \qquad \text{[W]} \qquad (2)$$

in which

J_{evap}	=	heat transfer from evaporation and heating of the air	[W]
r_{met}	=	heat production by micro-organisms	[W]
J_{wall}	=	heat transfer through the wall	[W]
T_b	=	average temperature of the bed (Pt100 1&2, Fig. 1)	[°C]
M_i	=	weight component i (water, starch, protein etc.)	[kg]
$C_{p,i}$	=	heat capacity component i (water, starch, protein etc.)	[J·(kg·°C)$^{-1}$]

The mass accumulation term ($\Sigma dM/dt \cdot T_b \cdot C_p$) in this balance is neglected. For the case of evaporative cooling this term was 2.7 W maximum ($\Sigma dM/dt$ = 0.028 g/s; T_b = 35 °C; C_p = 2.77 J/g °C), which is a minor term compared with the maximum heat production rate of 100 W. In the equation, all losses are regarded as negative production terms. The physical constants used in the equations were taken from literature (Lide, 1993). The different contributions are now examined briefly.
The amount of heat lost by evaporation and heating of the air was calculated by :

$$J_{evap} = -\left(h_o - h_i\right) \cdot F_{air} \cdot \rho_{air} \quad \text{[W]} \qquad (3)$$

with

F_{air}	=	volumetric dry air flow rate at 273 K and $1.013 \cdot 10^5$ Pa	[m^3 dry air·s^{-1}]
ρ_{air}	=	1.293 density dry air at 273 K and $1.013 \cdot 10^5$ Pa	[kg·m^{-3} dry air]
h_o	=	enthalpy of the outcoming air	[J·kg^{-1} dry air]
h_i	=	enthalpy of the incoming air	[J·kg^{-1} dry air]

The enthalpy of the air (h) is:

$$h = C_{p,air} \cdot T_{air} + y_w \cdot \left(H_V + C_{p,V} \cdot T_{air}\right) \quad \text{[J·kg}^{-1}\text{ dry air]} \qquad (4)$$

with

$C_{p,air}$	=	1007	heat capacity dry air	[J·(kg·°C)$^{-1}$]
H_V	=	$2.501 \cdot 10^6$	heat of vaporization of water at 273 K	[J·kg^{-1}]
$C_{p,V}$	=	1870	heat capacity water vapor	[J·(kg·°C)$^{-1}$]
T_{air}	=	temperature of the air		[°C]
y_w	=	moisture content of the air calculated from dewpoint		[kg·kg^{-1} dry air]

The amount of heat that is removed through the wall is calculated from :

$$J_{wall} = -\alpha_{ov} \cdot A \cdot \left(T_b - T_{wall}\right) \quad [W] \quad (5)$$

with

α_{ov}	=	heat transfer coefficient of the wall	[W·(m^2·°C)$^{-1}$]
A	=	heat transfer area of the wall	[m^2]
T_{wall}	=	average temperature inlet and outlet cooling coil	[°C]

Roels (1983) and other authors have shown that for aerobic fermentation the heat production can be related to oxygen consumption:

$$r_{met} = \left(C_{O2,i} - C_{O2,o}\right) \cdot F_{air} \cdot 460 \cdot 10^3 \quad [W] \quad (6)$$

with

$C_{O2,i}$	=	inlet O_2 concentration at 273 K and 1.013·10^5 Pa	[mol·m^{-3} dry air]

The estimator for wall cooling calculates the temperature of the wall ($T_{wall,est}$) necessary to assure temperature control (*i.e.* $dT/dt = 0$). Substitution of equation (5) in equation (2) gives the estimated control variable $T_{wall,est}$:

$$T_{wall,est} = T_b - \frac{r_{met} + J_{evap}}{\alpha_{ov} \cdot A} \quad [°C] \quad (7)$$

where J_{evap} is calculated by equation (3), by using the dew-point measurement in the effluent air and the setpoints of the liquid- and gas-flow controllers.
The estimator for evaporative cooling calculates the air flow rate ($F_{air,est}$) necessary for temperature control (i.e. $dT/dt = 0$). Substitution of equation (3) in equation (2) gives the estimated control variable $F_{air,est}$:

$$F_{air,est} = \frac{r_{met} + J_{wall}}{\left(h_o - h_i\right) \cdot \rho_{air}} \quad [m^3 \cdot s^{-1}] \quad (8)$$

where J_{wall} is calculated with equation (5), by using the measured bed and wall temperatures, and the product of heat transfer coefficient and wall area estimated as explained in what follows.

Wall cooling is minimized in this situation by setting a small temperature difference (0.5°C) between the bioreactor and the wall, but was not neglected in the enthalpy balance.

A PI controller was used for feedback control and to correct for errors in the estimated control variable (O_{est}) as a result of measuring errors, wrong assumptions in the enthalpy balance or incorrect input parameters. The estimated control variable ($T_{wall,est}$) for wall cooling; $F_{air,est}$ for evaporative cooling) was corrected with a proportional-integral algorithm to give the controller output ($O_{control}$):

$$O_{control} = O_{est} + K_c \cdot \varepsilon(t) + \frac{K_c}{\tau_I} \cdot \int_0^t \varepsilon(t) \cdot dt \tag{9}$$

in which

K_c = proportional gain of the controller [-]

τ_I = integral time constant [h]

The input of the controller is the deviation (or error ε) between the actual substrate temperature and the desired setpoint:

$\varepsilon(t) = T_b(t) - T_{b\text{-}set}$

$T_{b\text{-}set}$ = set-point temperature for the bed of solids [°C]

Parameters

The values for K_c and τ_I used in the PI controller were -5 [-] and 1.4 h, respectively, for wall cooling, and 7.5 L·(min·°C)$^{-1}$ and 7.5 h, respectively, for evaporative cooling. The value for $\alpha_{ov} \cdot A$ was estimated using Equation 2 from data of the first 24 hours of the fermentation. The values for $\alpha_{ov} \cdot A$ used in the estimator for wall cooling and evaporative cooling were 6 and 8.5 [W·°C^{-1}], respectively. The difference between both values must be attributed to the rough estimation procedure used and perhaps also to differences in water flow rate through the cooling tubes.

Off-line analysis

Sample Preparation

Twice a day during the fermentation samples (± 30 g) were taken from the bioreactor. Moisture content and water activity were determined immediately after sampling. Approximately 5 g of wheat grains were transferred into a sample bottle and stored at -20°C for analysis of glucosamine.

Moisture Content & Water Activity

The moisture content of the sample was determined in duplicate by drying 6 g of wet grains at 80°C for 2 days in a preweighed dish. The water activity of the sample was determined in a Novasina Thermoconstanter (Type TH200, Switzerland) at 35°C.

Glucosamine

The glucosamine content in the samples was used as an indirect estimate of biomass. Because the starch in the sample interfered with the peak separation during high-performance liquid chromatography (HPLC) analysis, the starch was first removed from the sample with an enzymatic method.

After the sample bottle was thawed, the wheat grains were homogenized with water (grains : water = 1 g : 4 g) in an ultraturrax (Silverson L4R, UK). Three gram of this homogenate was added to 6.5 mL 13 mM phosphate buffer (pH = 4.5) and 20 µL amyloglucosidase (Sigma A-3042, USA) enzyme solution and incubated at 55°C for 1 hour. This suspension was centrifuged (20 min, 5500 rpm, Beckman centrifuge GS-15R), after which the supernatant was discarded. The pellet was washed with 5 mL distilled water, again centrifuged and then dried (50°C, 3 days).

The dried pellet was prehydrolyzed with 0.5 mL 10 M H_2SO_4 for 24 hours and occasionally stirred at room temperature. After prehydrolysis, 4.5 mL distilled water was added and further hydrolysis was continued at 100°C for 3 h in a thermal heating block (Grant QBT4, UK). After hydrolysis, the pH was adjusted to 5 with NaOH and the sample was filtered through a 0.45-µm membrane. The glucosamine content was measured by ion-exchange chromatography (Carbopac™ PA1 column with guard column, Dionex, Sunnyvale, USA) with pulse amperometric detection, at 25°C, using D-(+)-glucosamine hydrochloride (Sigma G-4875, USA) as reference solution and 20 mM NaOH (1 mL/min) was used as eluent.

Measurements of glucosamine content (grams per dry matter sample) are recalculated in order to express the concentration per gram of initial dry matter wheat. For this calculation it was assumed that CO_2 linearly correlates with loss of dry matter. The cumulative CO_2 production at the moment of sampling was used together with total dry-weight loss and total CO_2 production to calculate the total dry matter at the moment of sampling (term above the division sign in Equation 10). Glucosamine measurements are expressed per gram initial dry matter wheat as calculated by:

$$Gm = Gm` \cdot \frac{\left(IDM - CO_2^{\,t_{sample}} \cdot \frac{\left(IDM - DM_{t_{end}} \right)}{CO_2^{\,t_{end}}} \right)}{IDM} \qquad [mg \cdot g^{-1}\ IDW] \quad (10)$$

Gm	=	glucosamine content per gram initial dry matter	[mg·g^{-1} IDW]
$Gm`$	=	glucosamine content sample per gram dry matter	[mg·g^{-1} DW]
IDM	=	initial dry matter in bioreactor	[g]
DM_{tend}	=	measured final dry weight in bioreactor	[g]
$CO_2^{tsample}$	=	cumulative CO_2 production at sampling time	[g]
CO_2^{tend}	=	final cumulative CO_2 production	[g]

Mixing performance paddle mixer

To determine radial and axial mixing in the horizontal paddle mixer, three colored wheat grain fractions were used: red, green, and natural. For radial mixing the fractions were placed in three horizontal layers; for axial mixing the fractions were placed in three equal vertical sections. The hold up and moisture content of grains in the mixing experiments were equal to those in the fermentations. Samples were taken using a long plastic cylinder in opening 2 (Figure 1). The colored grain fractions were counted and calculated as a percentage of the total number per sample. Mixing experiments were done at 0.5 and 1 rpm.

Miniature packed bed and tray

Packed bed: aeration through the bed

The miniature packed bed consisted of a glass cylinder (∅ = 5 cm, h = 15 cm). A stainless-steel wire mesh at 7 cm from the bottom supported one layer of grains (10 g wet weight, moisture content 0.44 kg/kg wet weight). The packed bed was placed in a temperature-controlled cabinet at 35°C. The air flow (24 L dry air/h at 273 K and $1.013 \cdot 10^5$ Pa) was humidified (94.6 % relative humidity) using a 1.5-L bubble column with 0.5-cm Rashig rings. The air was filter sterilized using a 0.2-µm hydrophobic membrane (acros 50, Gellman, USA) before it was passed through the bed. The effluent air was dehumidified using a condenser at 2°C before it was analyzed for CO_2 and O_2 (see "Measurements On-Line" subsection).

Tray: aeration over the bed

A Petri dish (without the lid) containing 30.2 g wet weight grains (moisture content 0.48 kg/kg wet weight) was placed in a closed jar. The air inlet was situated beside the Petri dish. The same cabinet and air-conditioning system were used as described earlier. The air flow was 27 L dry air/h at 273 K and $1.013 \cdot 10^5$ Pa, and the temperature of the cabinet was controlled at 37°C.

Desorption isotherm

For the water desorption isotherm of wheat grains, autoclaved wheat grains were used as described earlier. Portions of wheat grains were transferred to predried and preweighed dishes (Novasina, Switzerland). The dishes were placed in a large vacuum desiccator with saturated LiCl solution (a_w=0.11). At regular time intervals, dishes were removed and sealed. After a few hours at room temperature, the water activity and the moisture content were determined. Water activity was determined in a thermoconstanter (Model TH200, Novasina, Switzerland) at 35°C.

RESULTS AND DISCUSSION

Bioreactor performance

Several mixing experiments were done to determine the radial and axial mixing performance of this bioreactor. Radial mixing is easily accomplished in a paddle mixer. For axial mixing, however, V-shaped paddles had to be used that could push the solid substrate sideways. Axial mixing is important for homogeneous water distribution in the bed, because industrial spraying nozzles usually cannot spray evenly over the total surface of the bed. Adequate radial mixing is achieved after six revolutions (Figure 4), implying a mixing time of 12 min at 0.5 rpm, which was used during the fermentations. Axial-mixing experiments showed that, after 120 revolutions, the bed was well mixed (Figure 4). The number of revolutions needed to achieve radial or axial mixing was the same for both mixing frequencies tested (0.5 and 1 rpm). Although the axial-mixing time was rather long (4 h), it was brief compared with the time needed (30 h) to evaporate all the water in the bed, given a maximum heat generation of 100 W. Furthermore, the spraying frequency was about once every hour and full-cone spraying nozzles were used, and therefore good water distribution could be assured.

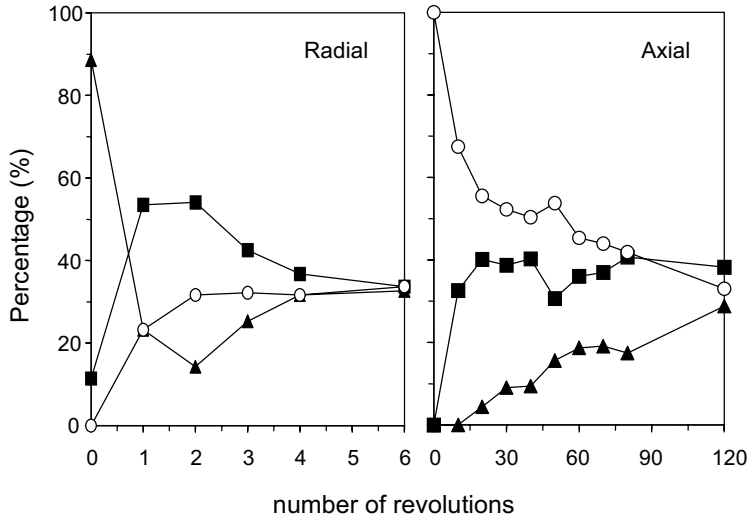

Figure 4. Axial and radial mixing at 1 rpm in the 35-L horizontal paddle mixer. Percentages of colord wheat grains in the sample taken from the position underneath the right nozzle (red ■; green ▲; natural color ○).

The next aim was to measure mixed-bioreactor performance and to compare it with measurements in a packed bed containing one layer of grains and literature data for a 1 kg packed-bed bioreactor. Bioreactor performance was determined from the maximum oxygen consumption rate per kilogram initial dry matter (*IDM*). When measuring the maximum oxygen consumption rate it is important to control the temperature and moisture content in order to allow comparison between different experiments. Wall cooling was applied to control the temperature and to minimize dehydration effects in the paddle mixer. The cultivations were done twice using similar conditions and reproducible results were obtained.

The temperature of the solid substrate could be controlled adequately using wall cooling in the 35-L paddle mixer (Figure 5). The oxygen consumption rate hardly showed an exponential-growth period, but rather a linear increase in consumption rate to 0.17 mol/(h·kg IDM) (Figure 5).

The maximum oxygen consumption rate measured in the miniature packed bed of grains with forced aeration through the bed was 0.20 mol/(h·kg IDM). Although the oxygen-consumption rate in this one-layer packed bed was slightly greater, probably due to ideal circumstances for oxygen transfer, bioreactor performance in our mixed system was satisfactory. Its results are comparable to those of a previously described packed-bed bioreactor with temperature and moisture-content control (Narahara *et al.*, 1984). A maximum oxygen-consumption rate equal to 0.138 mol/(h·kg IDM) was measured in a one-layer tray system when the air was blown over the layer instead of through the layer. This value is lower than the 0.2 mol/(h·kg IDM) measured in the 35-L bioreactor, despite the slightly more favorable temperature in the tray. This is probably attributable to less ideal oxygen transfer caused by the different aeration method. Table 1 summarizes the performance of the SSF systems discussed here.

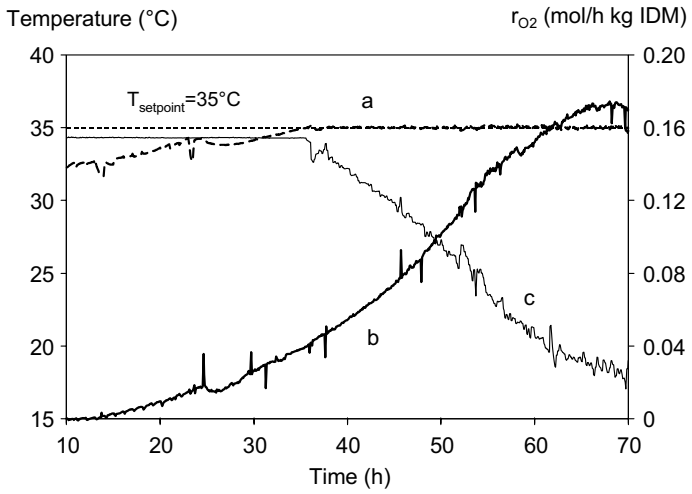

Figure 5. The course of the reactor temperature (dashed line, a), control variable T_{wall} (thin line, c) and oxygen consumption rate (thick line, b) during cultivation of *Aspergillus oryzae* on wheat grains in a 35-L paddle mixer in which the temperature was controlled with wall cooling.

Table 1. Bioreactor performance – expressed as oxygen consumption rate per kilogram initial dry matter (IDM) – of static and mixed solid-state cultivations of *Aspergillus oryzae* with temperature control and little moisture-content variation.

System and wet weight (ww)	Substrate	T [°C]	Water content (kg /kg ww)	Aeration	r_{O2} [mol·h^{-1}·kg IDM^{-1}]
Paddle mixer 8 kg[a]	Wheat grains	35.0	0.46	Forced through	0.172
Packed bed 10 g	Wheat grains	35.4	0.44	Forced through	0.200
Tray system 30 g	Wheat grains	37.0	0.48	Surface	0.138
Packed bed 1 kg	Steamed rice	38.0	0.40	Forced through	0.134[b]

[a] The paddle mixer runs in wall-cooling operation mode.

[b] value represents an r_{CO2} [mol·h^{-1}·kg DM^{-1}] measurement (Narahara, 1984); the respiration coefficient was determined as 1 for this substrate and fungus (Narahara, 1982).

The good bioreactor performance of our mixed system indicates good mass and heat transfer and minimal shear effects on the fungus. Microscopic observations of various cross-sections of wheat grains revealed that the fungus grew inside the wheat grain. Microscopic observations of whole grains showed hardly any fungal biomass on the outside. Apparently, continuous mixing forced the fungus to grow inside the wheat grain and it seemed that the fungus was protected by the seed coat. Therefore, shear effects are thought to be minimal in this case. Furthermore, aggregate formation was prevented through continuous mixing. It can be stated that wheat grains are an ideal solid substrate to be used in continuously mixed bioreactors.

Scale-Up of Wall Cooling

During scale-up of geometrically similar drum-type bioreactors, the ratio between wall area and reactor volume will decrease. It can therefore be expected that, given a maximum heat production rate, wall cooling will become insufficient at a certain bioreactor volume. To develop scale-up rules for wall cooling it is necessary to calculate for which bioreactor volume the capacity of wall cooling becomes limiting. For the case of *Aspergillus oryzae* in a mixed bioreactor the ratio between maximum wall-cooling capacity and maximum heat production was calculated as a function of bioreactor volume.

Several assumptions were made in this calculation :

- There is a constant bioreactor temperature.
- There is negligible evaporation of water.
- There is a perfectly mixed solid substrate.
- Heat transfer occurs through the wheat bed only, not through the air in the headspace.
- There is a bed hold-up of 0.5 [m^3 bed·m^{-3} reactor].

The maximum metabolic heat production and the maximum heat transfer capacity for wall cooling as a function of bioreactor volume are then given by (see also Equation 6):

$$r_{met}\left(V_r\right) = -r_{O2}''' \cdot 0.5 \cdot V_r \cdot 460 \cdot 10^3 \qquad \text{[W]} \qquad (11)$$

and

$$J_{wall}(V_r) = -\pi \cdot \left(\frac{V_r}{2 \cdot \pi \cdot C} \right)^{2/3} \cdot (2C+1) \cdot \alpha_{ov} \cdot (T_b - T_{wall}) \qquad [\text{W}] \qquad (12)$$

in which

r'''_{O2}	=	maximum oxygen production rate	[mol·s^{-1}·m^{-3} bed]
V_r	=	bioreactor volume	[m^3]
C	=	ratio of length over diameter of the drum	[-]
α_{ov}	=	overall heat transfer coefficient	[W·m^{-2}·°C^{-1}]

The maximum heat production rate was taken from the previously discussed experiments in the 35-L bioreactor. The overall heat transfer coefficient (α_{ov} = 100 W·m^{-2}·°C^{-1}) was measured in an industrial solid mixer filled with moisturized oats and equipped with a stainless-steel water jacket (data not shown). The temperature difference between the bioreactor contents and the wall was assumed to be 20 °C.

Figure 6 shows that wall cooling becomes insufficient at 2-m^3 reactor volume for a length/diameter (C = L/D) ratio of 1.7, the value for the 35-L bioreactor. Increasing the L/D ratio improves the capacity of wall cooling but it becomes insufficient above 8 m^3, even for L/D = 15, which, from a practical point of view, is a rather unrealistic ratio.

In a bioreactor of 60 m^3 (≈ 22000 kg wet wheat), 30-50% of the maximum heat production can be removed with wall cooling, irrespective of the L/D ratio, due to the asymptotic behavior of the curves in Figure 6. Thus, although evaporative cooling is necessary to achieve temperature control on a large scale, wall cooling always removes a substantial part of the maximum heat production. Clearly, in the beginning and toward the end of the fermentation wall cooling alone has sufficient cooling capacity to control the temperature.

Effect of evaporative cooling

As discussed previously, evaporative cooling is inevitable on a large scale. Therefore, we quantified the effect of evaporative cooling on the growth of *A. oryzae* on wheat. A temperature-controlled fermentation using mainly evaporative cooling was compared with the previous fermentation with wall cooling. Both experiments were repeated and duplicates gave comparable results (data not shown).

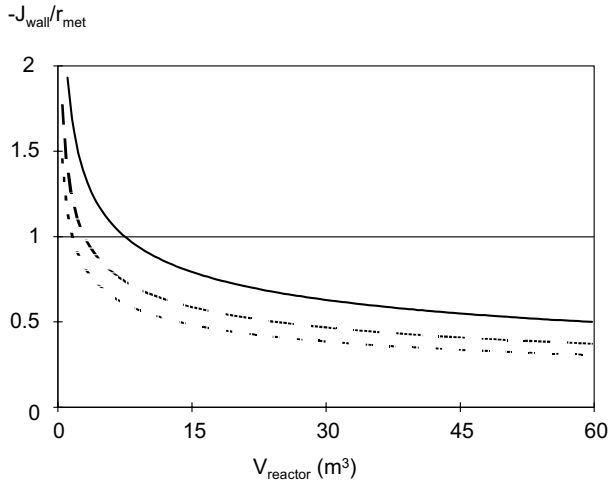

Figure 6. Ratio between maximum heat removal rate through the wall (J_{wall}) and maximum heat production rate (r_{met}) as a function of reactor volume, for three L/D-ratios: 1.7 (dotted line); 5 (dashed line) and 15 (solid line). Parameters used in the calculation are: $\dddot{r}_{O2}$ = 0.0191 mol·s^{-1}·m^{-3}; α_{ov} = 100 W·m^{-2}·C^{-1}; T_b-T_{wall} = 20 ºC.

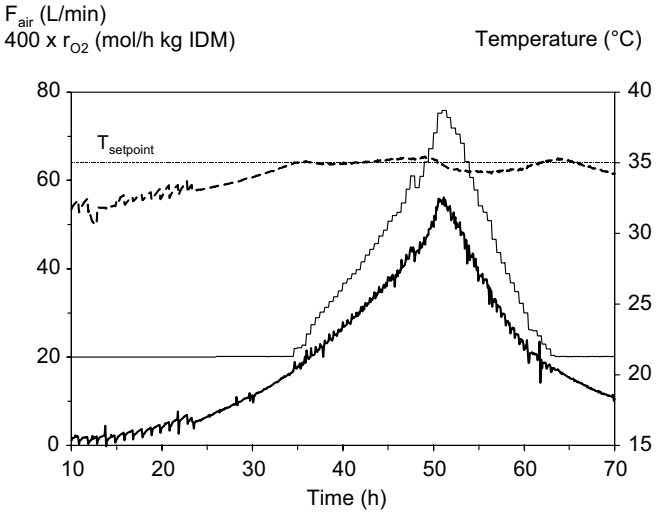

Figure 7. The course of the reactor temperature (dashed line), control variable F_{air} (thin line) and oxygen consumption rate (thick line) during fermentation of *Aspergillus oryzae* on wheat grains in a 35-L paddle mixer in which the temperature was controlled with evaporative cooling.

Figure 7 shows that adequate temperature control was possible in the fermentation with evaporative cooling, with a maximum deviation from the setpoint of 0.6°C. This deviation is acceptable for *A. oryzae* because the maximum specific growth rate is rather constant between 34 and 36 °C (Carlsen *et al.*, 1996). Furthermore, the parameters in the PI controller were not optimized for this purpose, so that better temperature control can be achieved in the future.

A comparison of the oxygen consumption rates for the two fermentations shows that, after a similar development in oxygen consumption rate up to 50 h, a sharp decline occurs when evaporative cooling was applied (Figure 8a).

Similar behavior could be observed with glucosamine measurements, which were used as an indirect estimate for fungal biomass (Figure 8b). These results can be explained by dehydration of the solid substrate caused by evaporative cooling, which eventually leads to a decrease in water activity that affects the growth rate and thus the oxygen consumption rate.

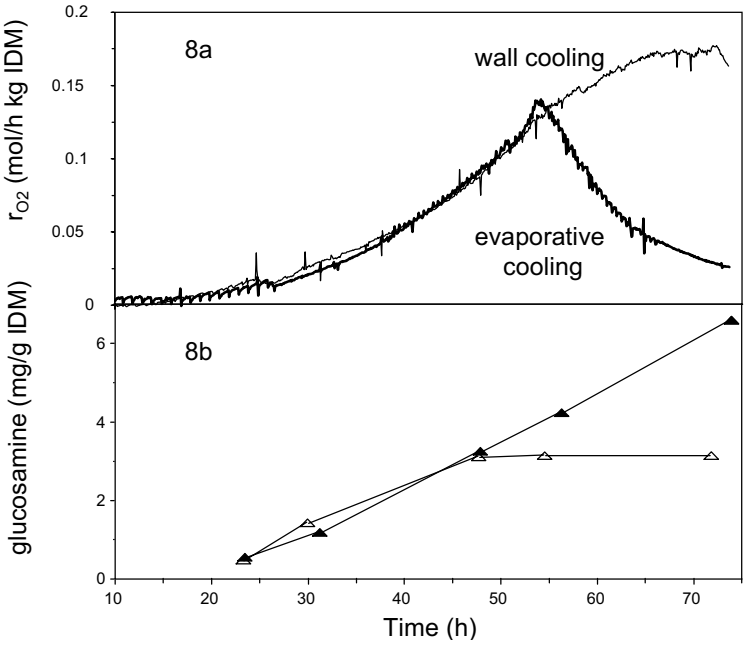

Figure 8. (a)The course of the oxygen consumption rate for a cultivation of *Aspergillus oryzae* with evaporative dooling (thick line) and with wall cooling (thin line). (b) Glucosamine measurements for the fermentation with evaporative cooling (△) and wall cooling (▲).

This is clearly supported by the moisture-content profile of the two fermentations and the measured water activities (Figure 9); that is, after 50-h fermentation, the moisture content dropped below 0.5 kg w/kg DM in the case of evaporative cooling. At that time, the water activity was estimated at 0.95 (linear interpolation between measurements) and it decreased rapidly thereafter. From radial-growth-rate data as a function of water activity for *A. oryzae* (Gibson *et al.*, 1994), the growth rate was estimated to be 70% of its maximum value at a_w=0.95. In other words, the observed decline in oxygen-consumption rate can be explained by a decrease in water activity. For the case of wall cooling, the water content and water activity remained constant ($a_w \approx$ 0.964 to 0.968) between 40- and 80-h fermentation times (Figure 9).

The observation that the oxygen consumption rate is only significantly affected after dehydration below 0.5 kg/kg dry matter (DM) also follows from the water-desorption isotherm of wheat grains. The water-desorption isotherm shows that below 0.5 kg/kg DM, water activity rapidly declines, and that, above 0.5 kg/kg DM, water activity remains almost constant at 0.995 (Figure 10). However, it should be noted that the moisture content of the solid substrate itself during fermentation is probably lower than the measured overall moisture content, because biomass, as part of the wheat grain, probably has a higher moisture content than the overall average (Larroche *et al.*, 1992; Oriol *et al.*, 1988).

In summary, evaporative cooling dehydrates the solid substrate, which eventually leads to a decrease in water activity that affects the growth and thus the oxygen consumption rate. Therefore, water addition becomes necessary when evaporative cooling is applied.

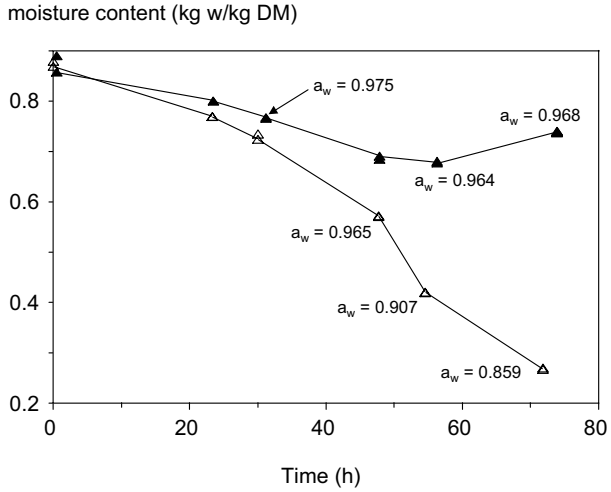

Figure 9. The course of the moisure content of wheat grains during cultivation of *Aspergillus oryzae* with evaporative cooling (△) and with wall cooling (▲).

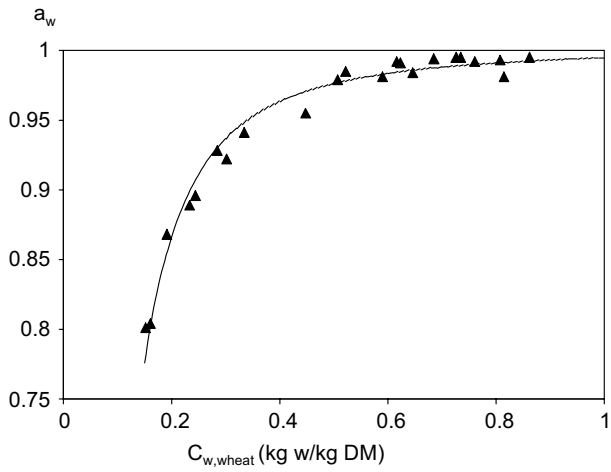

Figure 10. Water-desorption isotherm of moisturized and autoclaved wheat grains at 35ºC.

Validation of the enthalpy balance

Moisture-content control in SSF is difficult as there is no direct on-line measurement for the moisture content of the solid substrate. Therefore, a control strategy should be based on estimating the water balance and dry-weight variations in the system. For these estimations, reliable on-line measurements are a necessity. For example, air flow rate and dewpoint temperature of the effluent air determine the amount of water evaporated, which is the most important term in the water balance but also in the enthalpy balance. The aim was to validate the enthalpy balance in order to check the reliability of all measurements in the system that can be used later for moisture-content control. Furthermore, validation of the enthalpy balance will demonstrate that temperature control can be based on the enthalpy balance, as proposed in this study. The enthalpy balance was validated for the case of evaporative cooling.

On-line measurements and constants from literature were used to calculate the different terms in the enthalpy balance. The only unknown parameter that had to be determined experimentally was $\alpha_{ov} \cdot A$. This parameter (4.72 $W \cdot °C^{-1}$) was determined by fitting all results of the experiment in the 35-L bioreactor in which wall cooling was applied.

Figure 11 shows the absolute values of the individual terms in the enthalpy balance (equation 3). The summation of the individual terms should equal zero from 36 to 46 hours of fermentation in which temperature was adequately controlled, but a small average deviation of 2.4 ± 0.23 W (95% confidence) was found. Despite small deviations, the enthalpy balance is reasonably accurate and the applied on-line measurements can thus be used for moisture-content control. The obtained accuracy is certainly high enough if we take into account the water-desorption isotherm (Figure 10), which shows that a sufficiently high and virtually constant water activity can be maintained over a wide moisture content range above 0.5 kg w/kg dry substrate.

CONCLUSION

Aspergillus oryzae was successfully cultivated under continuous agitation in a new mixed bioreactor for SSF in which temperature could be adequately controlled by evaporative and wall cooling. The bioreactor performance approached the performance

of an ideal one-layer static system and was comparable to a well-controlled, small, packed-bed bioreactor from the literature.

Scale-up calculations for this mixed bioreactor demonstrated the importance of evaporative cooling in addition to wall cooling for cultivating *A. oryzae* on a large scale. Furthermore, it was demonstrated that water addition becomes necessary when evaporative cooling is applied. To assure homogeneous water addition and evaporation, the use of mixed bioreactors is a necessity. This research illustrates that, given a suitable solid substrate, mixing offers advantages, including improved bioreactor performance and facilitated scale-up of solid-state fermentation.

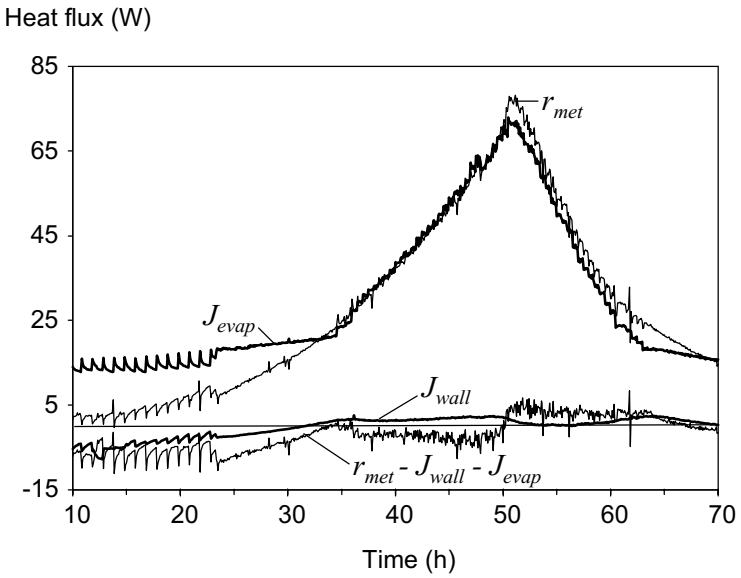

Figure 11. The course of the individual terms in de enthalpy balance during fermentation of *Aspergillus oryzae* on wheat grains in which the temperature was controlled by evaporative cooling.

ACKNOWLEDGEMENTS

The authors thank Dr. A.J.B. van Boxtel for the improvements made to the control strategy and G.M. Westhoff and J.C.A. Blonk for their contribution to this research program. We also thank the Central Services Department "de Dreijen" for the design and construction of the horizontal paddle mixer, particularly E. Janssen, M. Schimmel and A. van Wijk. This study was financially supported by the Dutch Graduate School on Process Technology.

REFERENCES

Aidoo KE, Hendry R, Wood BJB. 1984. Mechanized fermentation systems for the production of experimental soy sauce koji. J Food Technol 19: 389-398.

Barrios-Gonzalez J, Tomasini A, Viniegra-Gonzalez G, Lopez J. 1988. Penicillin production by solid state fermentation. Biotechnol Lett 10: 793-798.

Barstow LM, Dale BE, Tengerdy RP. 1988. Evaporative temperature and moisture control in solid substrate fermentation. Biotechnol Techn 2: 237-242.

Carlsen M, Spohr AB, Nielsen J, Villadsen J. 1996 Morphology and physiology of an alpha-amylase producing strain of *Aspergillus oryzae* during batch cultivation. Biotechnol Bioeng 49: 266-276.

Durand A, Chereau D. 1988. A new pilot reactor for solid-state fermentation: application to the protein enrichment of sugarbeet pulp. Biotechnol Bioeng 31: 476-486.

Durand A, Renaud R, Maratray J, Almanza S, Diez M. 1996. INRA-Dijon reactors for solid state fermentation: Designs and applications. J of Sci & Ind Res 55: 317-332.

Fernandez M, Perezcorrea JR, Solar I, Agosin E. 1996. Automation of a solid substrate cultivation pilot reactor. Bioproc Eng 16: 1-4.

Gibson AM, Baranyi J, Pitt JI, Eyles MJ, Roberts TA. 1994. Predicting Fungal Growth: The Effect of Water Activity on *Aspergillus Flavus* and Related Species. Int J Food Microbiol 23: 419-431.

Gupte A, Madamwar D. 1997. Solid state fermentation of lignocellulosic waste for cellulase and beta-glucosidase production by cocultivation of *Aspergillus ellipticus* and *Aspergillus fumigatus*. Biotechnol Prog 13: 166-169.

Gutierrez-Correa M, Tengerdy RP. 1998. Xylanase production by fungal mixed culture solid substrate fermentation on sugar cane bagasse. Biotechnol Lett 20: 45-47.

Hang YD, Woodams EE. 1998. Production of citric acid from corncobs by *Aspergillus niger*. Bioresource Technol 65: 251-253.

Kotwal SM, Gote MM, Sainkar SR, Khan MI, Khire JM. 1998. Production of alpha-galactosidase by thermophilic fungus *Humicola* sp. in solid-state fermentation and its application in soyamilk hydrolysis. Proc Biochem 33: 337-343.

Larroche C, Theodore M, Gros JB. 1992. Growth and sporulation behavior of *Penicillium roquefortii* in solid substrate fermentation: effect of the hydric parameters of the medium. Appl Microbiol Biotechnol 38: 183-187.

Laukevics JJ, Apsite AF, Viesturs UE, Tengerdy RP. 1984. Solid-substrate fermentation of wheat straw to fungal protein. Biotechnol Bioeng 26: 1465-1474.

Lekha PK, Lonsane BK. 1994. Comparative titers, location and properties of tannin-acyl-hydrolase produced by *Aspergillus niger* PKL 104 in solid-state, liquid surface and submerged fermentations. Proc Biochem 29: 497-503.

Lide DR. 1993. CRC Handbook of chemistry and physics. 74th edition. CRC Press Inc., Boca Raton.

Lonsane BK, Ghildyal NP, Budiatman S, Ramakrishna SV. 1985. Engineering aspects of solid-state fermentation. Enz Microbiol Technol 7: 258-265.

Lonsane BK, Saucedo-Castaneda G, Raimbault M, Roussos S, Viniegra-Gonzalez G, Ghildyal NP. 1992. Scale-up strategies for solid-state fermentation. Proc Biochem 27: 259-273.

Maldonado MC, de Saad AM. 1998. Production of pectinesterase and polygalacturonase by *Aspergillus niger* in submerged and solid-state systems. J Ind Microbiol Biotechnol 20: 34-38.

Mitchell DA, Lonsane BK. 1992. Definition, characteristics and potential. In: HW Doelle, DA Mitchell and CE Rolz (eds.) Solid Substrate Cultivation, Elsevier Science Publishers, London.

Narahara H, Koyama Y, Yoshida T, Atthasampunna P. 1984. Control of water content in a solid-state culture of *Aspergillus oryzae*. J Ferment Technol 62: 453-459.

Narahara H, Koyama Y, Yoshida T, Pichangkura S, Ueda R, Taguchi H. 1982. Growth and enzyme production in a solid-state culture of *Aspergillus oryzae*. J Ferment Technol 60: 311-19.

Ohnishi K, Yoshida Y, Sekiguchi J. 1994. Lipase production of *Aspergillus oryzae*. J Ferment Bioeng 77: 490-495.

Ohno A, Ano T, Shoda M. 1992. Production of antifungal antibiotic, iturin in a solid-state fermentation by *Bacillus subtilis* NB22 using wheat bran as a substrate. Biotechnol Lett 14: 817-822.

Oriol E, Raimbault M, Roussos S, Viniegra-Gonzales G. 1988. Water and water activity in the solid-state fermentation of cassava starch by *Aspergillus niger*. Appl Microbiol Biotechnol 27: 498-503.

Pandey A. 1991. Aspects of fermentor design for solid-state fermentations. Proc Biochem 26: 355-361.

Roels JA. 1983. Energetics and kinetics in biotechnology. Elsevier Biomedical Press, Amsterdam.

Ryoo D, Murphy VG, Karim MN, Tengerdy RP. 1991. Evaporative temperature and moisture control in a rocking reactor for solid substrate fermentation. Biotechnol Techn 5: 19-24.

Sargantanis J, Karim MN, Murphy VG, Ryoo D, Tengerdy RP. 1993. Effect of Operating Conditions on Solid-Substrate Fermentation. Biotechnol Bioeng 42: 149-158.

Saucedo-Castaneda G, Gutierrez-Rojas M, Bacquet G, Raimbault M, Viniegra-Gonzalez G. 1990. Heat transfer simulation in solid substrate fermentation. Biotechnol Bioeng 35: 802-808.

Saucedo-Castaneda G, Lonsane BK, Raimbault M. 1992. Maintenance of heat and water balances as a scale-up criterion for the production of ethanol by *Schwanniomyces castellii* in a solid-state fermentation system. Proc Biochem 27: 97-107.

Sekar C, Balaraman K. 1998. Optimization studies on the production of cyclosporin A by solid state fermentation. Bioproc Eng 18: 293-296.

Stuart DM, Mitchell DA, Johns MR, Litster JD. 1999. Solid-state fermentation in rotating drum bioreactors: Operating variables affect performance through their effects on transport phenomena. Biotechnol Bioeng 63: 383-391.

Torrado A, Gonzalez MP, Murado MA. 1998. PH regulation in solid state culture through the initial ratio between oxidized and reduced sources of nitrogen. A model applicable to the amylase production by *Aspergillus oryzae*. Biotechnol Techn 12: 411-415.

Xue M, Liu D, Zhang H, Qi H, Lei Z. 1992. A pilot process of solid-state fermentation from sugarbeet pulp for the production of microbial protein. J Ferment Bioeng 73: 203-205.

Chapter 4

Model for on-line moisture-content control

F.J.I. Nagel, J. Tramper, M.S.N. Bakker, A. Rinzema.
Biotechnology and Bioengineering (2001), 72: 231-243

SUMMARY

In this study we describe a model that estimates the extracellular (nonfungal) and overall water contents of wheat grains during solid-state fermentation (SSF) with *Aspergillus oryzae*, using on-line measurements of oxygen, carbon dioxide, and water vapor in the gas phase. The model uses elemental balances to predict substrate dry matter losses from carbon dioxide measurements, and metabolic water production, water used in starch hydrolysis, and water incorporated in new biomass from oxygen measurements. Water losses caused by evaporation were calculated from water vapor measurements. Model parameters were determined using an experimental membrane-based model system, which mimicked the growth of *A. oryzae* on the wheat grains and permitted direct measurement of the fungal biomass dry weight and wet weight. The measured water content of the biomass depended heavily on the moisture content of the solid substrate and was significantly lower than the estimated values reported in the literature. The model accurately predicted the measured overall water content of fermenting solid substrate during fermentations performed in a 1.5-L scraped drum reactor and in a 35-L horizontal paddle mixer, and is therefore considered validated. The model can be used to calculate the water addition required to control the extracellular water content in a mixed solid-state bioreactor for cultivation of *A. oryzae* on wheat.

INTRODUCTION

The growth of microorganisms on solid substrates under conditions of limited water availability is called solid-state fermentation (SSF). It can be used for the production of a wide range of biotechnological products such as spores (Whipps and Gerlagh, 1992), enzymes (Pandey, 1992) and fine chemicals (Shankaranand and Lonsane, 1994). The results presented here are part of a research project aiming to develop large-scale SSF bioreactors with simultaneous control of temperature and moisture content.

One of the main scale-up problems is the removal of heat generated by the metabolic activity of the microorganisms (Saucedo-Castenada *et al.*, 1992). In large-scale mixed bioreactors, evaporative cooling has to be applied due to limited heat removal through the bioreactor wall (Sargantanis, 1993; Nagel *et al.*, 2001). Evaporative cooling results

in large moisture losses and should therefore be combined with water addition to assure moisture-content control (Lonsane *et al.*, 1992; Ryoo *et al.*, 1991). For homogeneous water addition during cultivation, a continuously mixed bioreactor was developed (Nagel *et al.*, 2001). In the present article, a model is presented for automatic moisture-content control during SSF with *Aspergillus oryzae* grown on whole wheat grains. *A. oryzae* is a commonly used fungus for SSF (Pandey, 1992) and wheat grains are an ideal substrate for use in mixed bioreactors (Nagel *et al.*, 2001).

Process design and control for SSF must take into account the availability of water, as was clearly demonstrated in several previous studies (Oriol *et al.*, 1988; Larroche and Gros, 1992; Larroche *et al.*, 1992, Nagel *et al.*, 2001). Besides the evaporation needed for cooling, an important reason is the incorporation of water into new microbial cells. Oriol and coworkers (1988) showed that fungal growth can be hampered by limited water availability, even when the total water content of the fermenting mass increases in time. Their calculations showed that gradually increased water content is present inside the fungal cells and the residual water outside the cells, which determines the water availability or water activity of the substrate matrix, becomes limiting. Literature indicates that fungal mycelium grown in SSF contains approximately 3 kg water per kilogram cell dry weight (Oriol *et al.*, 1988; Larroche *et al.*, 1992). Taking this result, and using the model presented in what follows, we estimated that the water requirement for new cells would be ca. 45% of that for evaporative cooling. Furthermore, Larroche and Gros (1992) reported that the water content of mycelium of *Penicillium roquefortii* varies during cultivation. Therefore, experimental verification was warranted for this important water requirement. Preliminary experiments indicated that the intracellular water content of *A. oryzae* grown on wheat flour varies with the initial water content of the substrate matrix. A membrane model system was developed that mimics the growth conditions on wheat grains, which enabled us to analyze the substrate matrix and the fungal biomass separately.

In the literature, models have been described that predict the moisture content during SSF (Narahara *et al.*, 1984; Sargantanis *et al.*, 1993). These models do not distinguish between intracellular water (fungal biomass) and extracellular water (substrate matrix). In this article, we developed a model that allows calculation of the overall water content as well as the extracellular water content.

This model can be incorporated in an on-line control strategy aimed at maintaining a sufficiently high extracellular water content. Ideally, such a control strategy should aim at maintaining a sufficiently high water activity, but we decided not to include calculations of water activity, for several reasons. First, the desorption isotherm of the wheat used as substrate (Nagel *et al.*, 2001) indicated that the water activity remains very close to a_w=1 as long as the water content of the wheat matrix is > 0.5 kg per kilogram dry matter. Second, water activity may also be influenced by accumulation of monosaccharides, oligosaccharides, or other low-molecular-weight hydrolysis products. Incorporation of their effects in the calculations would require much more detailed information on the kinetics of hydrolysis and uptake reactions than is currently available. This would probably also make the control model too complex for on-line use.

Our model predicts the extracellular water content as well as the overall moisture content from on-line measurements of oxygen, carbon dioxide and moisture content of the air. The water balance in the model incorporates uptake of intracellular water, metabolic water production, water used for hydrolysis of starch, and evaporated water. Several attempts have been described in literature to estimate the intracellular water content of biomass indirectly (Larroche and Gros, 1992; Larroche *et al.*, 1992). We measured the intracellular water content of biomass directly using a model system, that can mimic the growth of *A. oryzae* on wheat grains and allows separate analysis of biomass and substrate matrix. We used elemental balances to estimate metabolic water production and loss of dry solid substrate using three experimentally determined yield coefficients. A systematic method (Wang and Stephanopoulos, 1983) was employed to identify possible gross measurement errors in the measured yield coefficients, and maximum-likelihood techniques were applied to obtain a consistent set of adjustments for the experimental data.

The model was validated using experiments in a 1.5-L scraped-drum reactor (Oostra *et al.*, 2000) and a 35-L horizontal paddle mixer (Nagel *et al.*, 2001). Relatively small deviations were observed between measured and predicted overall moisture contents.

A wide control range was found for the moisture content of the solid substrate. This control range followed from a combination of colony-growth-rate data (Gibson *et al.*, 1994) and the water desorption isotherm for wheat grains (Nagel *et al.*, 2001). In

summary, it may be stated that the proposed model is accurate enough to control the extracellular water content during SSF.

MODEL DEVELOPMENT

Moisture-content control during SSF is difficult because a direct on-line measurement of the overall moisture content is problematic. Furthermore, the extracellular-moisture content cannot be measured off-line because the fungal biomass cannot be separated from the substrate particles. A stoichiometric model is therefore developed that can be used for automatic moisture-content control during SSF. The model uses on-line measurements of O_2, CO_2, and dew-point in the effluent air, to predict the extracellular moisture content and the overall moisture content of the grains (Figure 1). The model is based on elemental balances and does not contain kinetic relations. Kinetics are given by the measured oxygen consumption rate. All yield coefficients in the model were determined using elemental balances and measured yields.

The reaction equation for growth of *Aspergillus oryzae* on glucose and wheat protein is:

$$Y_{S/O2}CH_2O + O_2 + Y_{N/O2}CH_{1.98}O_{0.63}N_{0.26} \rightarrow Y_{X/O2}CH_{1.72}O_{0.52}N_{0.17} + Y_{CO2/O2}CO_2 + Y_{W/O2}H_2O \quad (1)$$

in which

$Y_{S/O2}$	=	yield coefficient for substrate (*S*) on oxygen	[Cmol·mol^{-1} O_2]
$Y_{N/O2}$	=	yield coefficient for protein (*N*) on oxygen	[Cmol·mol^{-1} O_2]
$Y_{X/O2}$	=	yield coefficient for biomass (*X*) on oxygen	[Cmol·mol^{-1} O_2]
$Y_{CO2/O2}$	=	yield coefficient for carbon dioxide on oxygen	[mol·mol^{-1} O_2]
$Y_{W/O2}$	=	yield coefficient for water (*W*) on oxygen	[mol·mol^{-1} O_2]

The elemental composition of the biomass was assumed to be $CH_{1.72}O_{0.52}N_{0.17}$, which is the average biomass composition of *Aspergillus niger* (Nielsen and Villadsen, 1994). The elemental composition of protein ($CH_{1.98}O_{0.63}N_{0.26}$) was calculated from an average amino-acid composition of five different wheat-grain varieties (Shoup *et al.*, 1966). Production of α-amylase by *A. oryzae* was neglected because the ratio between

α-amylase and biomass was reported to be only 0.019 Cmol/Cmol (Agger *et al.*, 1998).

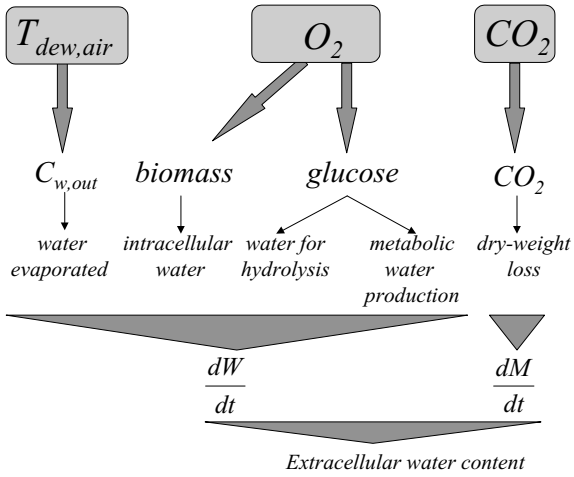

Figure 1. A schematic representation of the model used to estimate the extracellular water content during solid-state fermentation from on-line measurements (oxygen, carbon dioxide, and dewpoint temperature).

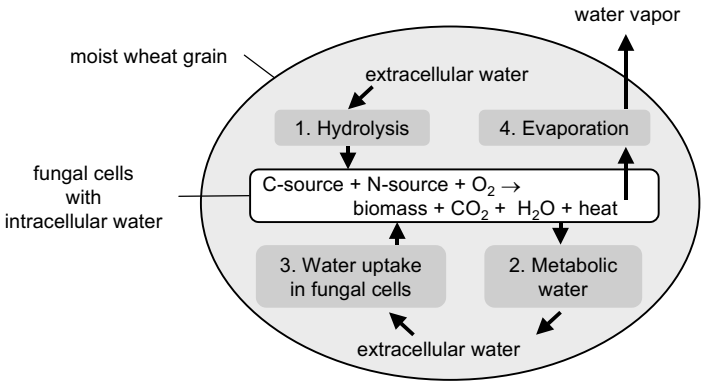

Figure 2. A schematic overview of the four different contributions in the water balance during solid-state fermentation on wheat grains. In order of increasing magnitude: (1) water for starch hydrolysis; (2) metabolic-water production; (3) water uptake in new biomass; and (4) water evaporation.

The water balance has four contributions (Figure 2):

1. Water needed for starch hydrolysis
2. Metabolic water production
3. Uptake of intracellular water during biomass production.
4. Water evaporation as a consequence of metabolic-heat production

All four contributions are taken into account in the mass balance for extracellular water (equation 2). In this balance, biomass production and substrate consumption are calculated from the measured oxygen consumption rate. In the following equations, all rates are production rates; consumption rates have a negative value.
Assuming that the air in the bioreactor is in steady state, the biomass has a constant water content, and accumulation of glucose or oligosaccharides is negligible, the balance for extracellular water is:

$$\frac{dW_{wh}}{dt} = F_{air} \cdot \left(C_{Win} - C_{Wout}\right) + X_{W,X} \cdot Y_{X/O2} \cdot r_{O2} \cdot Mw_X - Y_{W/O2} \cdot r_{O2} \cdot Mw_W + Y_{hyd} \cdot Y_{S/O2} \cdot r_{O2} \qquad [kg \cdot s^{-1}] \qquad (2)$$

in which

W_{wh}	=	weight extracellular water in wheat		[kg]
r_{O2}	=	oxygen production rate		[mol·s^{-1}]
F_{air}	=	volumetric gas flow at 273 K and 1.013·10^5 Pa		[m^3 dry air·s^{-1}]
C_W	=	water concentration in air recalculated to 273 K and 1.013·10^5 Pa		[kg·m^{-3} dry air]
$X_{W,X}$	=	water content of biomass		[kg·kg^{-1} DW]
Mw_w	=	18·10^{-3}	molecular weight water	[kg·mol^{-1}]
Mw_X	=	24.42·10^{-3}	molecular weight biomass	[kg·Cmol^{-1}]
Y_{hyd}	=	0.003	water needed to hydrolyze starch	[kg·Cmol^{-1} S]

The yield coefficients for starch and protein were used to relate dry-weight losses to the measured CO_2 production:

$$\frac{dM_{wh}}{dt} = -\left(\frac{Y_{S/O2}}{Y_{CO2/O2}} \cdot Mw_S + \frac{Y_{N/O2}}{Y_{CO2/O2}} \cdot Mw_N \right) \cdot r_{CO2} \qquad [kg \cdot s^{-1}] \qquad (3)$$

in which

M_{wh}	=	weight of wheat dry matter		[kg]
Mw_N	=	$27.63 \cdot 10^{-3}$	molecular weight protein	[kg·Cmol^{-1} N]
Mw_S	=	$30 \cdot 10^{-3}$	molecular weight starch	[kg·Cmol^{-1} N]
r_{CO2}	=	carbon dioxide production rate		[mol·s^{-1}]

The extracellular water content ($X_{W,wh}$) in time is then given by :

$$X_{W,wh}(t) = \frac{W_{wh}(t)}{M_{wh}(t)} \qquad [kg \cdot kg^{-1} \text{ DM}] \qquad (4)$$

The extracellular water content -that is, water outside the mycelium- can be estimated with the model, but it cannot be measured in the fermentations with grains. To validate the model, a prediction of the overall moisture content is necessary. The amounts of biomass dry weight and intracellular water are needed to calculate the overall moisture content of a fermented wheat grain; these are calculated from:

$$\frac{dM_X}{dt} = -Y_{X/O2} \cdot r_{O2} \cdot Mw_X \qquad [kg \cdot s^{-1}] \qquad (5)$$

$$W_X(t) = X_{W,X} \cdot M_X(t) \qquad [kg] \qquad (6)$$

in which

M_X	=	weight of biomass dry matter	[kg]
W_X	=	weight of intracellular water	[kg]

The overall moisture content of the cultivated wheat grains ($X_{W,ov}$) becomes:

$$X_{W,ov}(t) = \frac{W_{wh}(t) + W_X(t)}{M_{wh}(t) + M_X(t)} \qquad [\text{kg}\cdot\text{kg}^{-1}\ \text{DM}] \qquad (7)$$

MATERIALS AND METHODS

Micro-organism and inoculation

Aspergillus oryzae CBS 570.65 was obtained from Centraal Bureau voor Schimmelcultures (Baarn, NL). The preparation of a sporangiospore suspension has been described previously (Nagel *et al.*, 2001). Glycerol (20% [w/v] final concentration) was added to the spore suspension, which was stored at -80 °C for up to 3 months in 1-mL cryovials (Greiner, Germany) and 125-mL plastic bottles (Model 2105-0004, Nalgene, UK). The 125-mL plastic bottles contained 43.5 mL spore suspension and 16.5 mL of glycerol.

One 125-mL plastic bottle was used to inoculate the horizontal paddle mixer; the inoculation procedure has been described elsewhere (Nagel *et al.*, 2001). For experiments in the scraped drum reactor, three cryovials and 2 mL of peptone physiological salt solution were aseptically sprayed using a tube atomizer (Desaga, Germany) over 300 g of moisturized wheat grains. The contents of two 125-mL plastic bottles and 100 mL of peptone physiological salt solution were used for inoculation of the membrane model system.

Solid substrate

A single batch of wheat grains of commercial origin (Blok, Woerden, NL) was stored at 10°C (initial moisture content 0.12 kg/kg DM) and used for all experiments.

Wheat dough

Whole wheat grains were milled in a mill (Retsch, NL). Milled wheat grains and distilled water were mixed to obtain the desired moisture content of the wheat dough. At moisture contents > 1.5 kg/kg DM wheat, agar (final concentration 0.04 kg/kg total) was used to give sufficient strength to the wheat dough. It was not possible to prepare homogeneous dough below a moisture content of 0.8 kg w/kg DM.

Wheat grains

Whole wheat grains were soaked for 2.5 h in excess water at 60°C to give a final moisture content of 0.87 kg w/kg DM. After sieving, the soaked grains were autoclaved (1.5 h, 121°C).

Cultivation methods

Membrane model system

All parts of the membrane model system (Figure 3) were manufactured by the Mechanical workshop at Wageningen University. The wheat dough was transferred into a sausage maker (Figure 3b), autoclaved (1.5 h, 121 °C) and cooled down to room temperature. Wheat disks (4.5 cm diameter, 0.5 cm height) were prepared in a laminar flow cabinet, using a previously sterilized wire cutter. Each wheat disk was weighed and placed in a previously autoclaved polypropylene (PP) dish (Figure 3a). A sterile 0.45 µm polyamide membrane (Schleicher & Schuell, NL17 ST) was applied on the disk. A glass cylinder was placed on top of the membrane and the cylinder was closed with a lid of a petri dish (Greiner, ø = 4.5 cm).

For each cultivation, 20 PP dishes were prepared and 19 were inoculated by spraying a spore suspension onto the membrane using a moving-belt device (Mechanical workshop, Wageningen University, NL). One PP dish remained uninoculated in order to measure possible evaporation losses and to check for sterility.

Three PP dishes without lids were placed in the middle of a closed jar, which contained a layer of water on the bottom to prevent desiccation, in order to measure O_2 consumption and CO_2 production. The closed jar was placed in a temperature-controlled cabinet at 35°C. The closed jar was aerated (15 L/h at 273 K, $1.013 \cdot 10^5$ Pa) using a mass flow controller (Brooks Instruments BV, NL). To accurately determine CO_2 production, CO_2 was removed from the inlet air using a 1.5 M NaOH solution. The inlet air was further humidified (relative humidity 94.6% at 35°C) using a temperature-controlled water column (height 40 cm; diameter 10 cm) filled with Raschig rings (height 1 cm, diameter 5 mm). The inlet air was filter sterilized using a 0.2 µm hydrophobic membrane (Acros 50, Gelman, USA). The effluent air was first analyzed for dewpoint (DEWMET SD, Michell Instruments Ltd., UK), and then dehumidified (16% relative humidity at 30°C) using a condenser before it was analyzed for CO_2 and O_2 (see later). The remaining PP dishes were placed in a partially

opened box (25L) filled with a layer of water to prevent evaporation losses, which was placed in the same temperature-controlled cabinet as the closed jar. The duration of these cultivations was usually 80 h.

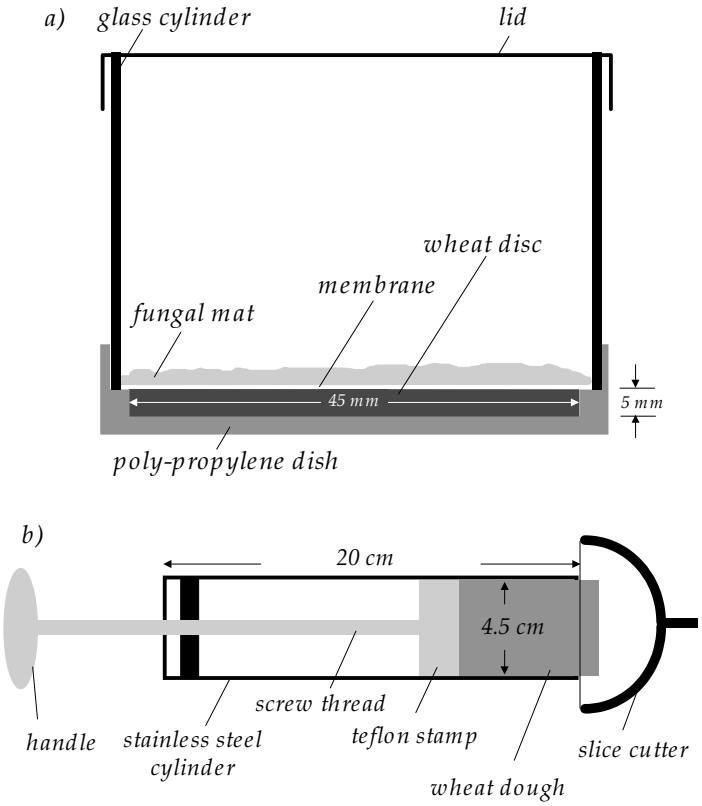

Figure 3. (a) Membrane model system for solid-state fermentation on wheat grains used to measure the moisture content of biomass and all other model parameters. (b) Apparatus used to aseptically prepare wheat disks for the membrane model system.

Scraped Drum Bioreactor (1.5 L)

The Scraped Drum Reactor (SDR, length 20 cm, diameter 5 cm, Figure 4) consisted of a glass cylinder, sealed on both sides with a stainless-steel flange. A hollow rotating shaft was mounted between the flanges. One end of the shaft was connected to the motor; the other end was used for the air inlet. A hollow scraper, mounted in the middle of the shaft, scraped along the wall to achieve radial mixing. Perforations in the scraper allowed sufficient air distribution in the reactor. The SDR was filled with 100 g wet inoculated wheat grains and placed in a temperature-controlled cabinet. The SDR was aerated (90 L/h at 273 K, $1.013 \cdot 10^5$ Pa) using a mass flow controller (Brooks Instruments BV, NL) and mixed continuously (1 rpm). The air-conditioning system for these experiments was the same as described earlier.

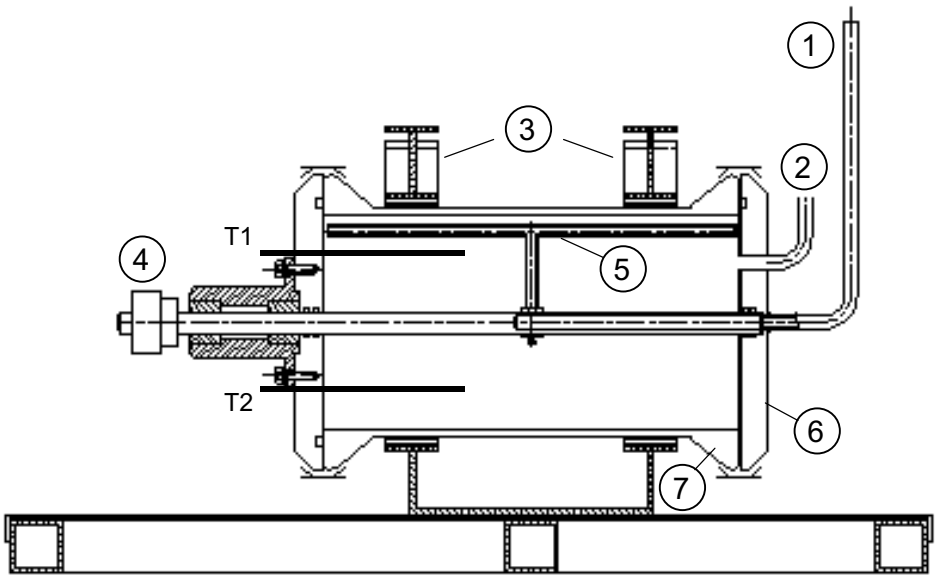

Figure 4. Schematic diagram of 1.5-L scraped drum reactor: (1) air inlet; (2) air outlet; (3) reactor fixings; (4) drive shaft; (5) scraper with fine holes for air distribution; (6) steel side plate; (7) glass cylinder. T1 and T2 are temperature sensors.

Horizontal Paddle Mixer (35 L)

Two cultivations in the horizontal paddle mixer were used to validate the model. A detailed description of the bioreactor and auxiliary equipment is given elsewhere (Nagel *et al.*, 2001). *A. oryzae* was cultivated on 8 kg of moistened wheat grains (moisture content 0.87 kg w/kg DM) for 3 days. The temperature of the solid substrate was maintained at 35°C using evaporative cooling for one cultivation and wall cooling for the other cultivation.

Sampling

Membrane model system

Twice a day, two PP dishes were removed for measurements. The biomass was pulled from the membrane and the membrane was easily peeled from the wheat-dough disk. The wet weights of biomass and wheat disk were recorded. Virtually complete recovery of biomass and dough was possible and virtually nothing adhered to the PP dish or membrane. Two grams of wheat dough from one PP dish was used to determine its water activity before it was transferred into a sample bottle and stored at -20°C for further analysis of glucose. The 2 g of wheat dough from the other PP dish was transferred directly into the sample bottle. The moisture content was determined for the remaining wheat dough and wet biomass.

Scraped Drum Reactor (1.5 L)

Three hunderd grams of inoculated wheat grains was prepared for this cultivation and 100 g of it was used to determine the initial moisture content and the initial concentration of total glucose. This initial moisture content was used to calculate the initial amounts of water and dry matter in the SDR. No samples were taken during cultivation. Instead, the whole bioreactor content was used to determine the final amounts of water and dry matter. Five grams was used to measure the glucosamine content and total glucose concentration.

Horizontal Paddle Mixer (35 L)

Twice a day during the fermentation, a sample (± 30 g) was taken from the bioreactor. Moisture content and water activity were determined immediately after sampling, as

described later. Approximately 5 gram of wheat grains was transferred into a sample bottle and stored (-20 °C) for further analysis of glucosamine and glucose.

Analysis

Moisture content & Water activity

The moisture content of biomass, wheat dough, and wheat grains were calculated from the weight loss after drying the sample at 80°C for 2 days in a preweighed dish. The water activity of the sample was determined in a Novasina Thermoconstanter (Type TH200, Switzerland) at 35°C.

Total and free glucose

After the sample bottle was thawed, the wheat dough or wheat grains were homogenized with water (dough : water = 1 g : 4 g) in an ultraturrax (Model L4R, Silverston, UK). For determination of total glucose, 0.1 g of this homogenate was added to 4.5 mL 13 mM phosphate buffer (pH 4.5) and 202 U amyloglucosidase (Sigma A-7255, 1 U will liberate 1.0 mg of glucose from starch in 3 min at 55 °C, pH 4.5). This mixture was continuously shaken in a water bath (Model 1083, GFL, Germany) at 55°C for 1 h and then filtered using a 0.45-µm membrane filter (Model FP 030/2, Schleicher and Schuell, Germany) after which total glucose was determined. Three milliliters of homogenate was divided into two Eppendorf tubes and centrifuged at 15300 rpm for 20 min (Model GS-15R centrigue, Beckman instruments, Germany) after which the supernatant was used to determine free glucose. Glucose was determined using a Peridochrom Glucose Kit (Cat. no. 676543, Boehringer Mannheim, Germany).

Glucosamine

The glucosamine content of dry biomass was measured over time during cultivation to convert the glucosamine measurements in wheat grains to dry biomass. The procedure for wheat-grain sample preparation and the glucosamine measurement has been described elsewhere (Nagel *et al.*, 2001). To determine the glucosamine content of dry biomass, 0.1 g dry biomass was prehydrolyzed instead of the dried pellet that was used for the glucosamine measurement in wheat grains.

CO_2 and O_2 consumption

Oxygen and carbon dioxide were analyzed using a paramagnetic O_2 analyzer (Xentra 4100, Servomex Zoetermeer, NL) and an infrared CO_2 analyzer (Servomex Series 1400). The oxygen analyzer was fitted with a second channel to measure the O_2 concentration of the outside air, in order to accurately determine O_2 consumption. Both O_2 sensors corrected the readings for pressure fluctuations.

Expression of the results

Measurements of glucose and glucosamine content obtained from the samples taken from cultivations in the membrane model system and SDR were expressed per unit weight of initial dry matter.

RESULTS AND DISCUSSION

Model parameters

Yield coefficients

A biochemical reaction equation (Equation 1) was used together with three measured yield coefficients ($Y_{X/O2}$, $Y_{S/O2}$, $Y_{CO2/O2}$; Table 1) to determine: (1) the metabolic water production ($Y_{W/O2}$), which cannot be measured directly; and (2) the yield coefficient necessary for the calculation of the dry-weight-loss factor ($Y_{N/O2}$). Due to various types of errors in measured yield coefficients, raw measurements rarely form a consistent set of data that satisfies the elemental balance equation (Equation 1). We used a systematic method (Wang and Stephanopoulos, 1983) that: (1) identified measurements that are most likely to contain gross errors; and (2) leads to a consistent set of adjustments on the experimental values. This method was used for our overdetermined system with five unknown yield coefficients, four elemental balances and three measured yield coefficients. Yield coefficients were calculated from the data of two experiments with the membrane model system. Only the data of the three dishes in the closed jars, after approximately 70 h of cultivation, were used to calculate the yield coefficients (Table 1). The measured data were not corrected for maintenance metabolism. Average yield coefficients were calculated from these values and used in the systematic method mentioned earlier. The measurement errors used in this method were estimated by

calculating the average of the two relative standard deviations obtained for each set of three measurements. These errors were 3.9%, 7.3%, 3.4% and 10.7 % for CO_2, O_2, biomass, and glucose, respectively. The value of the test function, 3.17, was compared with the chi-square (χ^2) distribution function for two degrees of freedom (two constraint equations).

Because $\chi^2_{0.9}(2) = 4.61 > 3.17$, the hypothesis test in this method was passed and we could state with 90% confidence that these yield coefficients do not contain gross errors (*i.e.* errors that are much larger than can be reasonably expected based on the measurements errors). The maximum-likelihood estimates for the yield coefficients are given in Table 1.

The yield coefficient for biomass on glucose was 0.8 Cmol/Cmol, which seems very high. It should be noted, however, that protein was also used as carbon source, and the yield of biomass on total carbon source (protein + glucose) was 0.52 Cmol/Cmol, which is in agreement with yield coefficients (0.5 to 0.6) normally found in literature (van 't Riet and Tramper, 1991).

Water content of biomass

The intracellular-water content of biomass ($X_{W,X}$) is an important parameter in the model because it is used to quantify the amounts of intracellular water in biomass and extracellular water in the solid substrate matrix ($X_{W,wh}$). Preliminary experiments indicated that $X_{W,wh}$ influenced $X_{W,X}$. Furthermore, it was uncertain if $X_{W,X}$ remained constant during cultivation. To answer these questions, a membrane model system (Figure 3) was developed that mimics the growth of *Aspergillus oryzae* on wheat grains and that allows direct measurement of $X_{W,X}$ and $X_{W,wh}$. Figure 5 shows the results of four experiments with the model system in which the initial moisture content of the wheat flour discs was 1 kg/kg DM, each with 9 to 12 separate measurements of wet and dry weight of the biomass layer. It shows that $X_{W,X}$ could be determined accurately and was constant during the whole cultivation period (80 h). Linear regression through the origin yielded $X_{W,X} = 2.08 \pm 0.0673$ kg/kg DM (± 95% confidence).

Table 1. Yield coefficients derived from measurements of two experiments (I and II) in a membrane model system. [a]

Yield coefficient	Measurement		Parameter value	Unit
	I	II		
$Y_{X/O2}$	1.06	1.16	1.16	Cmol X·mol O_2^{-1}
$Y_{S/O2}$	1.76	1.55	1.46	Cmol S·mol O_2^{-1}
$Y_{W/O2}$			1.22	mol W·mol O_2^{-1}
$Y_{CO2/O2}$	0.99	1.00	1.06	mol CO_2·mol O_2^{-1}
$Y_{N/O2}$			0.76	Cmol N·mol O_2^{-1}

[a] A systematic method (Wand and Stephanopoulos, 1983) was applied to determine the maximum-likelihood estimates for the yield coefficients used in the model.

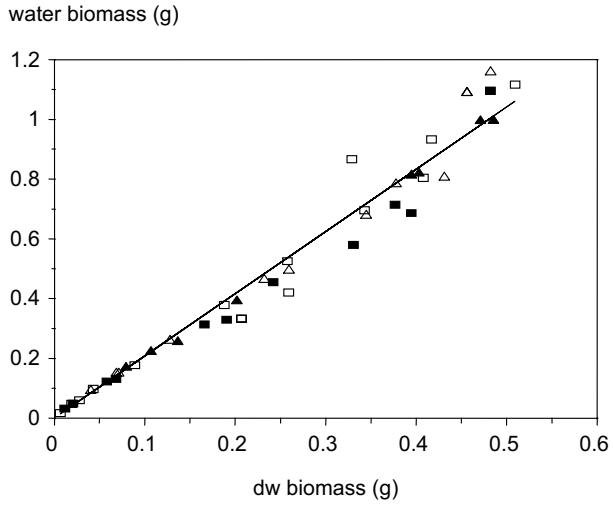

Figure 5. The amount of intracellular water in biomass of *Aspergillus oryzae* plotted against biomass dry weight for four separate experiments ($X_{W,wh}$ = 1 kg /kg DM) (▲, △, □, ■) with the membrane model system. The moisture content of fresh biomass was estimated from the straight line (——), which was determined by linear regression.

Figure 6 shows that the moisture content of the substrate ($X_{W,wh}$) influences $X_{W,X}$, especially at moisture contents > 1 kg/kg DM substrate. The influence of $X_{W,wh}$ on $X_{W,X}$ below 1 kg/kg DM was considered to be insignificant based on the 95% confidence intervals for the average values of $X_{W,X}$. It should be noted that only initial moisture levels of < 1 kg/kg are relevant for cultivation on wheat in our fermentors, because the grains are too quickly damaged by the mixing when the moisture content is higher. Therefore, the water content of biomass ($X_{W,X}$) was taken as a constant in the model for the cultivation of *A. oryzae* on wheat grains; its value was 2.08 kg/kg DM. This constant value is in accordance with results of the four experiments shown in Figure 5, in which $X_{W,wh}$ decreased during cultivation from 1 to 0.8 kg/kg DM, without affecting $X_{W,X}$.

The reasons for this dehydration of wheat dough were the water uptake for biomass production and water evaporation as a result of metabolic heat generation. No water losses were found in the PP dish that was not inoculated. We did not succeed in preparing homogeneous wheat flour discs with water contents of < 0.8 kg/kg. In some of the fermentor experiments presented in what follows, the water content of the wheat matrix dropped below 0.8 kg/kg. In these cases, model predictions were clearly extrapolations.

The value for the intracellular water content of fungal biomass used in our model is lower than the values of around 3 kg/kg DM reported previously for *Aspergillus niger* cultivated on cassava flour (Oriol *et al.*, 1988) and *Penicillium roquefortii* cultivated on buckwheat seeds (Larroche *et al.*, 1992). This may be due to differences in water content or binding of the substrates used; Figure 6 shows that wheat gave similar values. The difference may also be due to differences in measurement methods. Larroche and coworkers (1992) calculated the water content of the mycelium from the protein content and the initial water content of fermented buckwheat samples. Their calculation involved assumptions about the protein content of the biomass, water losses by evaporation and metabolic water production. Although a direct comparison is difficult, due to differences in strain and substrate, we believe that our value is more reliable because it was measured directly.

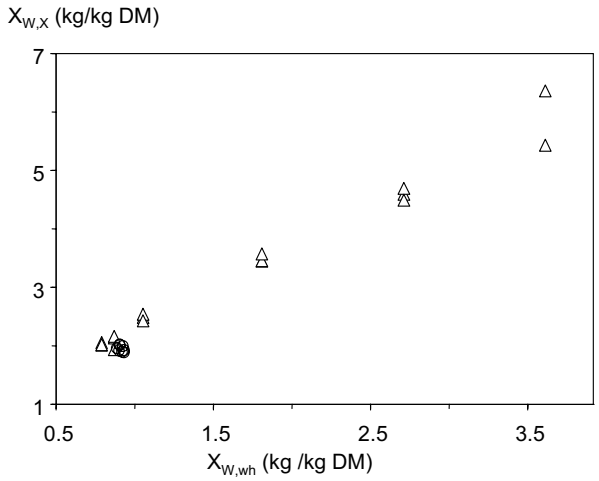

Figure 6. Intracellular moisture content of *Aspergillus oryzae* biomass ($X_{W,X}$) as a function of the moisture content of wheat dough ($X_{W,wh}$) after 60-h cultivation time, measured using a membrane model system. Samples of all four experiments from figure 5 at 60 h cultivation time are also displayed (○).

Dry-weight balance

To predict the extracellular water content $X_{W,wh}$, an accurate description of dry substrate loss is indispensable. Dry substrate loss is simply protein and starch that are consumed as given in Equation 3. For on-line dry substrate estimation, yield coefficients (Table 1) were recalculated based on CO_2:

$$Y_{S/CO2} = Y_{S/O2} / Y_{CO2/O2} = 1.38 \text{ Cmol/mol}$$

$$Y_{N/CO2} = Y_{N/O2} / Y_{CO2/O2} = 0.72 \text{ Cmol/mol}$$

so that the dry-weight loss could be easily estimated from the measured CO_2 production (r_{CO2}). Based on these yield coefficients the value in brackets in Equation 3 amounts to 61.1 g/mol CO_2. With this dry-weight loss factor, the total weight of the wheat matrix can be calculated on-line during cultivation.

Several investigators (Larroche *et al.*, 1998; Smits *et al.*, 1998) characterized dry-weight loss as the overall weight loss of the fermenting matter (substrate and biomass).

Overall dry-weight loss can be measured easily, whereas the weight of dry substrate cannot be measured directly because biomass and substrate are difficult to separate. To check the validity of our approach, the dry-weight loss factor mentioned earlier (61.1 g/mol) was recalculated to give an overall dry-weight loss factor (Equation 8), which was compared with literature data. The overall dry-weight-loss factor was 34.5 g/mol CO_2. Smits (1998) reported a ratio between overall dry-weight loss and CO_2 evolution equal to 32.6 g/mol CO_2 for *Trichoderma reesei* cultivated on wheat bran, which is very similar to our value.

$$f_{DMloss} = Y_{S/CO2} \cdot Mw_S + Y_{N/CO2} \cdot Mw_N - Y_{X/CO2} \cdot Mw_X \qquad [g \cdot mol^{-1}\ CO_2] \quad (8)$$

Our approach is applicable for any type of cultivation if a consistent biochemical reaction equation is available. Furthermore, dry-weight loss can be coupled to any compound (*e.g.* oxygen) present in the biochemical reaction equation. The approach can easily be extended with maintenance metabolism for a better description of the stationary phase.

Glucosamine content of biomass

In order to estimate biomass dry weight in wheat samples taken during cultivation in mixed bioreactors, the glucosamine content was measured. A conversion factor (G_X) is needed to convert the measured glucosamine content to biomass dry matter. Although glucosamine is a widely used indicator for biomass dry weight, two drawbacks are reported in literature: (1) the glucosamine content is dependent on the substrate and cultivation method used (Sakurai *et al.*, 1977); and (2) the glucosamine content is dependent on the age of the mycelium (Sakurai *et al.*, 1977; Arima and Uozumi, 1967). These drawbacks were circumvented by using the membrane model system so that glucosamine and biomass dry weight could be measured simultaneously during cultivation on a substrate with the same composition as that used in bioreactor cultivations. Results of three separate cultivations with the membrane model system showed an increase in the glucosamine content of biomass with cultivation time (Figure 7). The observed increase is best described by a sigmoidal curve fitted through the data:

$$G_X\left(t-\lambda\right)=44.61+\frac{43.65}{\left(1+\exp\left(-\frac{\left(\left(t-\lambda\right)-61.70\right)}{12.34}\right)\right)} \qquad [\text{mg}\cdot\text{g}^{-1}\text{dry biomass}] \quad (9)$$

in which

G_X	=	glucosamine content of biomass	[mg·g^{-1} DM]
t	=	time	[h]
λ	=	lag time	[h]

The cultivation time for experiments with the model system was corrected for a lag time so that this relation could be applied for recalculation of glucosamine measurements in the bioreactors, where the lag phase was shorter due to a higher inoculation density. In the model system, we found a linear increase of biomass dry weight in time (results not shown). In the paddle mixer, the glucosamine content of the grain increased linearly (Nagel *et al.*, 2001). The lag time was determined from the intersection of a regression line through the biomass dry matter values or glucosamine values and the time axis. It remains uncertain whether this correction of the cultivation time is legitimate. Nevertheless, this approach is believed to be the best possible way to deal with glucosamine measurements for indirect biomass dry-weight estimation and certainly no worse than other indirect biomass estimates.

Model validation

Although the model predicts both the total water content of the fermented grains and the extracellular water content of the wheat matrix, only the former can be measured. Validation of the predicted extracellular water content can only be achieved indirectly, by checking predictions for biomass and residual starch. Validation experiments were conducted with wheat grains in a scraped drum reactor and a paddle mixer.

We intend to apply a control strategy based on the model developed in this paper in the paddle mixer. The scraped drum was used, because it allows further reduction of water evaporation (more wall area available for cooling) and measurements on the whole amount of fermented grains.

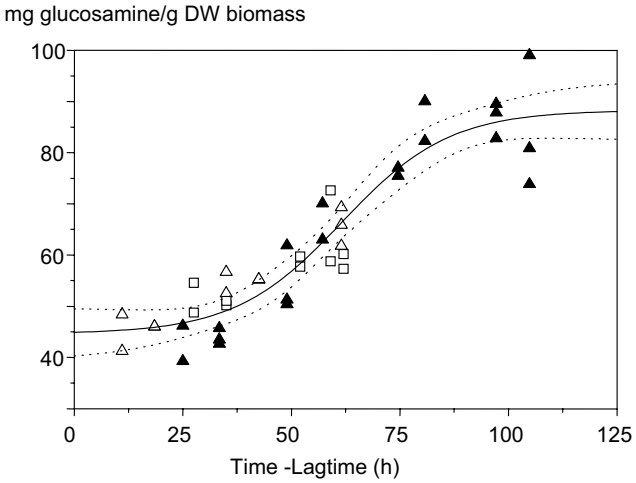

Figuur 7. Glucosamine content of dry-weight biomass as a function of the difference between cultivation and a lag time (time – lag time) in order to estimate biomass from experiments involving whole wheat grains. The different symbols represent three separate experiments. The straight line is the sigmoid fit through all measurements [Eq. (9)]. The dotted line is the 95% confidence interval for the fit.

Scraped drum reactor (1.5 L)

The model was validated with four cultivations in a 1.5-L scraped drum reactor (Table 2). These cultivations used only 100 g wet-weight grains to minimize heat generation and subsequent problems with temperature control. Nevertheless, temperature increased during these cultivations with a maximum of 37.5 °C attained in experiment B. This means that temperature did not limit fungal growth during these fermentations.

Water evaporation was minimized during these fermentations to increase the relative significance of other terms in the water balance; that is, metabolic water production and water used for hydrolysis. In this way, we tried to determine the sum of metabolic water production and water used for hydrolysis (= net water production, Table 2) from the water balance during fermentation, in order to validate the model. No samples were taken during these cultivations and, in the end, the whole bioreactor content was used

to determine final amounts of water and dry weight. A sample was taken in the end to measure glucosamine and glucose.

The model predicted the overall moisture content very well (Table 2). $X_{W,ov}$ increased during these cultivations, despite water evaporation, due to significant dry-weight losses and metabolic water production. Water evaporation could not be prevented completely, mainly due to the increasing substrate temperature during cultivation.

The prediction of metabolic water production was reasonably accurate (Table 2), as indicated by the small difference between measured and predicted net water production. The average deviation between predicted and measured final water amount was 2.1% of the initial amount of water present. Metabolic water production was significant as the amount was 20% of the water initially present after 70 hours of cultivation. The water needed to hydrolyze starch proved to be a minor term in the water balance, as expected.

The prediction of the final amount of dry matter was slightly less accurate. The average deviation between predicted and measured final amounts of dry matter was 4.2% of the initial amount of dry matter. Both deviations between predicted and measured amounts of water and dry matter can lead to a maximum deviation of the predicted moisture content equal to 6.3%.

Significant deviations were observed between model predictions and experimental data for biomass and consumed glucose (Table 2).

Model predictions became more accurate for longer cultivation times (experiments B and C) as more biomass was formed and glucose consumed. Both measurement methods (glucose and glucosamine) contain many steps to prepare the sample, which probably makes them less accurate. In addition, the conversion factor (G_X) is hampered by a large 95% confidence interval (Figure 7), and uncertainty in the lag-time correction, which may lead to a large error in the biomass determination.

Table 2. Validation of a model for the predicton of the extracellular and overall water content during solid-state fermentation of *Aspergillus oryzae* in a 1.5-L scraped drum reactor.[a]

	A (55.2 h)		B (71.1 h)		C (66.4 h)		D (49.4 h)	
Experiment (t_{end})	exp. data	Model	exp. data	Model	exp. data	Model	exp. data	Model
1. $X_{w,ov}$ t_0 [kg/kg DM]	1.02	[c]	0.95	c	1.00	c	0.96	c
2. $X_{w,ov}$ t_{end} [kg/kg DM]	1.23	1.21	1.38	1.23	1.02	0.96	0.98	0.94
3. Water t_0 [g]	53.84	c	50.53	c	52.23	c	50.41	c
4. Water evaporated [g]	2.22	c	13.90	c	22.85	c	8.08	c
5. Water t_{end} [g]	52.59	54.88	46.36	44.98	36.62	36.07	44.62	44.45
6. Metabolic water [g]		+ 4.08		+10.44		+ 8.37		+ 2.60
7. Water hydrolysis [g]		- 0.82		- 2.09		- 1.68		- 0.53
8. Net water production [g]	0.97	3.26	9.73	8.35	7.24	6.69	2.29	2.07
9. *DM* t_0 [g]	52.67	c	53.34	c	52.43	c	52.69	a
10. *DM* t_{end} [g]	42.74	45.20	33.61	36.56	36.06	37.70	45.45	47.24
11. Biomass [b] [g]	8.5 (±1.3)	5.3	11.8 (±1.8)	13.5	8.7 (±1.3)	10.8	4.3 (±0.6)	3.4
12. Substrate loss [g]		12.8		30.3		25.5		8.9
13. *DM* loss [g]	9.9	7.5	19.7	16.8	16.4	14.7	7.2	5.5
14. Glucose consumed [b] [g]	15.2 (±1.9)	8.2	23.2 (±1.7)	20.9	21.7 (±1.8)	16.8	9.9 (±2.2)	5.3
15. Intracellular water [g]		11.0		28.1		22.5		7.1
16. O_2 [g]	9.18	c	21.80	c	18.41	c	6.39	c
17. CO_2 [g]	5.97	c	15.28	c	12.25	c	3.88	c
18. $X_{w,wh}$ t_{end} [kg/kg DM]		1.10		0.73		0.50		0.85

[a] Four batch experiments were each harvested at different timepoints to validate the model.

[b] Values in parentheses indicate absolute measurement error and were calculated using a relative measurement error (15.25% for biomass, 7.33% for glucose) determined from 15 separate duplicate measurements for biomass and glucose.

[c] Experimental data in the left column of every experiment is used as input in the model. Calculations as follows: row 8, (Exp. data and model colomn), net water production = (water t_{end} – water t_0) + water evaporated [row 8= (row 5 – row 3) + row 4]; row 13 (Exp. data and model) column, DM loss = DM t_0 – DM t_{end} [row 13 = row 9 – row 10]; row 15 (Model) column, biomass (row 11) * water content biomass ($X_{W,X}$ = 2.08 kg/kg DM); row 18 (Model) column (water t_{end} – intracellular water)/(DM t_{end} – biomass) [(row 5 – row 15)/(row 10-row 11)].

Horizontal paddle mixer (35 L)

Two cultivations were done in the 35-L horizontal paddle mixer to validate the model: one cultivation in which evaporative cooling was applied and one in which mainly wall cooling was applied (Nagel *et al.*, 2001). This validation differs in two aspects from the aforementioned validation in the SDR. First, one of the cultivations better reflects the situation in which the model will be actually applied; that is temperature-controlled cultivations in which evaporative cooling is applied. Second, samples were taken during cultivation instead of measuring the whole bioreactor content in the end. The model was validated by comparing model predictions for $X_{W,ov}$ with measurements. The model predicted $X_{W,ov}$ very well throughout the whole fermentation for both cultivations (Figure 8).

Figure 9 shows the model prediction of $X_{W,wh}$ during the cultivation in which wall cooling was applied. It is impossible to measure the extracellular water content, but we can estimate such measured values ($X_{W,wh,exp}$) from biomass measurements ($M_{X,exp}$), predicted values of the overall water content ($X_{W,ov}$) and the remaining amount of wheat dry matter (M_{wh}):

$$X_{W,wh,\exp} = \frac{X_{W,ov} - \frac{M_{X,\exp}}{\left(M_{X,\exp} + M_{wh}\right)} \cdot X_{W,X}}{\left(1 - \frac{M_{X,\exp}}{\left(M_{X,\exp} + M_{wh}\right)}\right)} \qquad [\text{kg} \cdot \text{kg}^{-1}\ \text{DM}] \qquad (10)$$

Note that the remaining amount of wheat dry matter cannot be measured directly during the fermentation, and the predicted overall water content agrees well with measured values.

The calculated extracellular water content ($X_{W,wh,exp}$) has a large error, mainly due to the large measurement error (14.9%) for biomass (Table 2). The average deviation between the calculated value for $X_{W,wh,exp}$ and the model prediction for $X_{W,wh}$ between the 30- and 80-h cultivation time was 0.05 kg/kg DM.

To determine the suitability of the model for $X_{W,wh}$ control, the effect of this deviation on the growth rate was examined. For this purpose, a relation between colony growth rate and water activity, as determined by Gibson *et al.* (1994) was combined with a relation between water activity and moisture content (desorption isotherm) for

moisturized wheat grains (Nagel *et al.*, 2001), to give a relation between growth rate and moisture content:

$$u_{col} = \exp\left(-0.3915 + 5.571\sqrt{1-a_w} - 25.16\left(1-a_w\right)\right)$$

$$a_w = -2.917 + \frac{3.919}{\left(1+\left(X_{w,wh}/0.0344\right)^{-1.861}\right)} \quad [-] \qquad (11)$$

in which

u_{col} = colony growth rate of *Aspergillus oryzae* FRR1675 [mm·h^{-1}]

$X_{w,wh}$ = water content wheat grains [kg·kg DM^{-1}]

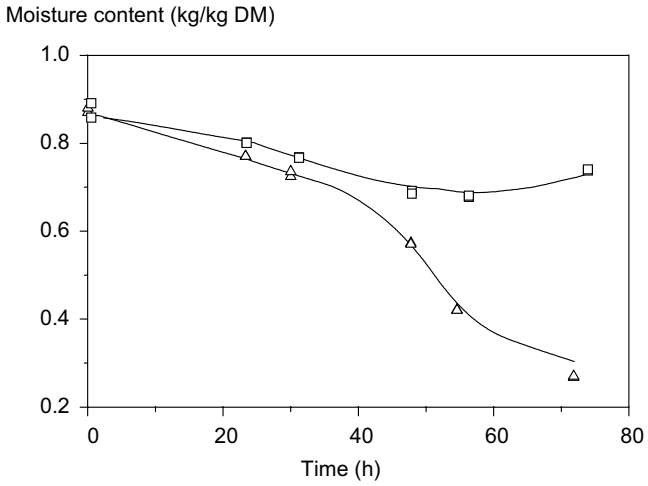

Figure 8. Model validation using two experiments in a 35-L mixed bioreactor with *Aspergillus oryzae*. Solid lines represent model predictions. Symbols represent duplicate measurements of the overall moisture content of wheat grains for an experiment with evaporative cooling (△) and wall cooling (□).

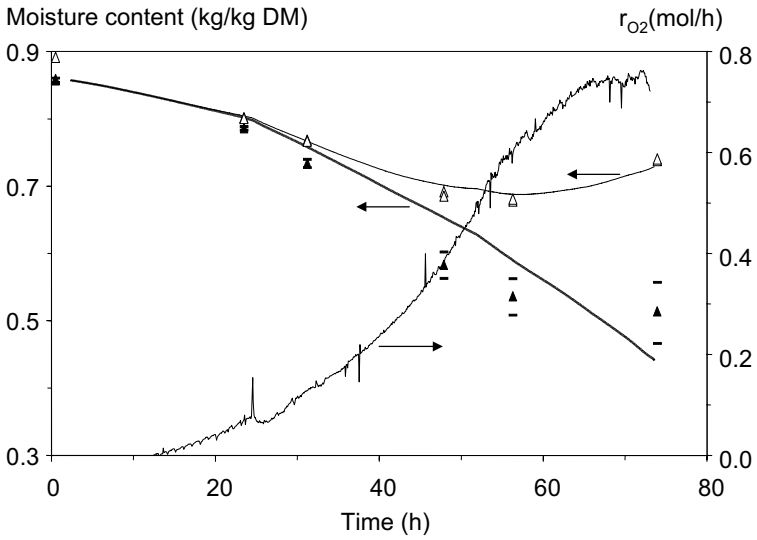

Figure 9. Model predictions of the overall water content (——) and extracellular water content (▲) and measurements of oxygen-consumption rate and overall moisture content $X_{w,ov}$ (△) are given for the cultivation in a horizontal paddle mixer in which wall cooling is applied. The extracellular water content $X_{W,wh}$ (▲) is calculated from Eq. (10). Error bars indicate absolute measurement errors.

Figure 10 shows that when $X_{W,wh}$ is controlled, for example, at 0.8 kg/kg DM, a very broad control range can be applied before the colony growth rate is affected by > 5%. The effect of a decreasing $X_{W,wh}$ on the growth rate can also be seen in Figure 9, as the oxygen-consumption rate leveled off when $X_{W,wh}$ fell below 0.5 kg/kg DM. The measured water activity at that moment was 0.965, which corresponds to 87% of the maximum colony growth rate. Although many assumptions are made when reasoning in this manner, we believe that the model is accurate enough to maintain a sufficiently high growth rate of *A. oryzae* on wheat by controlling $X_{W,wh}$. As mentioned earlier, water evaporation is a measured quantity in the model and, in these cultivations, it is the most important term in the water balance. To demonstrate the relative significance of the various terms in the water and dry-weight balance, a model prediction of absolute quantities is given for the cultivation in which wall cooling is applied (Figure 11). Evaporative cooling could not be prevented in this cultivation because water

condensation and subsequent clogging of the sterile filter had to be avoided. The pressure drop over the sterile air filter therefore limited the inlet air humidification. However, wall cooling prevailed and only about 36% of the total heat production was removed by evaporative cooling. Nevertheless, the total amount of evaporated water was estimated to be 1.5 kg compared to 3.7 kg water initially present, and was therefore the most important term in the water balance. The amount of evaporated water becomes even more important when mainly evaporative cooling is applied in large-scale bioreactors where the capacity of wall cooling is limited (Nagel *et al.*, 2001). The second most important term in the water balance is the amount of intracellular water in biomass (1.2 kg) followed by the metabolic-water production (0.5 kg). Metabolic-water production cannot be neglected (Figure 11) as was done by Oriol *et al.* (1988) and is not balanced by water needed for starch hydrolysis, as was assumed by Narahara *et al.* (1984) in his description of the water balance. The final amount of dry-substrate loss was 1.5 kg compared to the 4.3 kg initially present. Thus, for the prediction of moisture contents, the dry-weight balance is as important as the water balance.

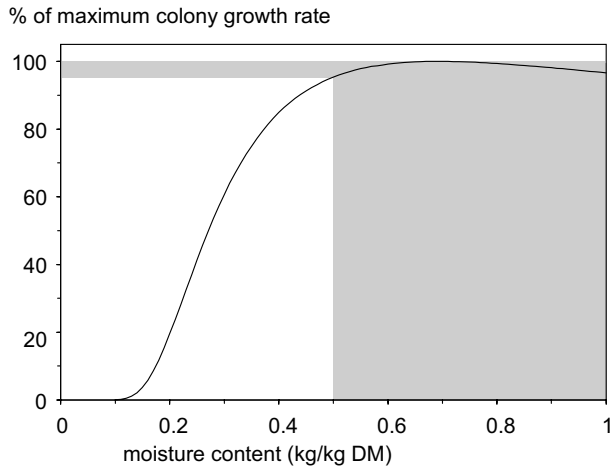

Figure 10. A desorption isotherm for wheat grains is combined with colony-growth-rate data as a function of water activity for *Aspergillus oryzae* to give a relation between colony-growth rate and moisture contents [Eq. (11)]. The gray area represents a suitable control range for the extracellular water content.

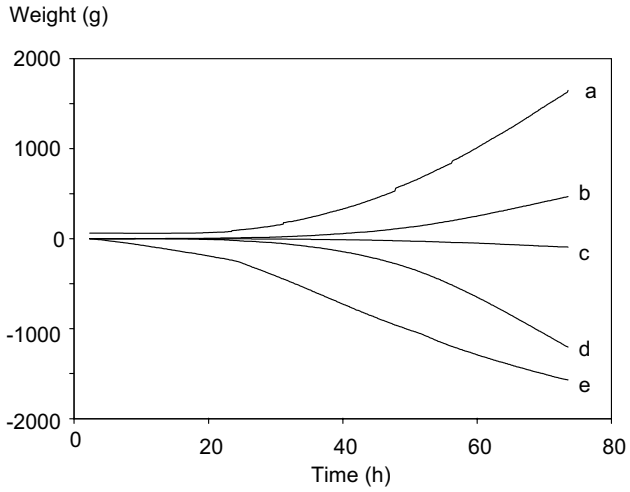

Figure 11. Model prediction of the absolute values of the different terms in the water- and dry-weight balance during an experiment in the 35-L mixed bioreactor in which wall cooling is applied. Curve *a* = dry-weight loss; curve *b* = Metabolic-water production; curve *c* = water for hydrolysis of starch; curve *d* = water in biomass; curve *e* = water evaporated.

Moisture-content control or water-activity control?

Water-activity control is necessary to maintain a sufficiently high growth rate during solid-state fermentation. Direct control of the substrate water activity is difficult as on-line monitoring in the substrate bed remains complicated, especially in a mixed bioreactor. The water activity of the solid substrate can decrease during SSF as a result of two processes: (1) dehydration of the solid substrate; and (2) accumulation of solutes in the substrate (glucose, amino acids etc.). In this article, a model has been developed and validated that can be used to control the extracellular water content, which is what accounts for the dehydration effect. However, the question remains whether it is valid to neglect accumulation of solutes.

We estimated the effect of the free glucose concentrations measured in the wheat grains to get an answer to this question. Free glucose concentrations were measured during all experiments mentioned in this study. The maximum free glucose weight fraction of fermented wheat grains found in the scraped drum reactor and paddle mixer varied between 0.12 and 0.14 kg/kg total DM. Assuming an extracellular water content

equal to 1 kg/kg substrate and a biomass dry-weight content of 0.3 kg/kg total DM (average SDR experiments B and C, Table 2), the glucose concentration can be estimated to be 170 to 200 g/L. According to the data of Bonner (1965), the water activity of a solution with 200 g/L glucose is 0.98. This water activity corresponds to 97% of the maximum colony growth rate for *A. oryzae*, according to data of Gibson *et al.* (1996). For this specific application the free glucose concentration does not seem to limit growth.

In SSF processes, we expect to find more cases in which there is not much free glucose accumulation, and in these cases control of the extracellular water content should keep water activity between acceptable limits. Even when more free glucose accumulates, this will not be important if the organism grows well over a relatively broad range of water activity values (*e.g.* 0.96 to 1.0). However, this does not negate the possibility that glucose, in some cases, accumulates to levels that affect growth significantly. We expect to see this in cases where glucose concentrations reach values of 100 to 200 g/L in the extracellular water, and where the growth of the organism falls significantly below the optimum as the water activity falls to values around 0.98. The proposed model, which aims at control of the extracellular (nonfungal) water content instead of the water activity, is a first step towards improved moisture control in SSF.

However, it may be insufficient; for example, when a microorganism with high amylolytic activity and poor a_w-tolerance has to be cultivated. The model would then have to be extended with hydrolysis and uptake kinetics in order to obtain predictions of the water activity. We expect that intra-particle transport of hyphae, enzymes, and sugars will also have to be taken into account, as this may cause strong glucose concentration gradients in substrate particles (Nagel *et al.*, unpublished). Extension of the model with these elements presents an interesting challenge for future work.

CONCLUSIONS

A model was developed for the prediction of the moisture content of wheat grains during SSF in mixed bioreactors, based on on-line measurements. The model is based on a complete water balance and elemental balances. Parameters for this model were determined from independent experiments using a membrane model system, which mimics the growth of *Aspergillus oryzae* on wheat grains as used in mixed bioreactors. Experiments in 1.5-L and a 35-L mixed bioreactors were used to validate the model. The model was able to predict the experimental moisture contents very well. We expect that the model can be used for automatic moisture-content control of the solid substrate in order to maintain a sufficiently high water activity during SSF in mixed bioreactors.

ACKNOWLEDGEMENTS

The authors thank J.C.A. Blonk for his contribution to this research. We also thank the central services department "de Dreijen" for the design and construction of the membrane model system and scraped drum reactor, in particular E. Janssen, M. Schimmel and A. van Wijk. This study was financially supported by the Dutch Graduate School on Process Technology.

REFERENCES

Agger T, Spohr A, Carlsen M, Nielsen J. 1998. Growth and product formation of *Aspergillus oryzae* during submerged cultivations: Verification of a morphologically structured model using fluorescent probes. Biotechnol Bioeng 57: 321-329.

Arima BK, Uozumi T. 1967. A new method for estimation of the mycelial weight in Koji. Agr Biol Chem 31: 119-123.

Bonner OD, Breazeale WH. 1965. Osmotic and activity coefficients of some nonelectrolytes. Carbohydr 10: 325-27.

Gibson AM, Baranyi J, Pitt JI, Eyles MJ, Roberts TA. 1994. Predicting Fungal Growth: The Effect of Water Activity on *Aspergillus Flavus* and Related Species. Int J Food Microbiol 23: 419-431.

Larroche C, Gros JB. 1992. Characterization of the growth and sporulation behavior of *Penicillium roquefortii* in solid-state fermentation by material and bioenergetic balances. Biotechnol Bioeng 39: 815-27.

Larroche C, Theodore M, Gros JB. 1992. Growth and sporulation behavior of *Penicillium roquefortii* in solid substrate fermentation: effect of the hydric parameters of the medium. Appl Microbiol Biotechnol 38: 183-187.

Larroche C, Moksia J, Gros JB. 1998. A convenient method for initial dry weight determination in samples from solid-state cultivations. Proc Biochem 33: 447-451.

Lonsane BK, Saucedo-Castaneda G, Raimbault M, Roussos S, Viniegra-Gonzalez G, Ghildyal NP. 1992. Scale-up strategies for solid-state fermentation. Proc Biochem 27: 259-273.

Nagel FJI, Tramper J, Rinzema A. 2001. Temperature control in a continuously mixed bioreactor for solid-state fermentation. Biotechnol Bioeng 72: 219-230.

Narahara H, Koyama Y, Yoshida T, Atthasampunna P. 1984. Control of water content in a solid-state culture of *Aspergillus oryzae*. J Ferment Technol 62: 453-459.

Nielsen J, Villadsen J. 1994. Bioreactor Engineering Principles. New York: Plenum Press.

Oostra J, Tramper J, Rinzema A. 2000. Model-based bioreactor selection for large-scale solid-state cultivation of *Coniothyrium minitans* spores on oats. Enz microbiol Technol 27: 652-663.

Oriol E, Raimbault M, Roussos S, Viniegra-Gonzales G. 1988. Water and water activity in the solid-state fermentation of cassava starch by *Aspergillus niger*. Appl Microbiol Biotechnol 27: 498-503.

Pandey A. 1992. Recent process developments in solid-state fermentations. Proc Biochem 27: 109-117.

Riet van 't K, Tramper J. 1991. Basic Bioreactor Design. New York: Marcel Dekker.

Ryoo D, Murphy VG, Karim MN, Tengerdy RP. 1991. Evaporative temperature and moisture control in a rocking reactor for solid substrate fermentation. Biotechnol Techn 5: 19-24.

Sargantanis J, Karim MN, Murphy VG, Ryoo D, Tengerdy RP. 1993. Effect of Operating Conditions on Solid-Substrate Fermentation. Biotechnol Bioeng 42: 149-158.

Saucedo-Castaneda G, Lonsane BK, Raimbault M. 1992. Maintenance of heat and water balances as a scale-up criterion for the production of ethanol by *Schwanniomyces castellii* in a solid-state fermentation system. Proc Biochem 27: 97-107.

Sakurai Y, Lee TH, Shiota H. 1977. On the convenient method for glucosamine estimation in Koji. Agr Biol Chem 41: 619-624.

Shankaranand VS, Lonsane BK. 1994. Coffee husk: an inexpensive substrate for production of citric acid by *Aspergillus niger* in a solid-state fermentation system. World J Microbiol Biotechnol 10: 165-68.

Shoup FK, Pomeranz Y, Deyoe CW. 1966. Amino acid compositions of wheat varieties and flours varying widely in bread-making potentialities. J Food Sci 31: 94-101.

Smits JP, Rinzema A, Tramper J, van Sonsbeek HM, Hage JC, Kaynak A, Knol W. 1998. The influence of temperature on kinetics in solid-state fermentation. Enz Microbiol Technol 22: 50-57.

Wang NS, Stephanopoulos G. 1983. Application of macroscopic balances to the identification of gross measurement errors. Biotechnol Bioeng 15: 2177-2208.

Whipps JM, Gerlagh M. 1992. Biology of *Coniothyrium minitans* and its potential use in disease biocontrol. Mycol Res 96: 897-907.

Chapter 5

Simultaneous control of temperature and moisture content in a mist bioreactor

F.J.I. Nagel, J. Tramper, M.S.N. Bakker, A. Rinzema.

Accepted for publication
Biotechnology and Bioengineering

SUMMARY

This article describes a control strategy for simultaneous control of the temperature and moisture content during solid-state fermentation, which can be used in large-scale mixed bioreactors that are cooled by water evaporation. We achieved simultaneous control of temperature and extracellular (non-fungal) water content during cultivation of *Aspergillus oryzae* on wheat in a continuously mixed paddle bioreactor (Nagel *et al.*, 2001a). Evaporative cooling with varying air flow rate was applied to control the temperature of the solid substrate. The extracellular water content was controlled by adding a fine mist of water droplets onto the mixed solid substrate, using a previously described model (Nagel *et al.*, 2001b) to calculate the required addition, based on on-line measurements. Temperature and extracellular water content were successfully controlled, which resulted in an improved biomass production compared to similar fermentations with temperature control only. No negative effects of water addition were observed with regard to biomass production. Control of the extracellular water content resulted in a sufficiently high water activity to assure good growth of *A. oryzae* on wheat grain, but it was not possible to maintain a constant water activity because glucose accumulated within the solid substrate. Control aimed at constant extracellular water content was shown to be superior to control aimed at constant overall water content of the fermented solids. The fully automatic control strategy employed in this study can improve bioreactor performance on a large scale and facilitate scale-up of SSF.

INTRODUCTION

The control of temperature and moisture content of the solid substrate is of critical importance for achieving a high productivity in solid-state fermentation (SSF) (Saucedo-Castaneda *et al.*, 1992). Conductive cooling is difficult -even in mixed bioreactors- because of the poor thermal conductivity of the solid substrate bed (Nagel *et al.*, 2001a; Oostra *et al.*, 2000). Therefore, evaporative cooling is needed in large-scale fermentations. It is achieved by supplying sufficient air to remove the amount of water vapor required for cooling; the inlet relative humidity can also be lowered to enhance the water vapor uptake capacity of the air (Laukevics *et al.*, 1984; Sargantanis

et al., 1993). However, evaporation results in dehydration of the solid substrate, so it is essential to combine temperature control with moisture-content control (Barstow *et al.*, 1988; Lonsane *et al.*, 1992; Ryoo *et al.*, 1991; Saucedo-Castaneda *et al.*, 1992). Direct on-line measurement of the moisture content in SSF is problematic. Therefore, mathematical models are needed to control the moisture content. Sargantanis *et al.* (1993) developed a model that estimates biomass content, total dry matter, temperature and total moisture content of the solid mass. This model was used for simultaneous control of temperature and overall moisture content in a rocking drum reactor (Ryoo *et al.*, 1991; Sargantanis and Karim, 1994). However, Oriol *et al.* (1988) demonstrated that the extracellular (non-fungal) moisture content limits growth; even when the overall water content of the fermenting solids increased, growth stopped due to limited availability of extracellular water. Therefore, the extracellular water content should be controlled. To our knowledge, no one has tried to achieve this.

In this article we demonstrate that simultaneous control of temperature and extracellular moisture content can be achieved for *Aspergillus oryzae* growing on wheat grain in a paddle mixer with evaporative cooling. Our control strategy differed from the one developed by Sargantanis and co-workers (1993) in several respects: (1) The extracellular (non-fungal) moisture content was controlled instead of the overall moisture content of the fermenting solids. (2) A different model (Nagel *et al.*, 2001b) was used for control purposes, which uses on-line measurements of O_2, CO_2 and dew point of the effluent air to predict the extracellular moisture content. (3) A different temperature-control strategy was used for evaporative cooling (Nagel *et al.*, 2001a). An aseptic bioreactor with internal mixing blades and spraying nozzles was used to ensure homogeneous water distribution and water evaporation. Control of the extracellular water content resulted in a sufficiently high water activity to assure good growth of *A. oryzae* on wheat grain, although it was not possible to maintain a constant water activity due to accumulation of glucose in the solid substrate. Biomass production and respiration were higher compared to previous experiments without water addition (Nagel *et al.*, 2001a). Furthermore, we show that control of the overall water content instead of the extracellular water content of the fermenting solids, gives a lower water activity and inferior growth of the fungus.

MATERIALS AND METHODS

Micro-organism and inoculation

Aspergillus oryzae CBS 570.65 was obtained from Centraal Bureau voor Schimmelcultures (Baarn, Netherlands). The preparation of a sporangiospore suspension is described previously (Nagel *et al.*, 2001a). The viable count of the spore suspension was approximately 9.7×10^6 spores per ml and 60 ml spore suspension was used to inoculate 8 kg moistened wheat grains. The inoculation procedure is described elsewhere (Nagel *et al.*, 2001a).

Preparation of the solid substrate

A single batch of wheat grain of commercial origin (Blok, Woerden, Netherlands) was stored at 10°C (initial moisture content 0.12 kg/ kg DM) and used for all experiments. Five kg of this batch was soaked for 2.5 h in excess water at 60°C. After sieving, the soaked grain was divided over four 25 L bottles (Nalgene 2251-0050,UK) and autoclaved (1.5 h, 121°C). The final moisture content was 0.92 kg /kg DM.

Fermentation process

Several fermentation runs were done in a 35-L horizontal paddle mixer in which the control strategy was adapted and optimized. Two fermentations are described in this article (experiments A and B) in which the same control strategy was used with the same parameters except for the outcome of the calibration of the mist-dosing nozzles. The extracellular moisture content was controlled at 0.78 kg/kg DM for both fermentations. The temperature of the solid substrate was maintained at 35°C. The temperature of the cabinet was maintained at 34.5°C. Fermentations were done under aseptic conditions for four or five days. The bioreactor contained 8 kg moistened wheat grains (moisture content = 0.92 kg w/kg DM). The bioreactor (Figure 1) consisted of a glass cylinder (Schott, Germany) with two stainless steel side plates. Along the central axis, 6 V-shaped paddles were placed at equal distance and a 90° angle to the adjacent paddle; two flat rectangular paddles were mounted at each end of the central axis. For the first 24 hours, the bioreactor content was mixed discontinuously (5 min, 1 RPM; 55 min 0 RPM) and after that continuous mixing (0.5 RPM) was applied.

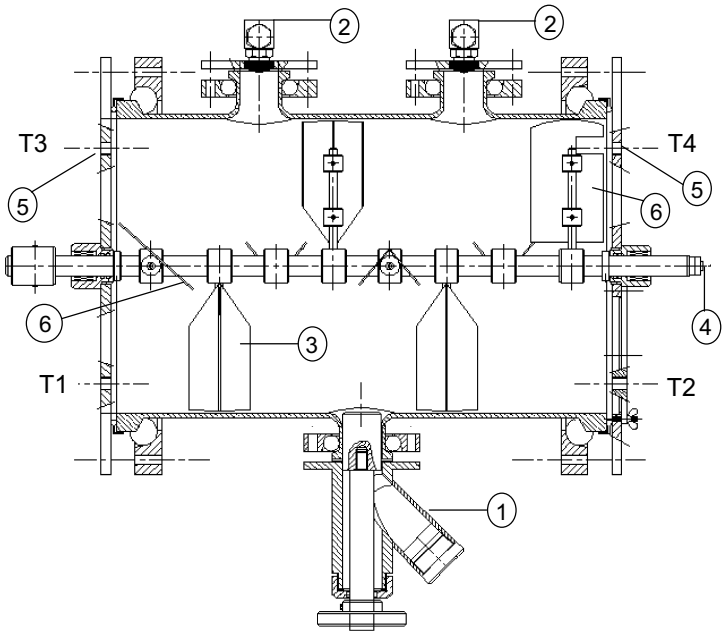

Figure 1. 35-L horizontal paddle mixer. 1: sampling device; 2: spraying nozzle; 3: V-shaped paddle; 4: air inlet; 5: air outlet; 6: rectangular paddle; T1 and T2: temperature sensors in the solid substrate bed; T3 and T4: temperature sensors in the headspace.

More details about the bioreactor, its operation and the ancillary equipment have been described previously (Nagel *et al.*, 2001a), except for the water addition system. The extracellular-moisture content was maintained by water addition using two spraying nozzles (Bète PJ8*5-1/8, Spraybest, NL). The nozzles used only pressurized demineralized water to produce a mist of water droplets. Water was pressurized (4 bar) in 20-L pressure tanks (Emergo, NL). A computer controlled on/off valve (220 V, Bruker, NL) regulated the mist dosing. A sterile 0.45-µm cellulose-acetate hydrophilic membrane filter (Sartobran 300, Sartorius, Germany) was used to filter-sterilize the water. A second mass-flow controller (0-100 Ln/min, Brooks, Veenendaal, NL) was added to the system to provide enough air for evaporative cooling. An overview of the air-conditioning and mist-addition system is given in Figure 2.

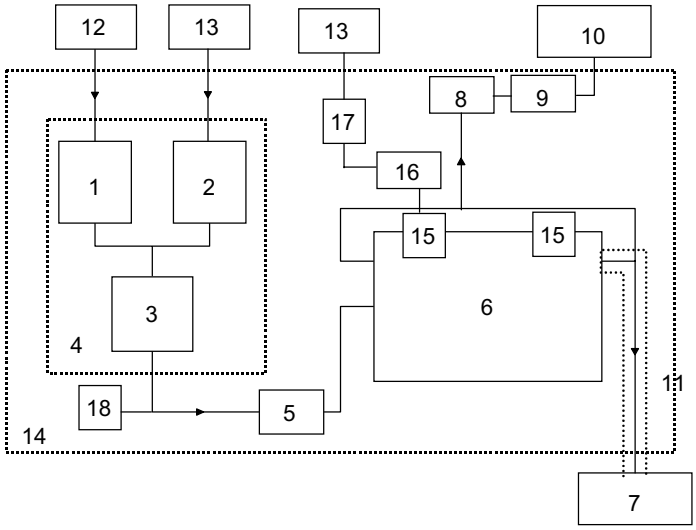

Figure 2. Schematic overview of the air-conditioning and mist-addition system used in the experiments. 1: mass-flow controller; 2: liquid-flow controller; 3: Controller-Mixed Evaporator (CEM); 4: "CEM"-Controlled-Vapor-Delivery System; 5: sterilizing membrane filter; 6: horizontal paddle bioreactor; 7: cooled-mirror dew point measuring system; 8: bioreactor pressure-control valve; 9: condenser; 10: oxygen/carbon-dioxide analyzer; 11: heated coil; 12: air pressure (6 bar); 13: pressure tank for water; 14: temperature-controlled cabinet; 15: spraying nozzle; 16: sterilizing membrane filter; 17: on/off valve for mist dosing; 18: mass-flow controller.

Sampling

Twice a day, a sample (± 30 g) was taken from the bioreactor. Moisture content and water activity were determined immediately after sampling. Approximately 5 gram of wheat grains were transferred into a sample bottle and stored (-20°C) for further analysis of glucosamine and glucose.

Analysis

The moisture content of the wheat grains was determined from the weight loss after drying the sample at 80°C for 2 days in a pre-weighed dish. The water activity of the sample was determined in a Novasina Thermoconstanter (type TH200, Switzerland) at

35°C. For starch, glucose and glucosamine analysis, the wheat-grain sample was homogenized with water in an ultra turrax (Silverson, L4R, UK). Free glucose was determined in the supernatant of the homogenate (Peridochrom glucose kit, Cat. no. 676543, Boehringer Mannheim, Germany). For the determination of total glucose, the starch in the homogenate was hydrolyzed with amyloglucosidase (Sigma A-3042, USA) and glucose was determined in the supernatant of the hydrolyzed sample. Supernatants were obtained by centrifugation (15300 rpm, 20 min, Beckmann GS-15R). Glucosamine content of samples was assayed by the method of Nagel *et al.* (2001a). The glucosamine content was converted to dry-weight biomass using the following equation which expresses the glucosamine content of biomass as a function of cultivation time (Nagel *et al.*, 2001b):

$$G_X\left(t-\lambda\right) = 44.61 + \frac{43.65}{\left(1+\exp\left(-\frac{\left(\left(t-\lambda\right)-61.70\right)}{12.34}\right)\right)} \qquad [\text{mg}\cdot\text{g}^{-1}\text{ dry biomass}] \quad (1)$$

in which

G_X	=	glucosamine content of biomass	[mg·g^{-1} DM]
t	=	time	[h]
λ	=	lag time	[h]

Oxygen and carbon dioxide were analyzed using a paramagnetic O_2 analyzer (Servomex, Xentra 4100, NL) and an infrared CO_2 analyzer (Servomex, Series 1400, NL), respectively. The humidity of the effluent air was measured in a cooled-mirror dew-point measuring system (DEWMET SD, Michell Instruments Ltd., UK).

CONTROL OF TEMPERATURE AND MOISTURE CONTENT

Temperature control

Temperature control started automatically when the substrate temperature exceeded 35°C. Temperature control was achieved through evaporative cooling by changing the dry-air flow rate. On-line measurements were used in a design equation for a steady-state feed-forward controller (ffc) that calculated the required dry-air flow rate from the energy balance over the bioreactor. All heat removal rates are considered as negative production rates. The air flow rate ($F_{air,ffc}$) necessary for temperature control was calculated every half hour from:

$$F_{air,ffc} = \frac{r_{met} + J_{wall}}{(h_o - h_i) \cdot \rho_{air}} \qquad [m^3 \cdot s^{-1}] \qquad (2)$$

in which

r_{met}	=	metabolic heat production by micro-organisms	[W]
h_o	=	enthalpy of the outcoming air	[J·kg^{-1} dry air]
h_i	=	enthalpy of the incoming air	[J·kg^{-1}dry air]
ρ_{air}	=	1.293 density dry air at 273 K and 1.013·10^5 Pa	[kg·m^{-3} dry air]

The following assumptions were made which lead to Equation 2:

- The fermenter is in steady state with respect to temperature;
- Mass accumulation is negligible;
- Heat dissipation by the stirrer is negligible.

Heat loss through the wall of the fermenter is calculated from:

$$J_{wall} = -\alpha_{ov} \cdot A \cdot (T_b - T_{wall}) \qquad [W] \qquad (3)$$

in which

J_{wall}	=	heat transfer through the wall	[W]
α_{ov}	=	heat transfer coefficient of the wall	[W·(m^2·°C)$^{-1}$]
A	=	heat transfer area of the wall	[m^2]
T_{wall}	=	external temperature of the wall	[°C]
T_b	=	temperature of the solid substrate	[°C]

In addition to the steady-state feed-forward controller (Equation 1), a PI controller was used for feed-back control of $F_{air,ffc}$ according to the set-point deviation of the bed temperature (Figure 3). The calculated air flow rate ($F_{air,ffc}$) was corrected with a discrete proportional-integral algorithm (sampling time = 2 s) to give the controller output ($F_{air,control}$) :

$$F_{air,control} = F_{air,ffc} + K_c \cdot \varepsilon(t) + \frac{K_c}{\tau_I} \cdot \int_0^t \varepsilon(t) \cdot dt \qquad [m^3 \cdot s^{-1}] \qquad (4)$$

in which

K_c	=	$1.667 \cdot 10^{-4}$	proportional gain of the controller	$[m^3 \cdot s^{-1} \cdot °C^{-1}]$
τ_I	=	4000	integral time constant	[s]

The input of the PI-controller is the deviation (or error ε) between the actual substrate temperature and the desired setpoint:

$\varepsilon(t) = T_b(t) - T_{b\text{-}set}$

$T_{b\text{-}set}$ = 35°C (set-point temperature for the bed of solids)

The PI controller was tuned based on experience and optimized during several test runs. The combination of feed-forward and feed-back control allowed us to study the effects of moisture content control at accurately controlled temperature. It was not compared to other control systems, as this was not the purpose of our work.

Moisture-content control

A model was developed which can be used for automatic extracellular moisture-content control during SSF (Nagel *et al.*, 2001b). The model uses on-line measurements of O_2, CO_2 and dew point of the effluent air, to estimate the extracellular moisture content of the grains (Figure 3). The model is based on elemental balances and does not contain kinetic relations. All values of the parameters used in the model are taken from Nagel *et al.* (2001a, b). In the following equations all rates are production rates; consumption rates have a negative value.

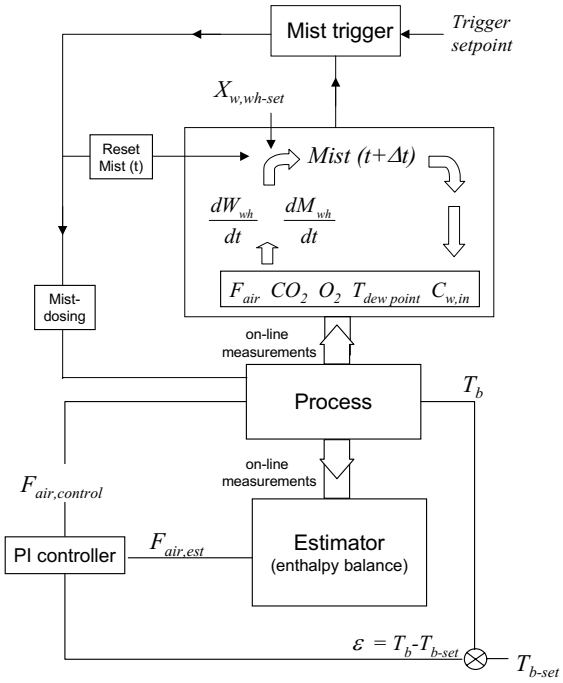

Figure 3. Schematic overview of the strategy used to control the temperature and moisture content of the solid substrate during solid-state fermentation.

Assuming that the air in the bioreactor is in steady state, the biomass has a constant water content and accumulation of glucose or oligosaccharides is negligible, the balance for extracellular water reads:

$$\frac{dW_{wh}}{dt} = F_{air} \cdot \left(C_{Win} - C_{Wout}\right) + X_{W,X} \cdot Y_{X/O2} \cdot r_{O2} \cdot Mw_X - Y_{W/O2} \cdot r_{O2} \cdot Mw_W + Y_{hyd} \cdot Y_{S/O2} \cdot r_{O2} \quad [\text{kg}\cdot\text{s}^{-1}] \qquad (5)$$

in which

W_{wh}	=	weight extracellular water in wheat		[kg]
r_{O2}	=	oxygen production rate		[mol·s^{-1}]
F_{air}	=	volumetric gas flow at 273 K and 1.013·10^5 Pa		[m^3 dry air·s^{-1}]
C_W	=	water concentration in air recalculated to 273 K and 1.013·10^5 Pa		[kg·m^{-3} dry air]
$X_{W,X}$	=	2.08	water content of biomass	[kg·kg^{-1} DW]
Mw_W	=	18·10^{-3}	molecular weight water	[kg·mol^{-1}]
Mw_X	=	24.42·10^{-3}	molecular weight biomass	[kg·Cmol^{-1}]
Y_{hyd}	=	0.003	water needed to hydrolyze starch	[kg·Cmol^{-1} S]
$Y_{W/O2}$	=	1.22	yield coefficient for water (W) on oxygen	[mol·mol^{-1} O_2]
$Y_{S/O2}$	=	1.46	yield coefficient for substrate (*S*) on oxygen	[Cmol·mol^{-1} O_2]
$Y_{X/O2}$	=	1.16	yield coefficient for biomass (*X*) on oxygen	[Cmol·mol^{-1} O_2]

The yield coefficients for starch and protein were used to relate dry-weight losses to the measured CO_2 production:

$$\frac{dM_{wh}}{dt} = -\left(\frac{Y_{S/O2}}{Y_{CO2/O2}} \cdot Mw_S + \frac{Y_{N/O2}}{Y_{CO2/O2}} \cdot Mw_N \right) \cdot r_{CO2} \qquad [\text{kg·s}^{-1}] \qquad (6)$$

in which

M_{wh}	=	weight of wheat dry matter		[kg]
$Y_{CO2/O2}$	=	1.06	yield coefficient for CO_2 on oxygen	[mol·mol^{-1} O_2]
$Y_{N/O2}$	=	0.76	yield coefficient for protein (N) on oxygen	[Cmol·mol^{-1} O_2]
Mw_N	=	27.63·10^{-3}	molecular weight protein	[kg·Cmol^{-1} N]
Mw_S	=	30·10^{-3}	molecular weight starch	[kg·Cmol^{-1} S]
r_{CO2}	=	carbon dioxide production rate		[mol·s^{-1}]

The initial weights of water and dry matter were input parameters for the model, and were determined from weight measurements during the preparation of the solid

substrate. From the beginning of the fermentation, the model estimates the extracellular moisture content of the solid substrate (X_W) every minute (Δt) as follows:

$$X_{W,wh}(t+\Delta t) = \frac{W_{wh}(t) + \frac{dW_{wh}}{dt}\cdot\Delta t}{M_{wh}(t) + \frac{dM_{wh}}{dt}\cdot\Delta t} \qquad [\text{kg}\cdot\text{kg}^{-1}] \qquad (7)$$

For the time step used (Δt = 60 s), this approximation is sufficiently accurate compared to the rigorous solution obtained using the chain rule.
The amount of water to be added for the desired set-point is calculated as:

$$Mist(t+\Delta t) = X_{W,wh}(setpoint)\cdot\left(M_{wh}(t) + \frac{dM_{wh}}{dt}\cdot\Delta t\right) - \left(W_{wh}(t) + \frac{dW_{wh}}{dt}\cdot\Delta t\right)$$

[kg] (8)

The nozzles are calibrated to determine the amount of water *(= Mist calibrated)* sprayed in 50 seconds. *Mist (t+Δt)* is calculated every minute *(Δt)* and if *Mist (t+Δt)* > *Mist calibrated*, mist addition is started and *Mist (t+Δt)* is set to zero.
A more detailed description of the above-mentioned events is programmed in a software program for data-acquisition and control (Viewdac®, Keithley Instruments Inc., USA) and is given in Table 1.

RESULTS AND DISCUSSION

The aim of our control strategy is to maintain a constant extracellular (*i.e.* non-fungal) water content of the fermenting solids. Experiment A below shows that this control strategy was quite successful. In experiment B a constant overall water content (*i.e.* water inside and outside fungal cells) was maintained and fermentation results were poorer. The control model employed here is evaluated at the end of the Results and discussion section.

Table 1. Scheme for on-line moisture-content control as programmed in the data-acquisition and control program in order to control the water addition during solid-state fermentation.

Step 1:	If *Mist* $(t+\Delta t) > Mist\ calibrated$ GOTO step 5
Step 2:	Calculate $\frac{dW_{wh}}{dt}$ $\frac{dM_{wh}}{dt}$ *and* $Mist\left(t+\Delta t\right)$
Step 3:	Calculate $W_{wh}\left(t+\Delta t\right)$ $M_{wh}\left(t+\Delta t\right)$
Step 4:	GOTO step 1 after 1 minute (Δt)
Step 5:	Calculate interval mist dosing $interval(\text{sec}) = \frac{Mist\left(t+\Delta t\right)}{Mist\ calibrated} \cdot 50\ sec.$
Step 6:	Set F_{air} to 0 L/min
Step 7:	Set rotational speed at 2 RPM
Step 8:	Open valve Mist addition
Step 9:	Close valve Mist dosing after mist dosing time interval
Step 10:	Set F_{air} to setpoint before mist addition
Step 11:	Set rotational speed to 0.5 RPM
Step 12:	Calculate $W_{wh}\left(t+\Delta t\right) = W_{wh}\left(t+\Delta t\right) + Mist\left(t+\Delta t\right)$
Step 13:	Set *Mist* $(t+\Delta t)$ to zero
Step 14:	GOTO step 1

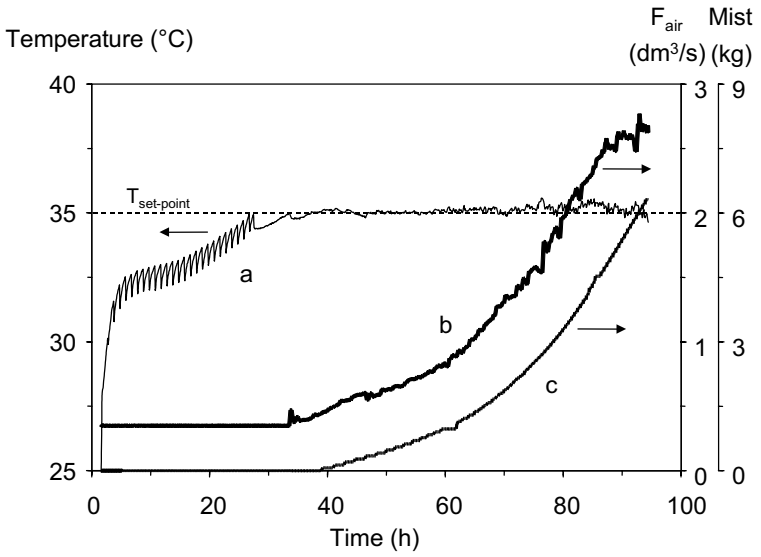

Figure 4. Experiment A: the course of the bioreactor temperature (*curve a*), dry air flow rate (F_{air}, *curve b*) and water addition (Mist, *curve c*) during cultivation of *Aspergillus oryzae* on wheat grain in a 35-L horizontal paddle mixer in which temperature and moisture content were controlled.

Experiment A – Control of extracellular moisture content

Overall description

The substrate temperature was controlled accurately with evaporative cooling, which was achieved by changing the airflow rate (Figure 4). The effect of discontinuous mixing during the first 24 hours can be seen from the saw-toothed pattern of the substrate temperature (Figure 4). The temperature control strategy was started after 34 hours, when the substrate temperature exceeded the set-point value of 35°C. From that moment on accurate temperature control was achieved. High airflow rates (≈150 L/min) with low incoming relative humidity were needed to evaporate enough water to cool the fermenting mass. The inlet relative humidity decreased automatically to a final value of ≈ 6% (= 2 g/kg dry air), because a constant water vapor flow was mixed with an increasing dry air flow (Figure 5). The effluent relative humidity of the air decreased to 60% (21.5 g/kg dry air) as the average residence time of the air decreased with increasing airflow rates.

Air entered the bioreactor via the hollow central axis and came out at the end of each paddle through a narrow nozzle, to provide a uniform air distribution through the bed. However, at any moment half of the paddles were in the headspace and the other paddles were in the bed, which implies that only part of the air contacted the bed efficiently. The evaporative cooling capacity could be increased by adapting the air inlet so that all the incoming air is injected into the bed.

After 40 h, mist addition started automatically (Figure 4) when the predicted extracellular water content dropped below the set-point value of 0.78 kg/kg DM (Figure 6). The saw-tooth pattern of the water content is the result of discontinuous water addition. Clearly, the overall moisture content increased when the extracellular moisture content (that is the water in the substrate, outside the fungal cells) was controlled, because in this fermentation the moisture content of biomass was twice the moisture content of the substrate (Nagel *et al.*, 2001b).

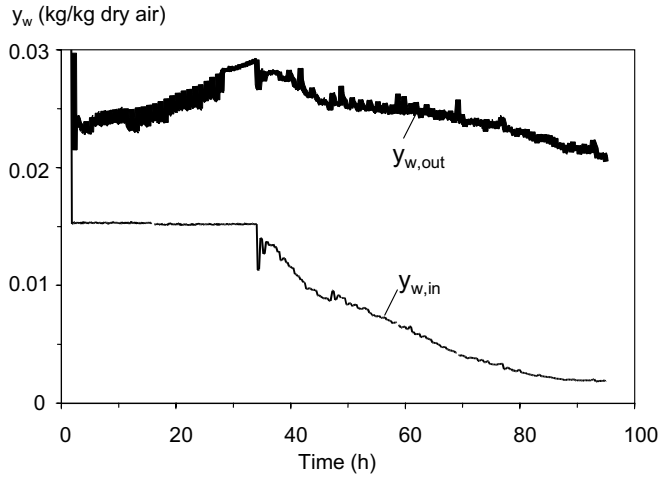

Figure 5. Experiment A: the course of the water content of the inlet air ($y_{w,in}$) and effluent air ($y_{w,out}$) during cultivation of *Aspergillus oryzae* on wheat grain in a 35-L horizontal paddle mixer in which temperature and moisture content were controlled.

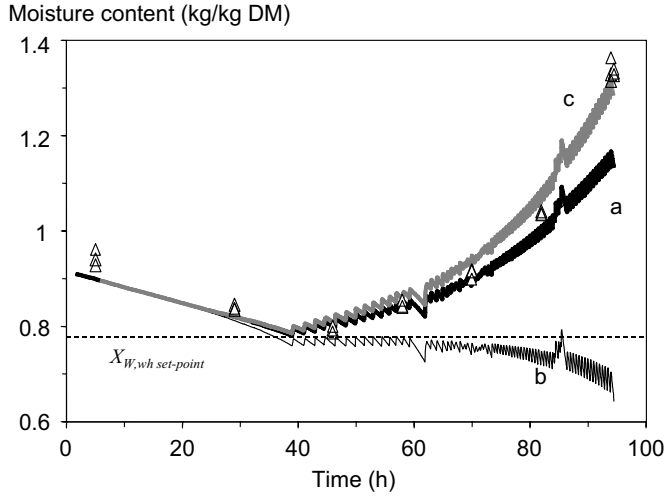

Figure 6. Experiment A: model predictions for the overall moisture content (*curve a*) and the extracellular-moisture content (*curve b*) compared with overall moisture content measurements (△) during cultivation of *Aspergillus oryzae* on wheat grain in a 35-L horizontal paddle mixer in which temperature and extracellular-moisture content were controlled. Model prediction (*curve c*) using a different overall dry-weight loss factor (39.5 g/mol CO_2), calculated from previously reported experiments (Nagel *et al.*, 2001b).

Moisture-content control

The combined water and dry matter balances over the bioreactor (Table 2) illustrate which terms are most important for moisture-content control. A large amount of water is lost due to evaporative cooling, viz. 7.5 kg compared to 4 kg water initially present. The total amount of mist addition (6.3 kg) is less than the amount of evaporated water, because (1) dry weight losses reduce the amount of water needed to maintain a constant extracellular water content, and (2) metabolic water is produced during the cultivation. The amount of water needed for starch hydrolysis is a minor term in the water balance. The dry matter loss is very important for moisture content control.

Figure 6 shows a comparison of calculated and measured overall water content of the fermenting solids, and the calculated extracellular water content. Note that the calculated values in this graph are not the ones that were calculated on-line, but recalculated values that take into account the water and dry matter lost by sampling, and a correction of the oxygen consumption for the water vapor left in the gas analysis sample stream. Until 80 hours fermentation time, the model prediction of the overall moisture content is quite accurate. At the end of the experiment, after 95 hours, there is however a rather large deviation.

This deviation is also evident from Table 2, which shows that the prediction of the final amount of water in the system is very accurate, but the prediction of the amount of dry matter should be improved. The difference between predicted and measured amounts after 95 h is 1% of the measured value for water and 15% for dry matter. This error in the prediction of dry matter caused about 90% of the deviation between measured and predicted overall moisture content after 95 hours shown in Figure 6 and Table 2.

Water activity

The water activity of the substrate is more important than its moisture content (Grajek and Gervais, 1987; Gervais *et al.*, 1988; Gervais, 1990). Based on the calculated extracellular moisture content (Figure 6) and the desorption isotherm of wheat grain (Nagel *et al.*, 2001a), we expected that the water activity would remain constant around 0.98. However, free glucose or other low molecular weight solutes will also lower the water activity (Nagel *et al.*, 2001b).

Table 2. Water and dry matter balance for experiment A in which *Aspergillus oryzae* was cultivated on wheat grains in a 35-L horizontal paddle mixer in which the temperature and moisture content were controlled. Final values after 95 hours.

	water (kg)			dry matter (kg)			
	extracellular	intracellular	total	extracellular	intracellular	total	
initial amount	4.00		4.00	4.30		4.30	
evaporated	-7.46		-7.46				1)
biomass production	-2.23	2.23	0.00		1.07	1.07	2)
metabolic production	0.80		0.80	-2.32		-2.32	2)
starch hydrolysis	-0.17		-0.17				2)
samples	-0.20		-0.20	-0.20		-0.20	
water added	6.31		6.31				3)
predicted final	1.05	2.23	3.28	1.78	1.07	2.85	
measured final			3.32			2.49	
	overall moisture content (kg/kg DM)						
predicted final	1.15						
measured final	1.33						

1) calculated from measured gas flow rate and the moisture content of the inlet and effluent air

2) model prediction, calculated from off-gas analysis (Nagel *et al.*, 2001b)

3) based on calibration before fermentation

The water activity during the fermentation inversely correlated with the free glucose concentration (Figure 7). According to data of Bonner and Breazeale (1965) a solution with a concentration of 0.17 g glucose per g water (the value shown in Figure 7) has a water activity of 0.98.

The Ross equation (Ross, 1975) was used to calculate the water activity of wheat grain with this glucose concentration:

$$\alpha_w^{mixture} = \alpha_w^{glucose} \cdot \alpha_w^{wheat} = 0.98 \cdot 0.98 = 0.96$$

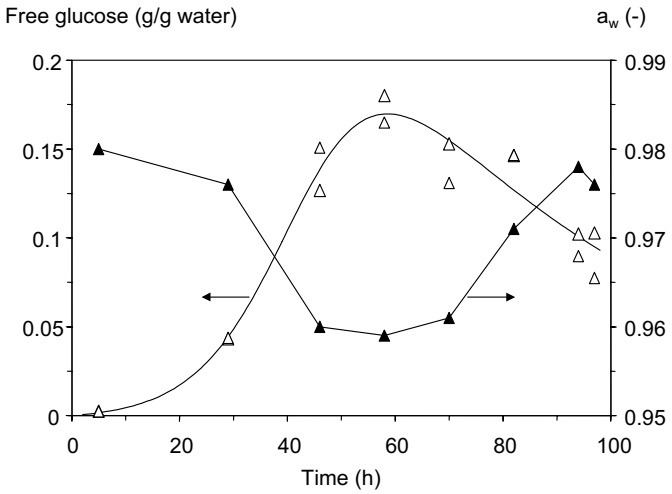

Figure 7. Experiment A: measurements of water activity (▲) and free glucose (△) during cultivation of *Aspergillus oryzae* on wheat grain in a 35-L horizontal paddle mixer in which temperature and moisture content were controlled.

We conclude that the observed decrease in water activity to 0.96 can be explained by a combination of the water sorption isotherm of the wheat solids and the increase in free glucose concentration in the wheat grains during the cultivation.
A water activity of 0.96 is not really limiting the growth of *Aspergillus oryzae*, as the colony radial growth rate is still approximately 85% of its maximum at this water activity (Gibson *et al.*, 1994). However, for many bacteria and some fungi a water activity of 0.96 seriously limits growth. Thus by controlling the extracellular moisture content in SSF, one can only control the water activity to a limited extent, depending on for example the α-amylase excretion and activity.

Biomass formation
Fungal biomass development is shown in Figure 8. Glucosamine was used as an indicator for fungal biomass and glucosamine measurements were converted to biomass dry-weight values taking into account the age dependence of the glucosamine content of the fungal cells as described previously (Nagel *et al.*, 2001b), in order to allow a comparison with model predictions. Measured and predicted amounts of

biomass dry matter after 95 hours were 0.17 g biomass/g IDM and 0.25 g biomass/g IDM, respectively. Part of the difference between measured and predicted values may be due to the measurement error in the glucosamine analysis. An uncertainty of 0.027 g biomass/g IDM in the measured value was calculated from the standard measurement error in the glucosamine content of biomass (Nagel *et al.*, 2001b). Another source of error in the measured biomass dry matter is the conversion of glucosamine to dry weight. This conversion is based on previously reported independent experiments with a wheat flour model substrate, which showed that the glucosamine content of fungal dry matter is highly dependent on the age of the biomass and the determination of the lag time used in this conversion is not very accurate (Nagel *et al.*, 2001b). Other explanations for the difference between predicted and measured biomass dry weight are discussed at the end of the Results and discussion section.

Mist-bioreactor performance

Bioreactor performance - measured as oxygen consumption rate and glucosamine production - of fermentation A is compared with a previously described experiment C in the same bioreactor with the same temperature control strategy but without mist addition (Figure 8, Nagel *et al.*, 2001a). This allows us to identify the influence of moisture-content control on bioreactor performance, measured as oxygen consumption rate (r_{O2} mol h^{-1}·kg DM^{-1}). The r_{O2} of experiment A lags behind from the moment that mist addition starts at 40 h (Figure 8a). A possible explanation for this observation could be that mist addition fills the open pores present in the wheat grain and thus hinders oxygen transfer. However, a high r_{O2} is measured at the end of the fermentation, where mist addition occurs more frequently. We cannot explain the observed temporary decline in the increase in respiration rate.

Besides oxygen consumption, glucosamine concentration was used as an indicator for bioreactor performance. Until the point where the peak in respiration rate occurs in experiment C, *i.e.* after 55 h, both experiments showed the same profile for the glucosamine concentration. After 55 h, the concentration increased to 14 g/kg IDM for experiment A (Figure 8b) while for experiment C the glucosamine concentration remained constant at 3.15 g/kg IDM.

Both, oxygen consumption rate and glucosamine measurements show that the bioreactor performance is improved by controlling the extracellular moisture content.

We have previously shown that growth stopped due to a lack of water after 55h, when no moisture content control was applied (Nagel *et al.*, 2001a). With moisture-content control, growth continued under otherwise comparable circumstances.

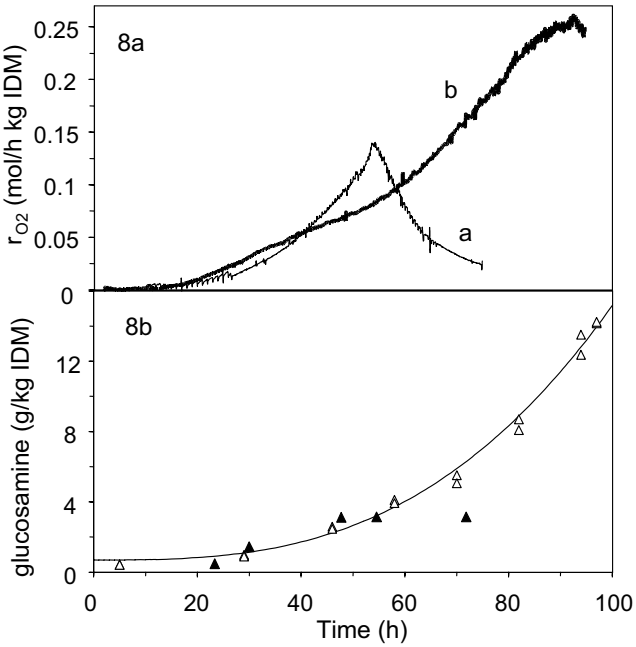

Figure 8a. A comparison between the oxygen consumption rates of a cultivation of *Aspergillus oryzae* in the horizontal paddle mixer with evaporative cooling (experiment C, *curve a*, data taken from Nagel *et al.*, 2001a) and with evaporative cooling and water addition (experiment A, *curve b*). **Figure 8b.** Glucosamine measurements for the fermentation with evaporative cooling and water addition (experiment A, △) and evaporative cooling (experiment C, ▲). The solid line (——) represents a fit on the data.

Experiment B – Control of overall moisture content

Experiment B (Figure 9) shows that control of extracellular water content is superior to control of overall water content. For unknown reasons, the flow rate of the mist-dosing nozzles sometimes decreased during fermentations. In experiment B, such a decrease accidentally resulted in a constant overall moisture content (0.75 kg/kg DM, Figure

10b), instead of a constant extracellular water content. The effect of a constant overall water content is clearly demonstrated by a comparison of the maximum oxygen consumption rate for both experiments (experiment B: 0.2 mol/h kg IDM; experiment A: 0.26 mol/h kg IDM) and the glucosamine concentrations (experiment B: 6.8 g/kg IDM; experiment A: 14 g/kg IDM, Figure 10a). Water activities were also lower for experiment B (Figures 7 and 10c). The lower water activity is probably the main cause for the observed difference in biomass production and oxygen consumption. The effect of a constant overall water content -and thus a lower extracellular water content- on water activity is self-enhancing. As the specific growth rate is lowered by a small decrease in water activity, the free glucose concentration increases because glucose uptake decreases and starch breakdown is apparently less affected (Figure 10c). The water activity is then further lowered due to the increased glucose concentration, etc. In summary, this fermentation illustrates the need to control the extracellular water content of the solid substrate instead of the overall water content.

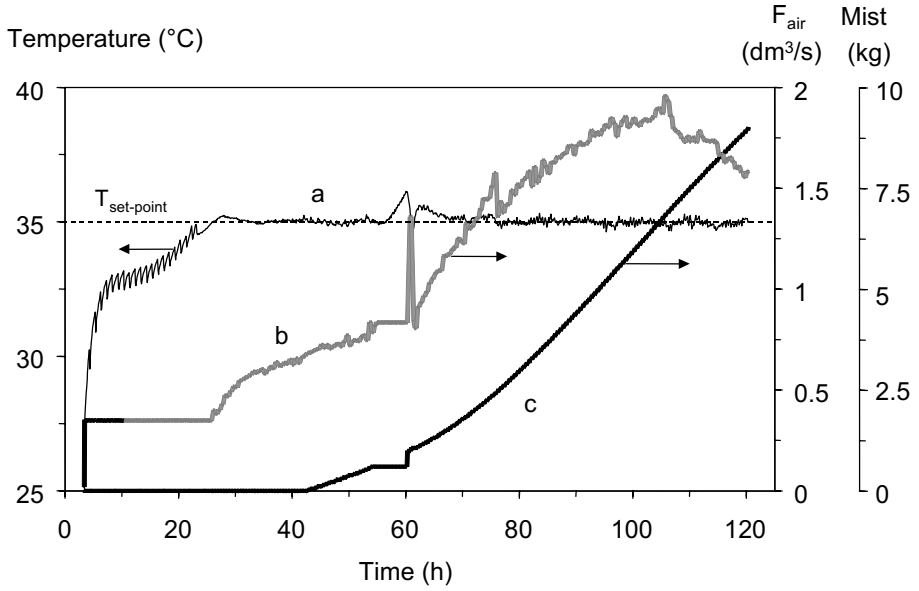

Figure 9. Experiment B: the course of the bioreactor temperature (*curve a*), air flow rate (F_{air}, *curve b*) and mist addition (Mist, *curve c*) during cultivation of *Aspergillus oryzae* on wheat grain in a 35-L horizontal paddle mixer in which temperature and moisture content were controlled.

A second effect illustrated by this experiment is that of failure of the control system. Temperature control stopped accidentally at 57 hours for about 3 hours (Figure 9). Due to the control failure, the substrate temperature rose 0.34 °C/h to 36°C, which clearly demonstrates the need for automatic temperature control in SSF. Note that a steeper increase would occur in a larger fermenter, which has a less favorable wall area/volume ratio. We are convinced that the short disturbance in temperature control does not affect the discussion above concerning the control of overall versus extracellular water content, because the temperature remained very close to the optimum for *A.oryzae*.

Evaluation of the extracellular moisture control strategy

Bioreactor performance, measured as biomass production or oxygen consumption, is clearly improved by controlling the extracellular moisture content, compared to a fermentation without moisture content control as well as a fermentation with overall moisture content control. The model underlying the control strategy gives adequate predictions of the overall moisture content during the first 80 hours of a fermentation of wheat grain with *A. oryzae* (Figure 6). Predictions of the overall moisture content after 80 hours were less accurate, but it should be emphasized that industrial fermentations with fast-growing fungi like *A. oryzae* usually have a far shorter duration, viz. under 50 hours. No direct evidence is available that a constant extracellular water content was maintained. However, the accurate prediction of the overall water content leads us to believe that this was indeed the case. This is supported by calculations of the water activity presented earlier.

A decrease in water activity of the substrate occurred, due to accumulation of glucose. This decrease did not interfere with process control, because the fungus used is not very sensitive to water activity and the sorption isotherm of the wheat grain (Nagel *et al.*, 2001a) leaves sufficient latitude. The model would have to be considerably more complex to predict glucose accumulation and actually control the water activity; this presents an interesting challenge for further research.

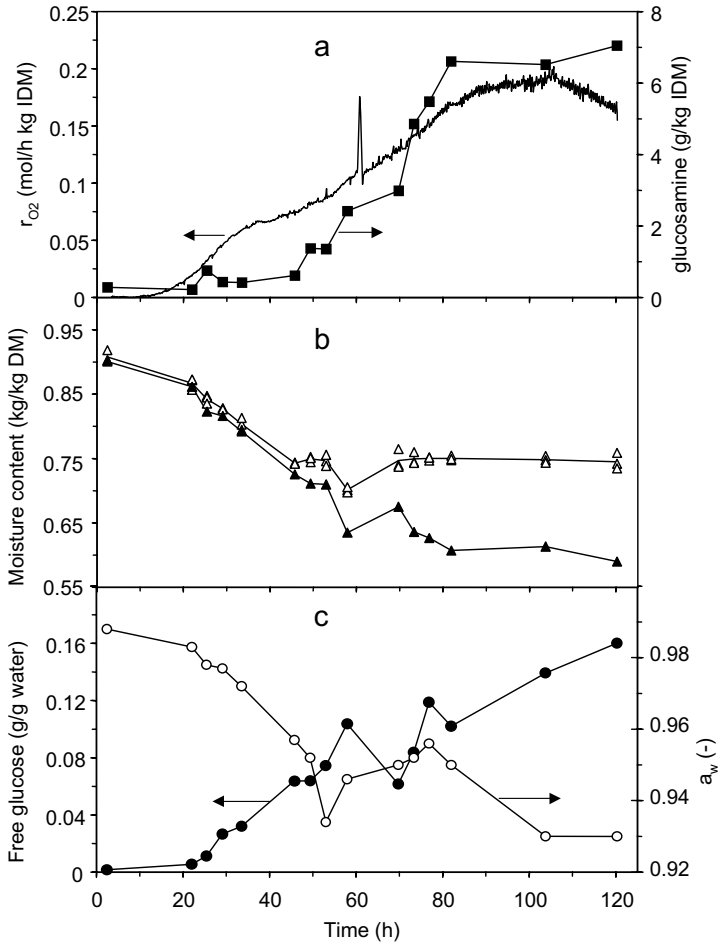

Figure 10. Experiment B: cultivation of *Aspergillus oryzae* on wheat grain in a 35-L horizontal paddle mixer in which temperature and moisture content were controlled. **10a:** oxygen consumption rate (—) and glucosamine concentration (■); **10b:** measured overall moisture content (△) and calculated extracellular moisture content (▲); **10c:** water activity (○) and free glucose concentration (●).

Apart from the water activity prediction, the existing model may be improved in some respects. Improvement would have to focus on dry matter predictions if we want to predict the behavior of lengthy fermentations better (Table 2, Figure 6). After 95 hours fermentation time, the error in the total dry matter prediction caused more than 90% of the difference between measured and predicted overall moisture content. This can be due to errors in the prediction of substrate dry matter losses (Eq. 6) or errors in the prediction of biomass dry matter. Substrate dry matter losses cannot be measured directly in an experiment with wheat grain, as it is impossible to separate substrate and biomass dry matter. Biomass dry matter can only be assessed through measurement of cell components such as glucosamine. The difference between predicted biomass dry matter and the biomass dry matter derived from the glucosamine measurement is virtually equal to the error in the total dry matter prediction. However, as discussed above, there are uncertainties in the glucosamine measurement as well as in the conversion of glucosamine to biomass dry matter. Therefore, it is not certain that the biomass prediction is the source of all errors in the moisture content prediction.
The ratio between overall dry matter loss, *i.e.* combined substrate dry matter losses and biomass production, and C_{O2} production is related to the yield coefficients in our model by

$$f_{ov,DMloss} = Y_{S/CO2} \cdot Mw_S + Y_{N/CO2} \cdot Mw_N - Y_{X/CO2} \cdot Mw_X \qquad [\text{g·mol}^{-1}\ CO_2] \qquad (9)$$

The overall dry weight loss factor ($f_{ov,DMloss}$) in our model is 34.5 g/mol C_{O2}, based on yield coefficients determined previously using a wheat flour model substrate (Nagel *et al.*, 2001b). Evidently, this is lower than the measured value. It is also lower than the value found in previous experiments in a scraped drum reactor (Nagel *et al.*, 2001b, experiments B and C), which on average was 39.5 g/mol C_{O2}. If we use this higher value, the model describes the experimental data for the overall moisture content accurately (Figure 6). Two factors may cause a higher dry matter loss, viz. errors in the yield coefficients and maintenance.
Previously, we have shown (Nagel *et al.*, 2001b) that the yield coefficients in our model do not contain gross errors at the 90% confidence level. However, an evaluation of results reported here and results reported previously (Nagel *et al.*, 2001b), shows that the biomass/oxygen yield coefficient used in the model is slightly higher than the

average observed value in virtually all fermenter runs and in the independent experiments with a model substrate that were used to set up the stoichiometric model (Nagel *et al.*, 2001b). Furthermore, the evaluation shows that the glucose/oxygen yield coefficient in the model is below the observed values. This may indicate that an oxidized metabolite was formed, which was not taken into account in the model. Overestimation of the amount of biomass formed combined with underestimation of the amount of glucose consumed will result in underestimation of dry matter loss and overall moisture content. This may explain the deviation in remaining total dry matter.

Maintenance is another factor that may explain the differences between calculated and measured amounts of total dry matter and biomass. Maintenance activity over the first 70 hours was taken into account implicitly in the determination of yield coefficients from experiments with a wheat flour model substrate (Nagel *et al.*, 2001b). A calculation using the maintenance coefficient reported for *A. oryzae* (Carlsen *et al.*, 1996) indicates that after 70 hours slightly more than 50% of the oxygen consumption found in the experiments with the model substrate was due to maintenance. Between 70 and 95 hours progressively more oxygen will be used for maintenance. Consequently, the biomass produced per mol of O_2 is expected to decrease and the dry weight loss per mol of O_2 is expected to increase.

It is recommended to study the formation of oxidized metabolites and expand the model with maintenance metabolism in order to better predict a lengthy stationary phase. In addition, we recommend improving moisture-content control with feed-back control of the mist addition by on-line adaptation of the dry-weight loss factor. This could be based on (1) on-line measurement of the bioreactor weight or (2) rapid off-line moisture-content measurements.

CONCLUSIONS

We achieved simultaneous control of temperature and extracellular (non-fungal) water content during cultivation of *Aspergillus oryzae* on wheat in a continuously mixed paddle bioreactor. This bioreactor was cooled by evaporation, the most important cooling mechanism in large solid-state fermenters. Adding a fine mist of water droplets onto the mixed solid substrate, using a previously described model to calculate the required addition, controlled the moisture content. The temperature and moisture content were adequately controlled and a large improvement in bioreactor performance was achieved compared to a similar experiment without moisture control, *i.e.* both the respiration rate and the final biomass were higher. No negative effects of water addition on the biomass production rate could be observed, but an unexplained delay in the increase in respiration rate occurred after water addition had started. Furthermore, it was demonstrated that control of the extracellular-water content resulted in improved bioreactor performance compared to control of the overall water content. The extracellular water content control strategy can be further optimized and improved by expanding the model with metabolites that were hitherto neglected and maintenance metabolism, and by on-line monitoring of added water and dry weight loss. Finally, this control strategy will improve bioreactor performance and facilitate the scale-up of SSF-bioreactors.

ACKNOWLEDGEMENTS

The authors thank M.S.N. Bakker for the experimental analysis and F.J. Weber for carefully reading the manuscript. We also thank the central services department "de Dreijen" for the design and construction of the horizontal paddle mixer, in particular E. Janssen, M. Schimmel and A. van Wijk. This study was financially supported by the Dutch Graduate School on Process Technology.

REFERENCES

Barstow LM, Dale BE, Tengerdy RP. 1988. Evaporative temperature and moisture control in solid substrate fermentation. Biotechnol Techn 2: 237-242.

Bonner OD, Breazeale WH. 1965. Osmotic and activity coefficients of some non-electrolytes. Carbohydr 10: 325-27.

Carlsen M, Nielsen J, Villadsen J. 1996. Growth and α-amylase production in *Aspergillus oryzae* during continuous cultivation. J Biotech 45:81-93.

Gervais P. 1990. Water activity: a fundamental parameter of aroma production by microorganisms. Appl Microbiol Biotechnol 33: 72-75.

Gervais P, Molin P, Grajek W, Bensoussan M. 1988. Influence of water activity of a solid substrate on the growth rate and sporogenesis of filamentous fungi. Biotechnol Bioeng 31: 457-463.

Gibson AM, Baranyi J, Pitt JI, Eyles MJ, Roberts TA. 1994. Predicting Fungal Growth: The Effect of Water Activity on *Aspergillus Flavus* and Related Species. Int J Food Microbiol 23: 419-431.

Grajek W, Gervais P. 1987. Influence of water activity on the enzyme biosynthesis and enzyme activities produced by *Trichoderma viride* TS in solid-state fermentation. Enz Microbiol Technol 9: 658-62.

Laukevics JJ, Apsite AF, Viesturs UE, Tengerdy RP. 1984. Solid-substrate fermentation of wheat straw to fungal protein. Biotechnol Bioeng 26: 1465-1474.

Lonsane BK, Saucedo-Castaneda G, Raimbault M, Roussos S, Viniegra-Gonzalez G, Ghildyal NP. 1992. Scale-up strategies for solid-state fermentation. Proc Biochem 27: 259-273.

Nagel FJI, Tramper J, Rinzema A. 2001a. Temperature control in a continuously mixed bioreactor for solid-state fermentation. Biotechnol Bioeng 72: 219-230.

Nagel FJI, Tramper J, Rinzema A. 2001b. Model for on-line estimation of moisture content during solid-state fermentation. Biotechnol Bioeng 72: 231-243.

Oostra J, Tramper J, Rinzema A. 2000. Model-based bioreactor selection for large-scale solid-state cultivation of *Coniothyrium minitans* spores on oats. Enz Microbiol Technol 27: 652-663

Oriol E, Raimbault M, Roussos S, Viniegra-Gonzales, G. 1988. Water and water activity in the solid-state fermentation of cassava starch by *Aspergillus niger*. Appl Microbiol Biotechnol 27: 498-503.

Ross KD. 1975. Estimation of water activity in intermediate moisture foods. Food Technol 29: 26-30.

Ryoo D, Murphy VG, Karim MN, Tengerdy RP. 1991. Evaporative temperature and moisture control in a rocking reactor for solid substrate fermentation. Biotechnol Tech 5: 19-24.

Sargantanis J, Karim MN, Murphy VG, Ryoo D, Tengerdy RP. 1993. Effect of Operating Conditions on Solid-Substrate Fermentation. Biotechnol Bioeng 42: 149-158.

Sargantanis J, Karim MN. 1994. Multivariable iterative extended kalman filter based adaptive control: case study of solid substrate fermentation. Ind Eng Chem Res 33: 878-888.

Saucedo-Castaneda G, Lonsane BK, Raimbault M. 1992. Maintenance of heat and water balances as a scale-up criterion for the production of ethanol by *Schwanniomyces castellii* in a solid-state fermentation system. Proc Biochem 27: 97-107.

Chapter 6

Water and glucose gradients in the substrate measured with NMR imaging during solid-state fermentation with Aspergillus oryzae

F.J.I. Nagel, H. Van As, J. Tramper, A. Rinzema

Submitted for publication
Biotechnology and Bioengineering

ABSTRACT

Gradients inside substrate particles cannot be prevented in solid-state fermentation. These gradients can have a strong effect on the physiology of the microorganisms, but have hitherto received little attention in experimental studies. We report gradients in moisture and glucose content during cultivation of *Aspergillus oryzae* on membrane-covered wheat-dough slices, that were calculated from ^{1}H-NMR images measured *in vivo*. We found that moisture gradients in the solid substrate remain small when evaporation is minimized. This is corroborated by predictions of a diffusion model. In contrast, strong glucose gradients developed. Glucose concentrations just below the fungal mat remained low due to high glucose uptake rates, but deeper in the matrix glucose accumulated to very high levels. Integration of the glucose profile gave an average concentration close to the measured average content. Based on published data, we expect that the glucose levels in the matrix cause a strong decrease in water activity. The results demonstrate that NMR can play an important role in quantitative analysis of water and glucose gradients at the particle level during solid-state fermentation, which is needed to improve our understanding of the response of fungi to this non-conventional fermentation environment.

INTRODUCTION

Solid-state fermentation (SSF) is defined as the growth of microorganisms, usually fungi, on a solid substrate in the absence of free-flowing water. For several biotechnological products, this cultivation method gives superior results compared to submerged fermentation (Oostra *et al.*, 2000; Nagel *et al.*, 2001a). Very little is known about the mechanistic background of the observed differences between SSF and submerged fermentation, although it is known that gene expression in SSF can differ from that in submerged cultures (Hata *et al.*, 1998; Ishida *et al.*, 1998). In Asia SSF is used on an industrial scale to produce enzymes such as amylases and proteases for hydrolysis of vegetable protein and starch during production of fermented foods such as soy sauce, tempe, miso and sake (Steinkraus, 1995). Application in Western countries is still unusual because there is insufficient insight in mechanisms that determine microbial behavior in SSF and a lack of well-established scale-up strategies.

A well-known problem in SSF is simultaneous control of temperature and moisture content of the solid substrate (Nagel *et al.*, 2001b): On an industrial scale temperature can only be controlled by evaporative cooling, which will result in a decrease in moisture content of the solids over time. The moisture loss is aggravated by the uptake of water in new microbial cells (Nagel *et al.*, 2001b). Simultaneously, extracellular microbial enzymes cause accumulation of e.g. sugars (Nagel *et al.*, 2001b). The water loss and solute accumulation will result in a decrease in water activity, which can have beneficial effects on metabolism (Gervais, 1990), but can also result in process failure (Nagel *et al.*, 2001a).

The aim of the work described in this article is to show the effect of fungal growth on gradients inside the substrate particles. The microorganism grows primarily near the outer surface of the substrate particle, due to oxygen supply limitations (Oostra *et al.*, 2001). The water uptake in new biomass and the evaporation are thus both localized at the particle surface, which will cause a moisture gradient in the particles. Furthermore, inhomogeneous distribution of microbial enzymes and uptake of sugars by the microorganisms will cause solute gradients. Intra-particle solute and moisture gradients have hitherto not been taken into account in physiological studies of SSF, because it is difficult to control and measure them.

We have used nuclear magnetic resonance imaging (MRI) to obtain spatially resolved moisture and glucose content measurements at the particle level during cultivation of *Aspergillus oryzae* on wheat dough slices. MRI allows non-destructive and non-invasive spatially resolved measurements in SSF systems at the particle level. NMR signals are characterized by a number of different parameters (Hills, 1998): The amplitude A is a direct measure for the amount of water in a sample. Two relaxation times (T_1 and T_2) of the excited nuclear spin system both correlate with the physical state of water in the sample (Van As and van Dusschoten, 1997; Van As and Lens, in press).

We show that both relaxation times (T_1 and T_2) linearly correlate with glucose and moisture content and that these correlations can be combined to calculate glucose and moisture content profiles in the dough from NMR images.

Water profiles in the dough calculated from the NMR images are compared to predictions of a mathematical model that describes water diffusion in the solid substrate driven by a constant water-uptake rate at the surface. Finally, the profiles for glucose and moisture content were used to estimate the water activity profile in the solid substrate.

WATER TRANSPORT MODEL

During growth of a fungus on the surface of a slab of solid substrate, the water content of the slab will decrease due to water uptake in new fungal cells and – depending on the mode and scale of operation - evaporation. The decrease in water content causes shrinkage of the substrate (Weber *et al.*, 1999; Oostra *et al.*, 2000).

Change in composition

The mass balance for water in an infinitesimal slice of the substrate slab reads

$$\frac{\partial}{\partial t}\left(\rho x_1 dz\right) = -\frac{\partial J_1''}{\partial z} dz \qquad [\mathrm{kg \cdot m^{-2} \cdot s^{-1}}] \qquad (1)$$

or

$$\rho dz \frac{\partial x_1}{\partial t} + x_1 \frac{\partial}{\partial t}\left(\rho dz\right) = -\frac{\partial J_1''}{\partial z} dz \qquad [\mathrm{kg \cdot m^{-2} \cdot s^{-1}}] \qquad (2)$$

where ρ is the density of the substrate matrix ($\mathrm{kg \cdot m^{-3}}$), X_1 is the mass fraction of water, J_1'' is the water flux ($\mathrm{kg \cdot m^{-2} \cdot s^{-1}}$), t is the time (s), z is the direction perpendicular to the slice surface (m), and dz is the slice thickness (m). At the top surface, where the fungus grows, we define z=0. The density of the substrate matrix depends on the moisture content.

The first term on the left-hand side in equation 2 represents the change in composition, the second the shrinkage of the slice. The shrinkage can be found from the mass balance for all components together. We assume that there is no flux of solids and solutes, which implies that the loss of dry matter due to fermentation is neglected. This

is further discussed in the Results and Discussion section. The mass balance for all components together reads:

$$\frac{\partial}{\partial t}\left(\rho dz\right) = -\frac{\partial J_1''}{\partial z} dz \qquad [\mathrm{kg \cdot m^{-2} \cdot s^{-1}}] \qquad (3)$$

Substitution of equation 3 in equation 2 gives

$$\frac{\partial x_1}{\partial t} = \frac{\left(1 - x_1\right)}{\rho}\left(-\frac{\partial J_1''}{\partial z}\right) \qquad [\mathrm{s^{-1}}] \qquad (4)$$

The flux J_1'' follows from Fick's first law

$$J_1'' = -D\frac{\partial}{\partial z}\left(\rho x_1\right) \qquad [\mathrm{kg \cdot m^{-2} \cdot s^{-1}}] \qquad (5)$$

If we neglect an influence of the matrix composition on the diffusion coefficient, equations 4 and 5 give the change in mass fraction of water

$$\frac{\partial x_1}{\partial t} = D\frac{\left(1 - x_1\right)}{\rho}\frac{\partial^2}{\partial z^2}\left(\rho x_1\right) \qquad [\mathrm{s^{-1}}] \qquad (6)$$

Boundary conditions for equation 6 are

$$z = 0 \qquad D\frac{d}{dz}\left(\rho x_1\right) = J_{1,0}'' \qquad (7)$$

$$z = L\left(t\right) \qquad \frac{d}{dz}\left(\rho x_1\right) = 0 \qquad (8)$$

Shrinkage

The mass balance for the dry matter over an infinitesimal slice gives the change in slice thickness dz. There is no transport of solids (or solutes), so this mass balance reads

$$\frac{\partial}{\partial t}\left(\rho x_2 dz\right) = 0 \tag{9}$$

where x_2 is the weight fraction of dry matter. Taking into account that $x_1 + x_2 = 1$, this gives

$$\rho\left(1-x_1\right)\frac{\partial}{\partial t}\left(dz\right) = dz\left(\rho - \left(1-x_1\right)\frac{\partial \rho}{\partial x_1}\right)\frac{\partial x_1}{\partial t} \tag{10}$$

The density of the slab is affected by the composition. Data on oat grains (Oostra *et al.*, 2000) show that the density can be described with a linear relation

$$\frac{1}{\rho} = \left(\frac{1}{\rho_1} - \frac{1}{\rho_2}\right)x_1 + \frac{1}{\rho_2} \tag{11}$$

where ρ_1 and ρ_2 are the densities of water and dry solids, respectively (kg·m^{-3}). Combination of equations 10 and 11 gives the change in slice thickness.

$$\frac{\partial}{\partial t}\left(dz\right) = dz\left(\frac{1}{\left(1-x_1\right)} + \left(\frac{\rho}{\rho_1} - \frac{\rho}{\rho_2}\right)\right)\frac{\partial x_1}{\partial t} \tag{12}$$

Numerical approximations

Equation 6 was solved with a Forward-in-Time-Centered-in-Space approximation that takes into account the variation in Δz caused by the shrinkage (Crank, 1975):

$$\frac{\Delta x_{1,i}}{\Delta t} = 2D\frac{\left(1-x_{1,i}\right)}{\rho_i}\frac{\dfrac{\Delta z_{1,i}}{\Delta z_{1,i+1}}\rho_{i+1}x_{1,i+1} - \left(1+\dfrac{\Delta z_{1,i}}{\Delta z_{1,i+1}}\right)\rho_i x_{1,i} + \rho_{i-1}x_{1,i-1}}{\Delta z_{1,i}{}^2 + \Delta z_{1,i}\Delta z_{1,i+1}} \tag{13}$$

For equation 12 we used as discrete solution

$$\Delta\left(\Delta z_i\right) = \frac{\Delta z_i}{2}\left[\left(\frac{1}{1-x_{1,i}} + \left(\frac{\rho_i}{\rho_1} - \frac{\rho_i}{\rho_2}\right)\right)\Delta x_{1,i} + \left(\frac{1}{1-x_{1,i-1}} + \left(\frac{\rho_{i-1}}{\rho_1} - \frac{\rho_{i-1}}{\rho_2}\right)\right)\Delta x_{1,i-1}\right] \tag{14}$$

In equations 13 and 14, i refers to the slice number and the grid point at the bottom of this slice, i-1 refers to the grid point at the top of this slice, and i+1 refers to the grid point at the bottom of the next slice.

The initial place step was set equal to the distance between two pixels in the NMR-image, viz. $\Delta z = 2.3438\cdot10^{-4}$ m; the initial slice thickness was $L=10.078\cdot10^{-3}$ m (44 grid points). The initial water content of the wheat dough was $x_1(t=0) = 0.483$ kg water per kg total weight. The time step used in the simulations was $\Delta t < 0.2\ \Delta x^2/D$ s.

Errors in the overall water balance were below 0.1% in all simulations.

Water flux at surface

Two values were used for the water flux at the top of the dough slab J_1'', viz. one based solely on water uptake in new-formed fungal cells and one that in addition takes evaporative cooling into account:

$$J_{1,0}'' = X_{W,X}\, r_X'' \tag{15}$$

$$J_{1,0}'' = X_{W,X}\, r_X'' + \frac{r_X''}{Y_{X/O}}\frac{\Delta H_O}{\Delta H_W} \tag{16}$$

where

$X_{W,X}$	= 2.08 kg·kg^{-1} DM	the moisture content of the fungal biomass, which was previously shown to remain constant during cultivation on wheat dough (Nagel *et al.*, 2001b),
$r_X^{"}$	:	the rate of increase in biomass dry weight found during cultivation of *Aspergillus oryzae* on wheat dough [kg·m^{-2}·s^{-1}]
$Y_{X/0}$	= 0.029 kg·mol^{-1}	the yield coefficient of biomass on oxygen in this system (Nagel *et al.*, 2001b),
ΔH_0	= 460 kJ·mol^{-1}	the reaction enthalpy per mol of oxygen (Roels, 1983),
ΔH_W	= 2419 kJ·kg^{-1}	the evaporation enthalpy of water at 35°C (Lide, 1993).

In equation 15 metabolic water production, water needed for starch hydrolysis and water evaporation are neglected. The first two terms were shown to be relatively small (Nagel *et al.*, 2001b); water evaporation was minimized in the experimental set-up for *in vivo* NMR.

Diffusion coefficient

We assumed that the water diffusion coefficient in the wheat dough is not affected by changes in dough composition. One value was estimated from a relation for the diffusion coefficient of water in gelatinized wheat flour (Andrieu and Stamatopoulos, 1986). For 35°C and the initial moisture content of our dough (0.483 kg water per kg total weight), this gave a diffusion coefficient of $6 \cdot 10^{-11}$ m^2·s^{-1}. Another value was estimated from published (Furuta *et al.*, 1984) diffusion coefficients in maltodextrin (partially hydrolyzed starch) solutions, which gave a value of $1.4 \cdot 10^{-10}$ m^2·s^{-1} for the temperature and initial water content of our dough.

MATERIALS AND METHODS

^{1}H-NMR-imaging

Nuclear magnetic resonance imaging (MRI) experiments were carried out with a 0.5 T NMR imager, equipped with an electromagnet (Bruker, Karlsruhe, Germany) and an S.M.I.S. console (Guilford, England) operating at 20.35 MHz. An NMR probe with an internal diameter of 4.5 cm and actively shielded gradients (Doty Scientific, Columbia, USA) was fitted in the 14-cm gap of the magnet. Donker *et al.* (1997) have previously described the applied Inversion-Recovery-Multiple-Spin-Echo (IR-MSE) pulse sequence. During the *in vivo* MRI experiment an image was recorded every 2 hours, alternatively in normal and perpendicular to normal direction (Figure 1). In total 19 images were recorded in normal view and 19 images perpendicular to normal, by recording the complex (real and imaginary) signal of 12 echoes at an inter-echo time of 2.7 ms for each image. The repetition time was set to 0.8 s and each measurement was repeated four times. In the Inversion-Recovery domain, we used 6 increments of 40 ms. The field of view was 3 cm x 3 cm and the images contained 128x128 pixels, thus the resolution was 234 μm. To reduce the effects of heterogeneity in the dough, 88 NMR data points obtained at the same height in the dough were averaged.

The obtained data were first filtered with a Gaussian filter (330Hz per pixel), before fast Fourier transformation and phasing. The real part of the MRI images was fitted simultaneously in the two dimensions assuming mono-exponential decay for both T_1 and T_2, and using a fitting routine based on the Marquardt-Levenberg algorithm (Press *et al.*, 1989). Amplitude, T_1 and T_2 images were obtained by fitting the following function for the decay of the signal intensity on the NMR data (Donker *et al.*, 1997):

$$S_{x,y}\left(T_{ir},t\right)=S_{x,y}\left(T_{ir}=\infty,t=0\right)\cdot\left(1-2\cdot e^{\left(-T_{ir}/T_{1,x,y}\right)}\right)\cdot e^{\left(-t/T_{2,x,y}\right)} \tag{17}$$

where $S_{x,y}$ (T_{ir},t) is the signal intensity in pixel x,y at time t in the inversion recovery step T_{ir}, $S_{x,}$y (T_{ir}=∞, t=0) is the extrapolated amplitude in pixel x,y at t = 0, representing the spin density, T_1 is the longitudinal relaxation time [s], T_2 is the transversal relaxation time [s], T_{ir} is the inversion recovery incrementing delay [s], and t is the time after the soft 90° pulse [s].

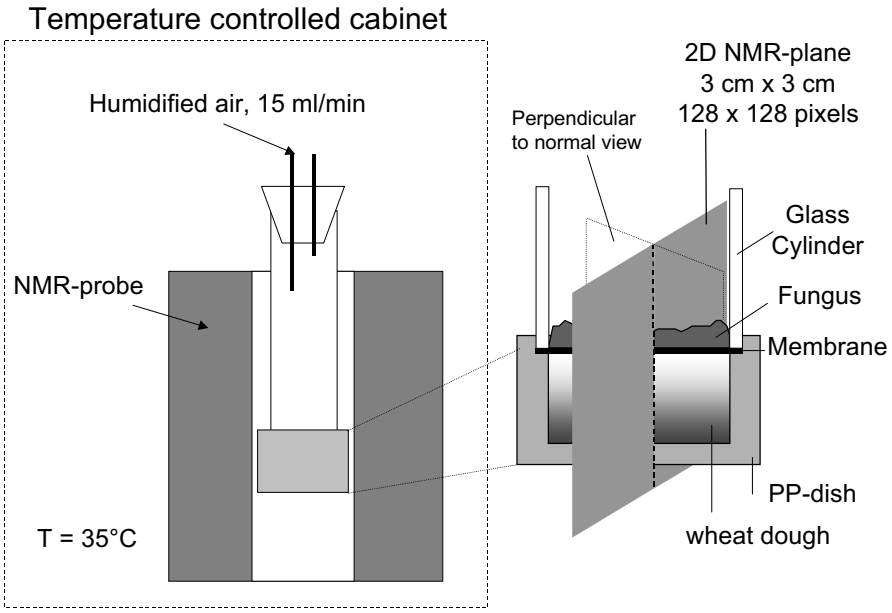

Figure 1. Experimental setup for the *in vivo* MRI experiment, in which *Aspergillus oryzae* was cultivated on a wheat-dough model substrate inside the NMR-probe. Two dimensional images were recorded every two hours, alternating in normal view and perpendicular to normal view.

Calibrations

Three wheat dough discs with moisture contents of 0.44, 0.5 and 0.55 kg/kg total and no added glucose were placed together in the NMR system to record amplitude, $1/T_1$ and $1/T_2$ images using the IR-MSE-sequence. Each calibration data point was obtained from an average of at least 728 pixels from the MRI images. The same procedure was followed with three wheat discs with different glucose concentrations (0.025, 0.05 and 0.075 kg/kg total) and a moisture content of 0.5 kg/kg total. Calibration measurements were conducted at 28°C. Linear regression analysis was applied to the amplitude data of the MRI images. We assumed that the effects of glucose and moisture content on T_1 and T_2 are not correlated and can be described by the following linear equations:

$$\frac{1}{T_1(x,t)} = \frac{1}{T_1(x,0)} - B_{WT1} \cdot \left[x_1(x,0) - x_1(x,t) \right] - B_{GT1} \cdot \left[x_G(x,0) - x_G(x,t) \right] \quad (18)$$

$$\frac{1}{T_2(x,t)} = \frac{1}{T_2(x,0)} - B_{WT2} \cdot \left[x_1(x,0) - x_1(x,t) \right] - B_{GT2} \cdot \left[x_G(x,0) - x_G(x,t) \right] \quad (19)$$

where

$T_i(x,t)$	=	the relaxation time (T_i) at position x and time t	[s]
$x_1(x,t)$	=	the moisture content at position x and time t	[kg·kg^{-1} total]
$x_G(x,t)$	=	the glucose concentration at position x and time t	[kg·kg^{-1} total]
B_{WTj} , B_{GTj}		coefficients for moisture content and glucose concentration respectively; j: 1 or 2	[kg total ·kg^{-1}·s^{-1}];

Regression coefficients B_{WTi} and B_{GTi} were determined using linear regression analysis on either the glucose or moisture data set. The average values for all pixels of both relaxation times at the start of the *in vivo* MRI experiment was used for $1/T_i(x,0)$ The equations were rearranged to allow direct calculation of $x_1(x,t)$ and $x_G(x,t)$ in Figures 7 and 8 from relaxation times.

Microorganism, substrate and incubation

Aspergillus oryzae CBS 570.65 was obtained from Centraal Bureau voor Schimmelcultures, Baarn, the Netherlands. A sporangiospore suspension was prepared and utilized for inoculation as described previously (Nagel *et al.*, 2001a). Wheat flour slices (diameter 3 cm, height 1.5 cm) were prepared as described previously (Nagel *et al.*, 2001b). Slices were placed in polypropylene petri dishes, covered with a sterile 0.45-µm polyamide membrane (Schleicher & Schuell, NL17 ST) and inoculated with ca. $3 \cdot 10^6$ spores evenly distributed on top of the membrane. The initial moisture content of the wheat flour slices was 0.483 kg/kg total. One dish was placed in the NMR probe at 35°C (Figure 1) and several others were placed in a temperature-controlled cabinet at 35°C for biomass measurements.

The dish in the NMR probe was aerated (airflow 15 ml/min, water-saturated at 35°C). The surroundings of the NMR probe were maintained at 35°C with air (30 L/min, RH ≈ 50%, T = 35°C).

Analysis

The moisture content of the wheat dough and biomass, the biomass dry weight and the glucose content of the dough were determined as described previously (Nagel *et al.*, 2001b).

Water activity

The water activity profile was calculated from the glucose and moisture concentrations using the Ross equation (Ross, 1975):

$$a_w\left(mixture, n \text{ components}\right) = a_w\left(1\right)\cdot a_w\left(2\right)\ldots\cdot a_w\left(n\right) \tag{20}$$

where $a_w\ (i)$ is the water activity in the binary mixture with component i. In our work this is either a water-glucose mixture, or a cooked mixture of water and wheat flour. Moisture-contents were converted to water activities using a desorption isotherm for wheat (Nagel *et al.,* 2001b); glucose concentrations were converted to water activities using data of Bonner and Breazeale (1965).

RESULTS AND DISCUSSION

Calibrations

NMR signals are characterized by a number of different parameters. The aim of the calibration was to quantitatively relate the parameters A ($=S_{x,y}(T_{ir}=\infty, t=0)$, equation 17), $1/T_1$ and $1/T_2$ deduced from NMR images to physical parameters in the solid substrate, viz. the glucose concentration and moisture content. Figure 2 shows the results of the calibration measurements. Table 1 shows the regression constants obtained by fitting equations 18 and 19. The first relaxation time (T_1) is more sensitive to glucose content and the second relaxation time (T_2) is more sensitive to moisture content. The combination of T_1 and T_2 allows the calculation of moisture and glucose concentrations. Apart from the effect of glucose, no additional effect of starch breakdown was observed in calibration measurements with dough incubated with amylase (results not shown).

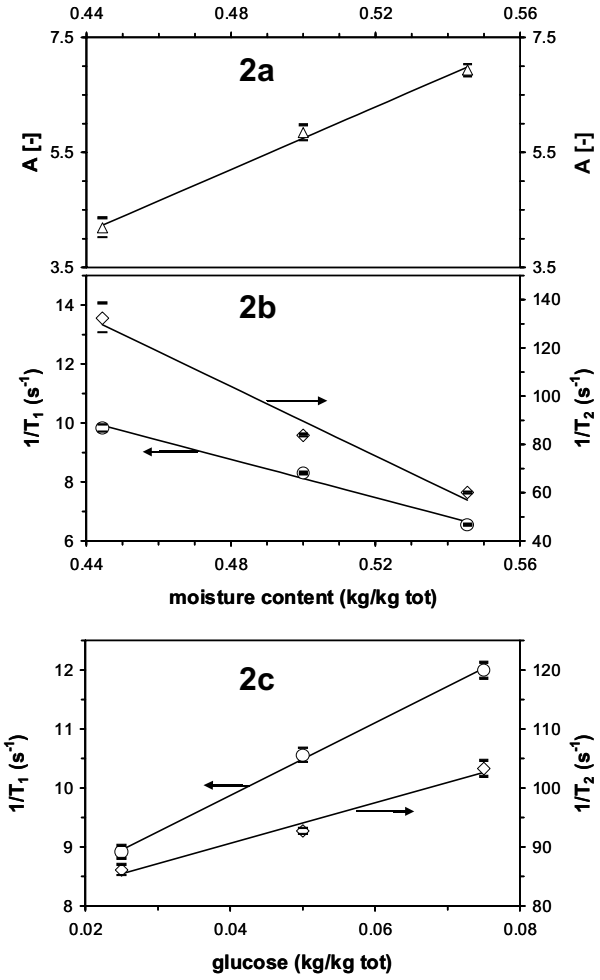

Figure 2a, 2b and 2c. Different wheat discs with variable concentrations of water and glucose were analyzed in the NMR system in order to calibrate NMR parameters A (**Fig. 2a,** △), T1 (**Fig. 2b**, ○) and T2 (**Fig. 2c,** ◇) for moisture content and glucose. The solid lines are fitted using linear regression. The horizontal bars represent the standard error in the measurement. The SR-MSE images from which the parameters are calculated are shown in the graphs; the images are turned 90° clockwise with respect to the wheat dough in Figure 1. Wheat discs with varying moisture content contain no glucose; moisture content of the wheat discs with varying glucose concentrations is 0.5 kg per kg total weight.

Table 1. Calibration of time constants T_1 and T_2 against glucose content and water content of wheat dough, and of the amplitude *A* against water content. Values in brackets are standard errors.

Regression analysis of T_1 and T_2 data versus water and glucose content (equations 18 and 19)		
Parameter	Value	r^2
$1/T_1$ (x,0)	7.358	
B_{WT1}	-32.3 (3.2)	0.981
B_{GT1}	61.6 (2.4)	0.997
$1/T_2$ (x,0)	103.733	
B_{WT2}	-720.4 (100.3)	0.962
B_{GT2}	343.6 (45.5)	0.966

Regression analysis of amplitude data versus moisture content ($x_1 = C_A + B_A \cdot A$)		
B_A	0.037 (0.002)	0.993
C_A	0.29 (0.01)	

Growth experiments

Aspergillus oryzae was cultivated on wheat dough in a membrane model system (Nagel *et al.*, 2001b). After a lag phase of ca. 29 hours a linear increase in biomass dry weight ($5.8 \cdot 10^{-3}$ kg·m^{-2}·h^{-1}) was found (Figure 3), which is in agreement with results of previous experiments with this system (Nagel *et al.*, 2001b). The relative standard deviation was 17% for three experiments. From this biomass formation rate, we calculated a water flux of $1.2 \cdot 10^{-2}$ kg·m^{-2}·h^{-1} for use in the diffusion model.

In order to study water-potential gradients in the solid substrate during SSF, *A. oryzae* was cultivated inside the NMR probe (Figure 1) for three days. Figure 4 shows MRI images in normal view with a 12-hours interval.

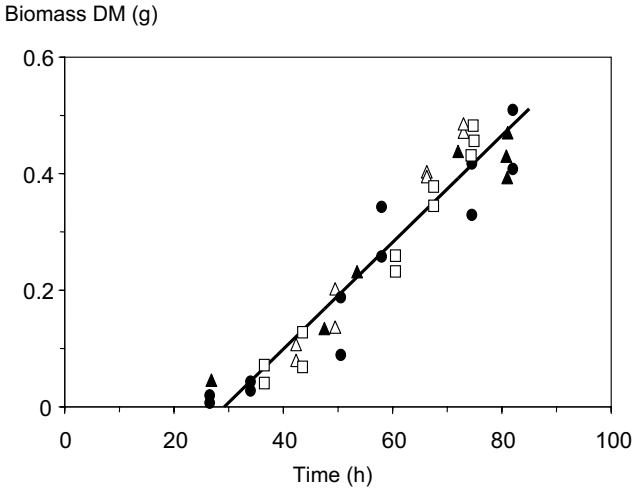

Figure 3. Biomass production during four different cultivations of *Aspergillus oryzae* on the membrane model system (Nagel *et al.*, 2001b). The biomass production rate ($5.8 \cdot 10^{-3}$ kg·m^{-2}·h^{-1}) was estimated by linear regression analysis of all data (—).

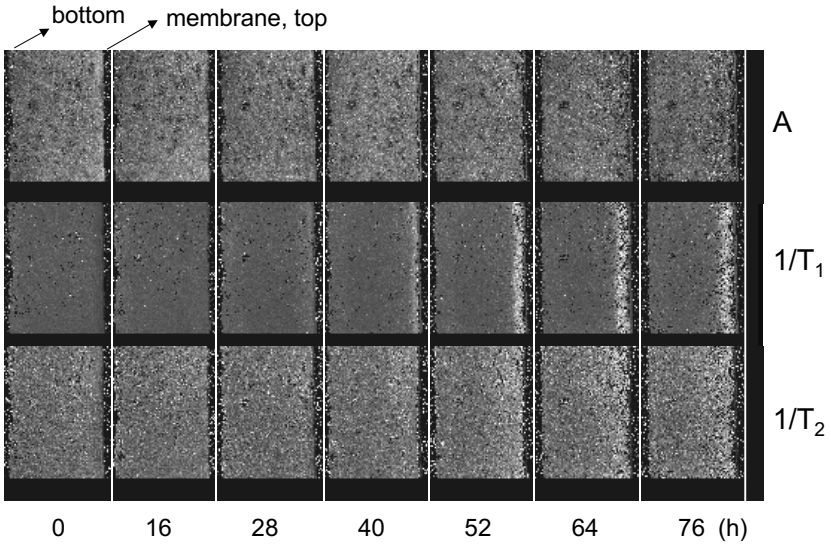

Figure 4. MRI images for amplitude (A) and both reciprocal relaxation times ($1/T_1$ and $1/T_2$) during cultivation of *Aspergillus oryzae* on a membrane model system. The time axis is displayed horizontally with the cultivation time shown below the images. The images are turned 90° clockwise with respect to the wheat dough in Figure 1.

The images perpendicular to normal view gave similar results. Figures 5 and 6 show T_1 and T_2 values obtained from these images as a function of substrate depth and time. The T_1 images show a clear gradient and the fungus - located on the right hand side of the images - is clearly visible. The measurement of T_1 is quite sensitive: the profile at t=0 shows the absorption of the inoculation liquid. High T_2 values are observed near the membrane where the fungus is present. This is explained by the fact that the moisture content of fungal biomass is twice that of the solid substrate and that T_2 is much more sensitive to moisture content (Table 1) than to glucose content. The T_2 images display high heterogeneity, but nevertheless a gradient in T_2 can be observed. The amplitude images do not show much variation during the course of fermentation.

These images are not homogeneous, which is an indication for heterogeneity in the dough. The scatter that is observed mainly in A and T_2, is probably due to inhomogeneous spatial distribution of dough components, flour particle size distribution and problems that are intrinsic to NMR imaging of systems with low moisture content. In such systems, part of the water is strongly bound to the substrate matrix and exhibits a different relaxation behavior. This results in short T_2 values, which are difficult to determine accurately. Furthermore, in non-imaging NMR measurements of wheat dough we observed multi-exponential decay for T_2 (data not shown). All MRI measurements were interpreted assuming mono-exponential decay, which may have caused part of the observed scatter.

Figure 7 shows the glucose content as a function of depth in the wheat dough, calculated from T_1 and T_2 values after 64 hours cultivation time. Just below the top surface the glucose concentration is very low after 64 hours, but strong glucose accumulation occurs between 1 and 2 mm depth. The absence of glucose deeper in the matrix is in accordance with the slow diffusion of amylase in a concentrated starch matrix found by Mitchell *et al.* (1991). The glucose uptake in the fungal mat explains the concentration decrease towards the membrane. The average glucose concentration of the whole dough calculated from the glucose profile after 64 hours is 0.094 kg per kg DM, which agrees well with the average concentration of 0.092 kg per kg DM (with a relative standard deviation of 8.7%) that was measured after ca. 64 hours in three previous experiments with this model system (Nagel *et al.*, 2001b).

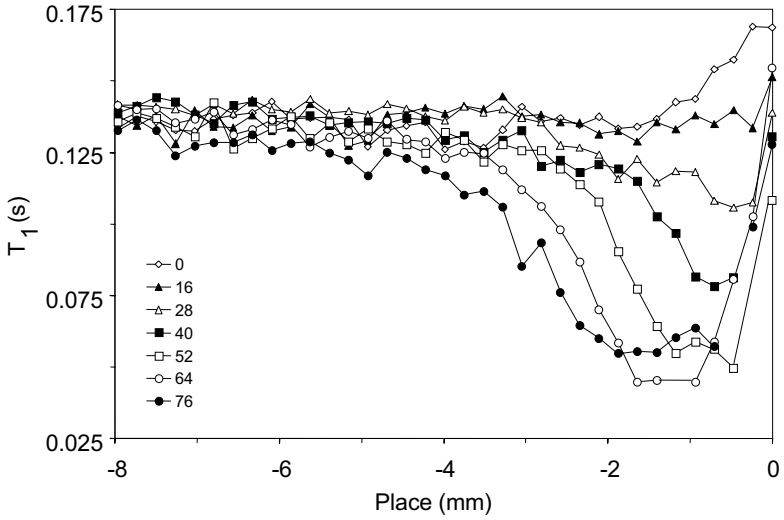

Figure 5. T_1 profile as a function of depth in the wheat dough deduced from MRI images during cultivation of *Aspergillus oryzae* on a membrane model system. Numbers in the legend represent the cultivation time in hours. Position 0 indicates the position of the membrane.

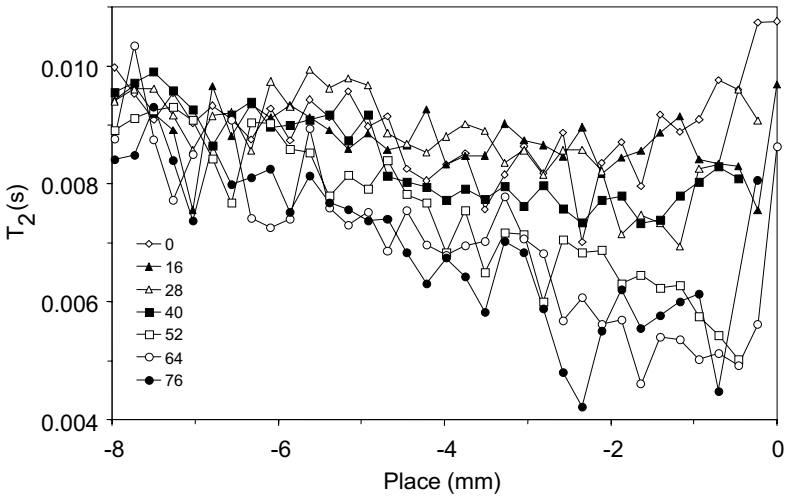

Figure 6. T_2 profile as a function of depth in the wheat dough deduced from MRI images during cultivation of *Aspergillus oryzae* on a membrane model system. Numbers in the legend represent the cultivation time in hours. Position 0 indicates the position of the membrane.

Figure 8 shows a moisture-content profile calculated from T_1 and T_2 values using equations 18 and 19, and one calculated from amplitude values, both after 64 hours cultivation. It is not possible to verify which of the two moisture-content profiles calculated from the NMR data is most realistic, due to the scatter in the underlying measurements. The deviation in the moisture content calculated from T_1 and T_2 between 1 and 2 mm depth probably indicates that glucose and moisture content no longer contribute independently to the relaxation behavior at high glucose concentrations. The local glucose concentrations found here are far higher than average values found previously that were used to set the calibration interval. With respect to the amplitude, one should note that the high glucose concentrations occurring between 1 and 2 mm depth could cause a significant contribution of the protons of glucose to the amplitude measurement.

Two predictions of the water-diffusion model are also shown in Figure 8, which were calculated with different values of the diffusion coefficient (see model section). For the densities in equation 11 we used ρ_1= 1000 kg·m^{-3} and ρ_2=1564 kg·m^{-3}; the latter value was derived from measurements of wet wheat dough density. Considering the scatter in experimental data, the water-diffusion model describes the overall behavior of both measured profiles adequately. This is remarkable, considering that solute diffusion and matrix effects on the diffusion coefficient were neglected.

The simulation profiles and the two experimental profiles show a relatively small moisture-content gradient in the wheat dough, from ca. 0.5 kg per kg total weight at the bottom of the substrate to ca. 0.4 kg per kg total weight underneath the membrane. The model predicts a loss of 8.3% of the initial amount of water between 29 and 64 hours, and a reduction in dough volume of 4.2% of the initial value. Water uptake in new fungal biomass alone does not cause serious moisture shortage during a 64-hours cultivation of *A. oryzae* on wheat. This is in agreement with results obtained in fermenters in which evaporation was minimized (Nagel *et al.,* 2001a).

In summary, glucose and moisture-content profiles have been estimated from relaxation times deduced from MRI images. The glucose profile correlates well with a previously measured average glucose concentration, and the moisture profile correlates reasonably with predictions of the water-diffusion model.

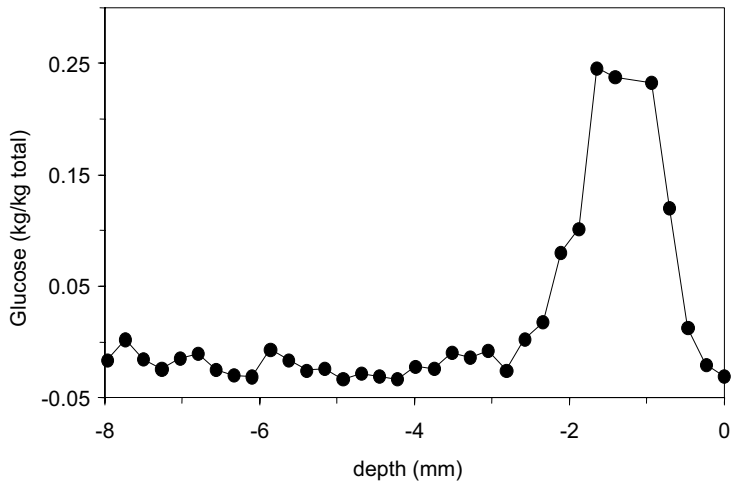

Figure 7. Glucose profile as a function of depth in the wheat dough calculated from both relaxation times (T_1 and T_2) after 64 hours (●) cultivation of *Aspergillus oryzae* on wheat dough. Position 0 indicates the position of the membrane.

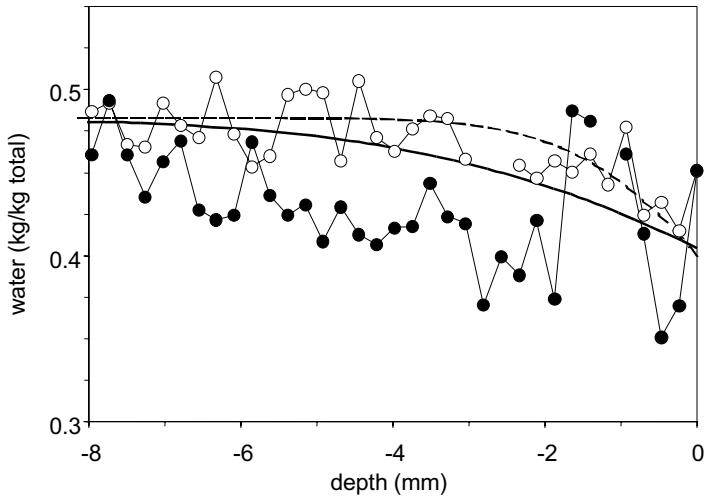

Figure 8. Moisture-content profile as a function of depth in the wheat dough calculated from relaxation times (●) and amplitude (○) after 64 hours cultivation of *Aspergillus oryzae* on wheat dough. The curved lines represent profiles calculated with the water-diffusion model for 64 hours cultivation time with different diffusion coefficients, viz. D=6·10^{-11} m^2·s^{-1} (- - -) and D=1.4·10^{-10} m^2·s^{-1} (——). Position 0 indicates the position of the membrane.

Water activity

Besides water, glucose can have a significant effect on the water activity in SSF (Nagel *et al.*, 2001b). Although other solutes might be present in the wheat dough, we believe that glucose is the most important one, given the relative abundance of starch compared to e.g. protein in wheat and the high glucose levels measured. Figure 9 shows the combined effect of water and glucose on the water activity after 64 hours, calculated with equation 20 (Ross, 1975). Comparison of Figures 7-9 shows that free glucose is mainly responsible for the observed a_w decrease between 1 and 2 mm depth. Immediately below the fungal biofilm, the water activity was not affected due to the glucose uptake into the fungal mat.

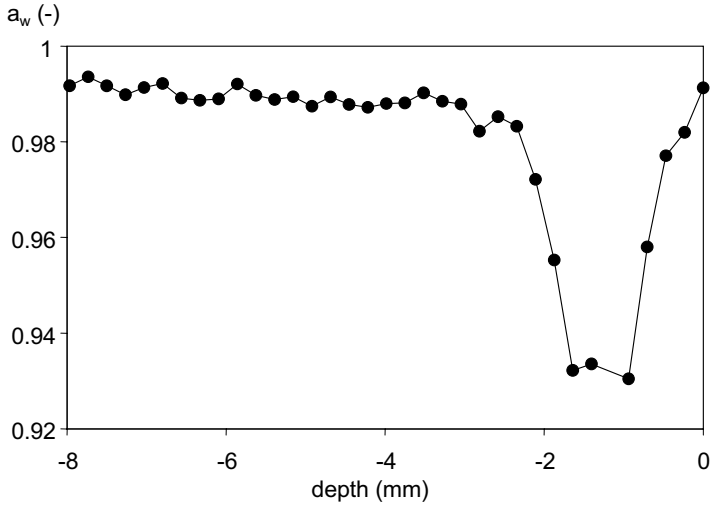

Figure 9. Water-activity profile as a function of depth in the wheat dough calculated using equation 20 (Ross, 1975) with glucose and moisture-content profiles after 64 hours cultivation of *A. oryzae* on wheat dough. Position 0 indicates the position of the membrane.

An important question is how an SSF culture without a membrane would behave. Hyphae of *A. oryzae* can penetrate into wheat dough at a rate of 0.25 $mm \cdot h^{-1}$, but oxygen diffusion limitation will prevent the mycelium in the dough from reaching the high cell density that is reached in the fungal mat on the surface (Rahardjo and Rinzema, manuscript in prep.). Consequently, these penetrating hyphae will not be

able to lower the glucose concentration in their vicinity as efficiently as the hyphae in the fungal mat did and will be subjected to a low water activity and low oxygen concentration. This may well trigger physiological responses that contribute to the unique results of SSF reported in literature (Ito, 1993).

The water activity of the solid substrate is one of the most important variables in SSF. It is influenced by a number of biochemical and physical processes, like enzymatic starch hydrolysis, microbial uptake of water and glucose and excretion of metabolites, and evaporation. In order to understand SSF, these processes have to be studied at the particle level. NMR imaging can play an important role in non-invasive studies of gradients caused by these processes. This article shows that moisture and glucose-content profiles can be determined simultaneously using the combined T_1 and T_2 measurements.

Simulations

Above we used the water diffusion model to verify the moisture-content profile calculated from NMR data. In this section we will discuss (1) predictions of the model for fermentations with evaporative cooling, and (2) assumptions and parameter estimates.

Evaporative cooling will drastically increase the amount of water lost from the substrate matrix compared to the loss in the NMR experiment (Nagel *et al.*, 2001b). This implies that the water activity at the particle surface may decrease even when glucose does not accumulate there. The water transport model has been used to simulate the effect of the higher moisture flux at the substrate surface that occurs in case of evaporative cooling (equation 16, Figure 10). The large difference between local water content and water activity at the dough surface and the average values shows that evaporative cooling causes sharp moisture gradients in the wheat dough slab. The model predicts that after 50 hours of evaporative cooling the moisture content at the wheat dough surface drops below 0.3 kg per kg total weight. This implies that the water activity drops below 0.925 (Nagel *et al.*, 2001a), assuming that fungal activity is not affected and the glucose concentration at the surface remains low due to uptake by the fungus. Such a low water activity would in fact lower the fungal growth rate by 50% (Gibson *et al.*, 1994). This simulation result is in agreement with the breakdown of fungal growth during fermentation of wheat in a paddle mixer with

evaporative cooling that was reported previously (Nagel *et al.*, 2001a). A more detailed comparison of predictions of the current model to the previously reported results obtained with wheat grains requires that the model be extended to take into account the degradation of substrate dry matter and differences in respiration kinetics between the wheat dough model substrate and whole grains.

After 64 hours fermentation, the predicted water loss with evaporative cooling is 34.4% of the initial amount of water and the shrinkage is 17.2% of the initial volume; both values are roughly four times higher than those found with water uptake in new cells only. Shrinkage causes serious problems in unmixed packed beds (Weber *et al.*, 1999; Oostra *et al.,* 2000). Losses predicted for the dough slab with evaporative cooling are still relatively small compared to those expected for real substrates such as wheat grain (diameter ca. 4 mm), due to the high initial thickness of the dough slab (height 1.5 cm).

In view of the complexity of the SSF system, models and advanced measurements are needed to elucidate the importance of gradients in the substrate particles. By necessity, such models are simplified. One of the main assumptions made in the current model is that there is no diffusion of glucose or other solutes. Obviously diffusion of solutes would affect the water transport. Extension of the model to include transport of solutes requires the incorporation of a bio-kinetic model to predict production of low molecular weight solutes such as glucose, which in turn requires the incorporation of fungal growth and enzyme production, transport of oxygen and enzymes, and hydrolysis kinetics. Current work in our laboratory aims at such model extensions.

Another important simplification in the current model is the use of a constant diffusion coefficient, despite the obvious influence of matrix composition on the diffusion coefficient. This is justified because our primary aims were verification and improvement of understanding, not validation. Furthermore, reduction of the scatter in NMR data and experiments designed to deliver more extreme moisture gradients would be more important than model refinement when validation is aimed for. If matrix effects on the diffusion coefficient are to be included in a future model, these could be verified directly using pulsed field gradient (PFG)-NMR (Van Dusschoten *et al.*, 1995; Beuling *et al.*, 1998). The value of spatially resolved diffusivity measurements for the interpretation of measured oxygen concentration profiles has recently been demonstrated for a microbial mat (Wieland *et al.*, in press).

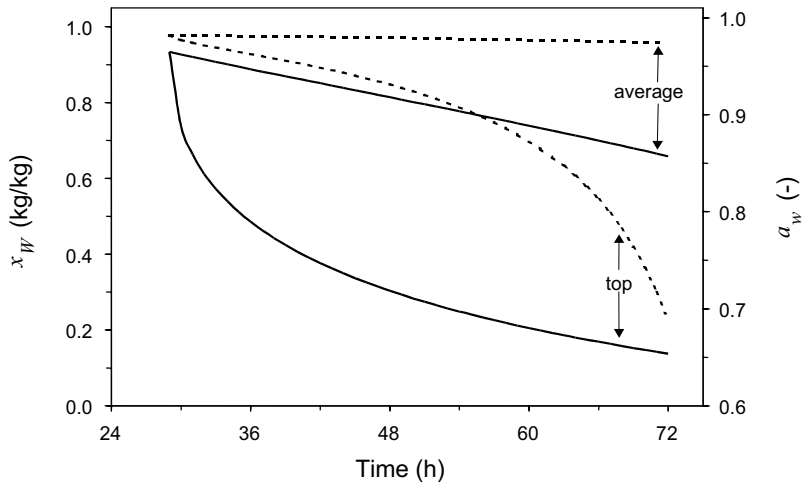

Figure 10. Simulated water content (x_W , drawn lines) and water activity (a_w, dashed lines) at the top surface of the dough and on average in the dough, taking into account water uptake in new fungal cells and evaporation (equation 16). The water content was calculated with the water transport model, using a diffusion coefficient of D=10^{-10} $m^2 \cdot s^{-1}$ and assuming that the fungal activity remains constant. The water activity was calculated from the sorption isotherm of wheat (Nagel *et al.*, 2001b), assuming that there is no solute accumulation. Fungal growth starts after 29 hours.

CONCLUSIONS

^{1}H-NMR imaging is a powerful technique to study solid-state fermentation at the particle level. The water potential of the solid substrate is one of the most important variables in SSF-research and is influenced by a number of biological processes near the biofilm, like enzymatic hydrolysis, water and glucose uptake and excretion of metabolites. In order to predict and model biomass formation, these processes have to be studied and measured non-invasively on particle level. This article shows how NMR-imaging can play an important role in elucidating complex biological processes.
Water-activity profiles in the solid substrate were estimated during fungal growth, based on moisture-content and glucose profiles calculated from relaxation times deduced from NMR-signals. The moisture-content profile was reasonably well

predicted with a water-diffusion model and the glucose profile correlated well with overall glucose measurements.
This article shows that ^{1}H-NMR imaging can be used for quantitative analysis of solid-state fermentation on particle level. Furthermore, this article is a first demonstration of using combined T_1 and T_2 measurements to measure moisture-content and glucose profiles during solid-state fermentation.

ACKNOWLEDGEMENTS

The Dutch Graduate School on Process Technology (OSPT) financed this study. The authors thank M.S.N. Bakker, F. Vergeldt and P.A. de Jager for assistance with the experiments.

LIST OF SYMBOLS

a_w	water activity	[-]
A	amplitude NMR signal	[-]
B_{WTj}	regression coefficient in equation 18	[-]
B_{GTj}	regression coefficient in equation 19	[-]
D	diffusion coefficient	[$m^2 \cdot s^{-1}$]
ΔH_O	reaction enthalpy per mol oxygen	[$kJ \cdot mol^{-1}$]
ΔH_W	evaporation enthalpy of water at 35°C	[$kJ \cdot kg^{-1}$]
i	slice or grid number	
J_1''	water flux	[$kg \cdot m^{-2} \cdot s^{-1}$]
$J_{1,0}''$	water flux at top surface	[$kg \cdot m^{-2} \cdot s^{-1}$]
r_X''	biomass production rate	kg DM$\cdot m^{-2} \cdot s^{-1}$
$S_{x,y}(T_{ir},t)$	signal intensity in pixel x, y at time t in the inversion recovery step T_{ir}	[-]
t	time	[s]
T_1	longitudinal relaxation time	[s]
T_2	transversal relaxation time	[s]
T_{ir}	inversion recovery incrementing delay	[s]
x_1	weight fraction of water	[kg·(kg total)$^{-1}$]
x_2	weight fraction of dry solids	[kg·(kg total)$^{-1}$]
x_G	weight fraction of glucose	[kg·(kg total)$^{-1}$]
$X_{W,X}$	moisture content of biomass	[kg·(kg DM)$^{-1}$]
$Y_{X/O}$	yield of biomass on oxygen	[$kg \cdot mol^{-1}$]
z	distance from top surface, along axis perpendicular to surface	[m]
ρ	matrix density	[$kg \cdot m^{-3}$]
ρ_1	density of water	[$kg \cdot m^{-3}$]
ρ_2	density of dry solids	[$kg \cdot m^{-3}$]

REFERENCES

Andrieu J, Stamatopolous A. 1986. Moisture and heat transfer modeling during durum wheat pasta drying. In: Mujumdar AS (ed.) Drying '86, Volume 2. London: Hemisphere Publishing Corporation.

Beuling EE, Van Dusschoten D, Lens P, Van den Heuvel JC, Van As H, Ottengraf SPP. 1998. Characterization of the diffusive properties of biofilms using pulsed field gradient-nuclear magnetic resonance. Biotechnol Bioeng 60: 283-291.

Bonner OD, Breazeale WH. 1965. Osmotic and activity coefficients of some nonelectrolytes. Carbohydr 10: 325-327.

Crank J. 1975. The mathematics of diffusion 2nd ed. Oxford: Clarendon press.

Donker H, Van As H, Snijder H, Edzes H. 1997. Quantitative 1H-NMR imaging of water in white button mushrooms (*Agaricus bisporus*). Magn Reson Imag 15: 113-121.

Furuta T, Tsujimoto S, Makino H, Okazaki M, Toei R. 1984. Measurement of diffusion coefficient of water and ethanol in aqueous malto dextrin solution. J Food Eng 3: 169-86.

Gervais P. 1990. Water activity: a fundamental parameter of aroma production by micro-organisms. Appl Microbiol Biotechnol 33: 72-75.

Gibson AM, Baranyi J, Pitt JI, Eyles MJ, Roberts TA. 1994. Predicting fungal growth: The effect of water activity on *Aspergillus flavus* and related species. Int J Food Microbiol 23:419–431.

Hata Y, Ishida H, Ichikawa E, Kawato A, Suginami K, Imayasu S. 1998. Nucleotide sequence of an alternative glucoamylase-encoding gene (glaB) expressed in solid-state culture (koji) of *Aspergillus oryzae*. Gene 207: 127-134.

Ishida H, Hata Y, Ichikawa E, Kawato A, Suginami K, Imayasu S. 1998. Regulation of glucoamylase-encoding gene (glaB) expressed in solid-state culture (koji) of *Aspergillus oryzae*. J Ferment Bioeng 86: 301-307.

Ito K. 1993. Studies on the Mycelial Growth of *Aspergillus oryzae* on Rice Grain. J Soc Ferment Bioeng 71: 115-127.

Lide DR. 1993. CRC Handbook of chemistry and physics, 74th edition. Boca Raton, FL: CRC Press.

Mitchell DA, Do DD, Greenfield PF, Doelle HW. 1991. A semi-mechanistic mathematical model for growth of *Rhizopus oligosporus* in a model solid-state fermentation system. Biotechnol Bioeng 38: 353-362.

Nagel FJI, Tramper J, Bakker MSN, Rinzema A. 2001a. Temperature control in a continuously mixed bioreactor for solid-state fermentation. Biotechnol Bioeng 72: 219-230.

Nagel FJI, Tramper J, Bakker MSN, Rinzema A. 2001b. Model for on-line estimation of moisture content during solid-state fermentation. Biotechnol Bioeng 72: 231-243.

Oostra J, Tramper J, Rinzema A. 2000. Model-based bioreactor selection for large-scale solid-state cultivation of *Coniothyrium minitans* spores on oats. Enz Microbiol Technol 27: 652–663.

Oostra J, Le Comte EP, Van den Heuvel JC, Tramper J, Rinzema A. 2001. Intra-particle oxygen diffusion limitation in solid-state fermentation. Biotechnol Bioeng 75: 13-24.

Press, WH, Flannery BP, Teukolsky SA, Vetterling WT. 1989. Numerical recipes in pascal: The art of scientific computing. Cambridge: Cambridge University Press.

Roels JA. 1983. Energetics and kinetics in biotechnology. Amsterdam: Elsevier.

Ross KD. 1975. Estimation of water activity in intermediate moisture foods. Food Technol 29: 26-30.

Steinkraus KH. 1995. Handbook of indigenous fermented foods, 2nd edition. New York: Marcel Dekker Inc.

Van As H, Lens P. Use of ^{1}H-NMR to study transport processes in porous biosystems. J Ind Microbiol Biotechnol (in press).

Van As H, Van Dusschoten D. 1997. NMR methods for imaging of transport processes in microporous systems. Geoderma 80: 389-403.

Van Dusschoten D, De Jager P, Van As H. 1995. Extracting diffusion constants from echo-time-dependent PFG NMR data using relaxation-time information. J Magn Resonance Series A 116: 22-28.

Weber FJ, Tramper J, Rinzema A. 1999. A Simplified Material and Energy Balance Approach for Process Development and Scale-Up of *Coniothyrium minitans*. Conidia Production by Solid-State Cultivation in a Packed-Bed Reactor. Biotech Bioeng 65: 447-458.

Wieland A, Van Dusschoten D, Damgaard LR, De Beer D, Kühl M, Van As H. Fine-scale measurement of diffusivity in a microbial mat with NMR imaging. Limnol Oceanograph (in press)

Chapter 7

Process control in commercial bioreactors for solid-state fermentation

SUMMARY

Over the latest decade it has been demonstrated that solid-state fermentation (SSF) can be used to produce a variety of biomolecules of interest to the food and pharmaceutical industry. These products can compete with those produced by submerged fermentation (SmF) and in many cases higher productivities or better product characteristics are obtained using SSF. The Western world still hesitates to apply SSF on a large scale, due to scale-up problems. This paper gives an overview of recent advances in process control in large-scale SSF systems. Two types of bioreactors are discussed that can facilitate industrial application of SSF: (1) the koji bioreactor, which is suitable mainly for low added-value products for the food and feed industries; and (2) alternative bioreactors based on industrial solids mixers that may facilitate the industrial production of pharmaceutical products.

INTRODUCTION

Solid-state fermentation (SSF) is defined as a fermentation process occurring in the absence of free-flowing water, employing a natural solid substrate or an inert carrier as solid support. SSF is applied since ancient times for the production of fermented foods like soy sauce, tempeh, mold-ripened cheeses (Wood, 1998) and solid-waste composting. Besides that, SSF has the potential to be used in a wide variety of other processes like bioremediation, biological feed detoxification, biotransformation, biopulping and the production of a variety of value-added products, which were recently reviewed by Pandey *et al*. (2000c). During the latest decade, research on SSF has shown many attractive products, mainly on lab-scale (Pandey *et al.*, 1999; Pandey *et al.*, 2000a, 2000b). For several enzymes (Pandey *et al*., 1999), flavours (Ferron *et al*., 1996), colorants (Johns and Stuart, 1991) and other substances of interest to the food industry, it has been demonstrated that SSF can give higher yields (Tsuchiya *et al*., 1994) or better product characteristics (Acuña-Arguelles *et al*., 1995; Solís-Pereira *et al*., 1993), compared to similar products obtained by submerged fermentation (SmF) (Maldonado and de Saad, 1998). We also observe an increasing number of commercially attractive applications, which produce molecules of interest to the pharmaceutical industry (Merck, 1990; 1991), like antibiotics (Ohno *et al*., 1995;

Venkateswarlu *et al*., 2000), fungicides (Sadhukhan *et al*., 1999), antigens (Maruyama *et al*., 2000) and cholesterol-lowering agents (www.biocon.com; Baxter *et al*., 1998). Some of these applications clearly show the superiority of SSF over SmF. For example, Maruyama *et al*. (2000) reported differences in glycosylation of heterologous protein produced by *A. oryzae* in SmF and SSF conditions. Besides that, important economic advantages of SSF are the lower power requirements, lower downstream-processing costs (Kumar and Lonsane, 1987) and lower investment costs (Castilho *et al*., 2000).

In the Western world, SmF has become the standard process for microbial products after WWII. This is due to (1) large R&D efforts in the penicillin industry; and (2) the developments in genetic engineering, which allow the production of almost any product using a standard organism in a standard submerged fermenter. In South-East Asia, research attention was directed towards the industrialization of fermented foods like soy sauce, miso, natto, sufu, tempeh, and the like, to meet the growing demand of these products caused by a rapidly increasing population (Steinkraus, 1989). These products were all made using SSF and large bioreactors were developed from 1950 onwards (Fukushima, 1989; Yokotsuka, 1985).

The Western world still hesitates to use SSF for industrial applications due to scale-up problems. This in contrast to Asia where SSF is applied on a large scale and apparently, scale-up problems have been solved. What is the reason for the success of these processes and how are scale-up problems solved? An example of such an application is Japanese soy-sauce production, where a koji bioreactor (very wide and shallow packed bed for SSF) is used to produce enzymes for the subsequent hydrolysis phase. This bioreactor is rarely discussed in literature, as there is a general perception that the knowledge behind its design is inaccessible. In this paper, the scarce knowledge present in literature is combined, to provide insight in the scale-up and process control applied in koji bioreactors. In our opinion this bioreactor concept can be further improved and adapted to serve a wide range of applications in the food industry.

Products of interest to the pharmaceutical industry and biological control agents based on fungal spores often require aseptic operation and advanced control possibilities with respect to moisture content and temperature. Commercially available solids mixers, which are already used in the pharmaceutical industry, could be a suitable alternative

for these applications and will facilitate approval by authorities based on FDA and GMP guidelines. In this paper we will outline the advantages and disadvantages of solids mixers, which could be used for these applications.

KOJI BIOREACTORS

Many reviews dealing with scale-up of SSF explain that commercialization of SSF is hampered by a lack of quantitative strategies for design and operation of large-scale SSF bioreactors (Lonsane *et al*., 1992; Pandey, 1991, 1992). On the other hand, many commercial applications in Asia use SSF in bed volumes of 250 m^3 or more (Yokotsuka, 1985). In literature, little attention is paid to these bioreactors, because it is generally believed that the details of these processes are either closely guarded trade secrets or described in Japanese literature. However, bioreactors that are successful on a large scale or pilot scale in Europe (Durand and Chereau, 1988; Lyven, www.lyven.com; Gerrits, 1996), Mexico (Anon., 1999), China (Xue *et al*., 1992) and Chili (Fernandez *et al*., 1996), show remarkable resemblance to bioreactors used in the koji industry. In this paragraph, the knowledge about koji bioreactors available in Western literature is reviewed (Yokotsuka, 1986; Yokotsuka, 1985; Xu, 1990; Fukushima, 1989; O'Toole, 1997; Shurtleff and Aoyagi, 1980).

In a koji bioreactor, a packed bed of solid substrate rests on a perforated plate. Continuous forced aeration is applied and intermittent mixing. Three types of koji bioreactors can be distinguished: a batch-type with a fixed rectangular perforated plate (12m x 5m), a batch-type with a moving circular perforated plate (∅ 15-30 m) and a continuous type with a moving circular perforated plate (∅ 38 m).

The circular koji bioreactor operated in batch-mode is most widely used in Japan and will be discussed in more detail. The diameter of the circular plate can be up to 30 m, which results in a maximum bed volume around 250 m^3, which is equal to ≈ 90 ton dry matter. A round perforated stainless steel plate is used to support the solid substrate with a bed-height between 30 and 40 cm (Yokotsuka, 1985). The packed bed is mixed two times during a two-days solid-state fermentation in order to prevent air channeling caused by shrinkage and breakage of the bed. The perforated plate rotates very slowly while several vertical screw mixers in a row mix the solid substrate. This set-up is

quite similar to the mixing screws mounted on a rotating arm used in the malting process in beer production.

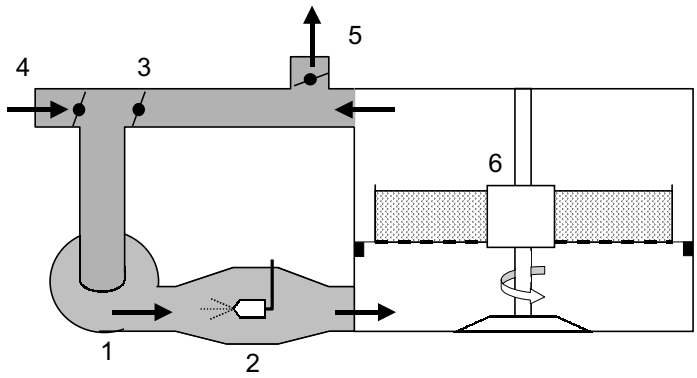

Figure 1. Schematic, simplified drawing of an air circulation loop of a koji bioreactor: 1 blower, 2 humidifier, 3 air control valve, 4 fresh-air inlet, 5 air outlet, 6 packed bed.

TEMPERATURE CONTROL

In soy-sauce koji cultivation, the temperature is kept at 30-35°C in the early stage for mycelium growth and less than 30°C in the later stage for protease formation. Two mechanical mixing periods (after ≈19h and ≈ 31h) are used to cool the solid substrate. Mixing is crucial for temperature control in these fermentations as it (1) reduces the pressure drop across the bed by disentangling the network of mycelia with the solid substrate; and (2) eliminates air channels caused by shrinkage and breakage of the packed bed. Both aspects are important for evaporative cooling as the air flow is inversely related to the overall pressure drop and air channels decrease the effective surface area for water evaporation and increase the mass transfer resistance for evaporation. Between the mixing events, the temperature of the bed is controlled with the control valves in the air-circulation loop (Figure 1). Depending on the temperature of the koji, air is recirculated or fresh air is taken from outside in order to slightly change the relative humidity. The relative humidity of the air is close to saturation throughout the koji cultivation. A high superficial air velocity (ca. 11 cm/s) is used in these bioreactors (Yokotsuka, 1986), which is equal to 16.5 - 22 vvm (F_{air} [L/min]/V_{bed} [L]), *i.e.* at least 10 times more than in SmF. This high air flow minimizes temperature

gradients in the packed bed and provides enough capacity for heat removal. The air is humidified close to saturation for two reasons: (1) a more even evaporation throughout the bed occurs; and (2) water evaporation is less compared to a situation where the inlet air is not saturated with water as explained in Table 1.

Table 1. Comparison between two temperature control strategies; (1) water-saturated air, RH = 100% and (2) unsaturated air, RH = 75%. Both strategies use the same air flow rate and the same inlet air temperature and remove the same quantity of metabolic heat production (27.9 W/kg DM). The temperature control strategy that uses water-saturated air has a larger difference between outlet and inlet temperature, which implies that more energy is needed for heating of the air and less water is evaporated.

	(1) saturated inlet air	(2) unsaturated inlet air
F_{air} (mol dry air/(s kg DM))	0.03272	0.03272
Inlet air conditions	T_{in}=30°C, RH = 100%	T_{out}=30°C, RH = 75%
Outlet air conditions	T_{out}=35°C, RH = 100%	T_{out}=32.34°C, RH = 100%
Metabolic heat production Q_{met} (W/kg DM)	27.9	27.9
$\Delta h_{a,evap}$ (J/mol dry air)	680.7	767.2
$\Delta h_{a,conv}$ (J/mol dry air)	171.3	84.7
Water evaporation rate Q_w (mol/(kg DM h))	1.910	2.064
% convection	20%	10%

The energy balance during SSF in pseudo-steady state reads:

$$0 = F_{air} \cdot \left(h_{a,out} - h_{a,in}\right) - Q_{met} \qquad [\text{J}\cdot(\text{kg DM}\cdot\text{s})^{-1}] \quad (1)$$

in which the enthalpy of moist air (h_a) is calculated as:

$$h_a = C_{p,air} \cdot T + a_w \cdot y_{w,sat} \cdot \left(C_{p,V} \cdot T + H_V\right) \qquad [\text{J}\cdot\text{mol dry air}^{-1}] \quad (2)$$

in which the moisture content of the saturated air ($y_{w,sat}$) is calculated as:

$$p_{wsat}(T) = \exp\left(23.59 - \frac{4045}{(T + T_{ref}) - 37.7}\right) \quad \text{[Pa]} \quad (3)$$

$$y_{w,sat}(T) = \frac{p_{wsat}(T)}{p - p_{wsat}(T)} \quad \text{[mol·mol dry air}^{-1}\text{]} \quad (4)$$

The enthalpy of the moist air is split into a convection part ($\Delta h_{a,conv}$, heating of the dry air and water vapor) and a water evaporation part ($\Delta h_{a,evap}$):

$$\Delta h_{a,conv} = C_{p,air} \cdot (T_{out} - T_{in}) + C_{p,V} \cdot \left(a_{w,out} \cdot y_{w,sat}(T_{out}) \cdot T_{out} - a_{w,in} \cdot y_{w,sat}(T_{in}) \cdot T_{in}\right)$$

$$\text{[J·mol dry air}^{-1}\text{]} \quad (5)$$

$$\Delta h_{a,evap} = H_V \cdot \left(a_{w,out} \cdot y_{w,sat}(T_{out}) - a_{w,in} \cdot y_{w,sat}(T_{in})\right) \quad \text{[J·mol dry air}^{-1}\text{]} \quad (6)$$

The water evaporation rate (Q_w) is calculated as:

$$Q_w = F_{air} \cdot (y_{w,out} - y_{w,in}) \cdot 3600 \quad \text{[mol·(kg DM·h)}^{-1}\text{]} \quad (7)$$

$$\%\, convection = \frac{\Delta h_{a,conv}}{\Delta h_{a,conv} + \Delta h_{a,evap}} \quad \text{[-]} \quad (8)$$

in which

$C_{p,air}$	=	29.2	heat capacity dry air	[J·(mol·°C)$^{-1}$]
$C_{p,V}$	=	33.7	heat capacity dry air	[J·(mol·°C)$^{-1}$]
T_{ref}	=	273		[K]
a_w	=	RH%/100	water activity	[-]
H_V	=	45000	heat of vaporization of water	[J·(mol)$^{-1}$]

MOISTURE CONTROL

The moisture content of the solid substrate is usually not controlled during koji cultivations. For example for soy-sauce koji, the preferred initial moisture content is about 0.75 g/g DM and drops to ≈ 0.43 g/g DM in the finished koji. This difference in initial and final moisture content provides enough water evaporation to absorb 77% of the total heat production of a koji cultivation (Box 1).

Box 1: Fate of water

The water balance during solid-state fermentation consists of 4 contributions as displayed in the figure below (Nagel *et al*., 2001b). First, during fungal growth extracellular water is incorporated into newly synthesized mycelium, which has a moisture content between 75% (Larroche *et al*., 1992 a,b) and 66% (Nagel *et al*., 2001b). Second, due to metabolic heat generation, extracellular water evaporates. Third, metabolic water is produced as a result of glucose breakdown. The fourth contribution is the water needed for breakdown of starch into glucose. For the estimation of the a_w, the dry-matter balance in such a model is just as important as the water balance. Solid substrate is converted into biomass, H_2O and CO_2 and this will affect the extracellular dry matter and therefore also the extracellular moisture content (Smits *et al*., 1998; Larroche *et al*., 1998; Nagel *et al*., 2001b). Solid substrate losses amount up to 25 - 50% of the initial substrate present (Nagel *et al*., 2001b).

In the following table, the water and dry matter balance are calculated for soy-sauce koji in order to estimate the extracellular moisture content at the end of the cultivation. Data are taken from literature and the equations are described by Nagel *et al*. (2001b).

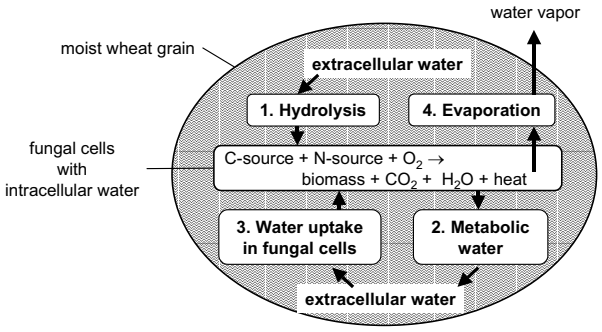

Symbol	Parameter	Reference	Value	Unit
ΔH_o	Metabolic heat generation	Roels, 1983	460	kJ/mol O_2
Mw_X	Molecular weight biomass	Lide, 1993	0.02442	kg/mol
$Y_{X/O2}$	Yield for biomass on oxygen	Nagel *et al*., 2001b	1.16	Cmol X/mol O_2
$Y_{W/O2}$	Yield for water on oxygen	Nagel *et al*., 2001b	1.22	mol W/mol O_2
Mw_w	Molecular weight water	Lide, 1993	0.018	kg/mol
H_v	Heat of vaporization	Lide, 1993	2500	kJ/kg water
$X_{W,X}$	Moisture content biomass	Nagel *et al*., 2001b	2	kg/kg DM
$\%Q_{conv}$	% convective air cooling	Table 1	20%	[-]
$Q_{heat,cum}$	Cumulative heat production	Yokotsuka, 1985	1965	kJ/kg IDM
$X_{W,ini}$	Initial moisture content koji	Yokotsuka, 1985	0.754	kg/kg IDM
$X_{W,end}$	Final moisture content koji	Yokotsuka, 1985	0.429	kg/kg DM
DM_{loss}	Overall dry matter loss	O'Toole, 1997	0.15	kg/kg IDM
Symbol	**Bioprocess quantity**	**Calculations**	**Value**	**Unit**
O_{2cum}	Cumulative oxygen consumption	$Q_{heat,cum} / \Delta H_o$	4.272	mol/kg IDM
$M_{Wtot,end}$	Final water amount koji	$X_{W,end} * (1- DM_{loss})$	0.365	kg/kg IDM
M_X	Biomass production	$O_{2cum} * Y_{X/O2} * Mw_X$	0.121	kg/kg IDM
$M_{W,met}$	Metabolic water	$O_{2cum} * Y_{W/O2} * Mw_w$	0.094	kg/kg IDM
$M_{W,X}$	Biomass water	$M_X * X_{W,X}$	0.242	kg/kg IDM
$M_{W,evap}$	Evaporated water	$X_{W,ini} - M_{Wtot,end} + M_{W,met}$	0.483	kg/kg IDM
$X_{W,ext}$ (t_{end})	Extracellular water content	$(M_{Wtot,end} - M_{W,X})/ (1- M_X - DM_{loss})$	0.168	kg/kg DM
$Q_{evap,cum}$	Cumulative water evaporation enthalpy	$M_{W,evap} * H_v$	1208	kJ/kg IDM
$Q_{conv,cum}$	Cumulative convective air cooling	$Q_{evap,cum} / (1- \%Q_{conv}) * \%Q_{conv}$	302	kJ/kg IDM
$\%Q_{evap}$	% evaporative cooling	$Q_{evap,cum} / Q_{heat,cum} * 100\%$	77%	[-]

Box 1 also shows that the fungal growth rate is probably limited by low water activities towards the end of the cultivation as the extracellular water content (outside fungal cells) of the finished koji is estimated at 0.168 g/g DM. On the other hand, these low water activities limit bacterial growth, which explains why these cultivations can be carried out under non-sterile conditions. A second advantage of these low water activities is that they stimulate protease production (Narahara *et al*., 1982), which is necessary for the subsequent hydrolysis phase in soy-sauce production.

SCALE-UP

Scale-up of these bioreactors for koji cultivation seems to be relatively straightforward and based on a few empirical design rules. The packed-bed height is kept constant at about 30 to 40 cm (Xu, 1990; Yokotsuka, 1985) and scale-up is usually realized by increasing the bed diameter. Temperature control is achieved by using a superficial air velocity of 11 cm/s (Yokotsuka, 1986). These design rules only apply for koji cultivation of a fast growing fungus, *Aspergillus oryzae*, on a mixture of soya flakes and wheat bran and these conditions may not be suitable or necessary for other SSF applications. For example, the superficial air velocity depends on the heat production rate of the fungus and the desired temperature profile over the packed bed (Weber *et al*., 1999; Oostra *et al*., 2000; Hardin *et al*., 2000), which can differ significantly between fermentations. The packed-bed height depends on the pressure drop and compressibility of the solid substrate. In box 2 we verified mechanistic scale-up models from literature against literature data on koji making (Terui *et al*., 1958). In this example, the superficial air velocity was calculated using the model described by Weber (1999), which yielded a similar value as reported by Yokotsuka (1986).
However, many design details still remain unknown and scale-up of these bioreactors is still mainly empirical. More research is needed for a better understanding of the rationale behind current design practice.

Box 2: Scale-up rules for evaporative cooling in a packed bed

The model of Weber and co-workers (1999) decribes a simplified energy balance for a packed-bed bioreactor that neglects heat losses via the wall. The necessary air flow is calculated for a constant inlet and outlet temperature of the air that differ 5°C (assumed). The maximum attainable oxygen consumption rate for soy-sauce koji is used in the energy balance to calculate the maximum air flow necessary to maintain this temperature difference in a large-scale bioreactor.

$$F_{air} = \frac{Q_{met}}{\left(h_{a,out} - h_{a,in}\right)} \qquad [\text{mol dry air}\cdot(\text{kg DM}\cdot\text{s})^{-1}] \quad (9)$$

$F_{air,max}$ is equal to 0.0425 mol dry air/(kg DM s) to maintain a temperature gradient of 5°C over the packed bed at maximum heat-production rate. The average heat production rate was equal to 14.7 W/kg DM which yielded an $F_{air,average}$ equal to 0.0172 mol dry air/(kg DM s)

The superficial air velocity is calculated using Equation 10:

$$v_{air} = \frac{F_{air} \cdot \rho_{DM,bulk} \cdot H \cdot R \cdot \left(T_i\right)}{P} \qquad [\text{m}\cdot\text{s}^{-1}] \quad (10)$$

The maximum superficial air velocity is equal to 0.15 m/s and the average value is 0.06 m/s. These values are similar to the value (0.11 m/s) reported by Yokotsuka (1986) for soy-sauce koji cultivation, for which it is unclear if this value represents the maximum or average air velocity.

List of symbols and values used in the equations 9 and 10 above:

Symbol	***Unit***	***Value***	***Reference***
$Q_{met,max}$	W/kg DM	36.3	Terui *et al*., 1958
$Q_{met,average}$	W/kg DM	14.7	Terui *et al*., 1958
$h_{a,out}$ - $h_{a,in}$	J/mol	853	Chosen, Table 1 T_{in}=30°C, T_{out}=35°C, $RH_{in\&out}$=100%
ρ_{bulk}	kg DM/m^3	347	Terui *et al*., 1958
H	m	0.40	Yokotsuka, 1986
R	J/(mol K)	8.314	Lide, 1993
T_i	K	303	Chosen
P	Pa	$1\cdot10^5$	Assumed

FUTURE PROSPECTS

We believe that the koji bioreactor is a promising bioreactor concept that could be applicable to many SSF applications. Many industrialized applications in Asia show that these bioreactors can be used successfully to produce low to medium-added-value products (Wood, 1998; Mudgett, 1986).

The bioreactor design provides a solution to prevent air channeling, caused by shrinkage and breakage of the bed, which currently limits the use of packed beds on a large scale (Weber *et al*., 2002). Furthermore, shear forces are low due to the small bed height combined with the small number of mixing events. Temperature control is adequate using this design due to mixing and the shallow bed combined with a high air velocity over the bed. Besides these advantages, improvements have to be made to the design in order to make the bioreactor more applicable for a wide range of applications. The bioreactor is operated non-aseptically and high bacterial counts of 10^8-10^9 g^{-1} are found in the final koji (Yokotsuka, 1985), which limits its use for other SSF applications. Furthermore, the moisture-content of the solid substrate is not controlled as heat is mainly be removed by evaporative cooling. Improvements should be made to the hygienic design, to allow better hygienic operation possibilities, similar to the aseptic SSF pilot bioreactors described in literature (Fernandez *et al*., 1996; Chamielec *et al*., 1994; Bandelier *et al*., 1997). Recently, a commercial aseptic pilot-scale koji bioreactor (∅ 1 m) was developed allowing hygienic operation with respect to aeration, sampling, inoculum addition and substrate sterilization (www.fujiwara-jp.com).

The design of the koji bioreactor permits that large-scale fermentation conditions can easily be mimicked on labscale using an insulated packed bed (height = 30 - 40 cm) with a mixing device and a similar air-flow and air-humidity control. Such a down-scaled, aseptically designed, lab-scale version of a koji bioreactor, could be used to evaluate this bioreactor concept and potential scale-up problems of commercially attractive applications for SSF.

INDUSTRIAL SOLIDS MIXERS: ALTERNATIVE BIOREACTORS FOR SSF?

In the latest decade, it has been demonstrated that many pharmaceuticals can be produced using SSF (Robinson *et al*., 2001; Pandey *et al*., 2000c). The production of pharmaceuticals by SSF has major implications on the design of the bioreactor, for it should comply with current FDA and GMP guidelines. These guidelines state that closed or contained equipment should be used that can be sanitized or sterilized to prevent contamination. The manufacturing process should be controlled and reproducible and the consistency of the process has to be validated.

In order to facilitate the validation of the process consistency, adequate control of the most important process parameters in SFF, which are temperature and moisture content, is a necessity. Besides that, some pharmaceutical applications require moisture-content control for optimal productivity (Liu and Tzeng, 1999; Sekar and Balaraman, 1998). As evaporative cooling is the most important cooling mechanism to control the temperature, dehydration is inevitable. The only possibility to control the moisture content of the solid substrate is to add water during fermentation. Water has to be added homogeneously to the solid substrate, which requires a mixing device inside the bioreactor. Summarizing, it can be stated that for the production of pharmaceuticals using SSF, a hygienically designed, mixed bioreactor is required with the ability to homogeneously add water during fermentation. Potential new bioreactors that meet all these requirements and that are already used in the pharmaceutical industry are commercially available solids mixers like orbiting-screw mixers (Box 3), plough/paddle mixers and ribbon mixers.

Mixing will certainly improve process control in SSF, but the effect of mixing on the productivity of SSF is a controversial subject. Some papers show that the improved heat and mass transfer caused by mixing outweighs the disadvantages of mixing (Aidoo *et al*., 1984; Stuart *et al*., 1999; Nagel *et al*., 2001a; Fung and Mitchell, 1995), while in other studies a reduced productivity is observed (Bajracharya and Mudgett, 1979; Silman, 1980; Desgranges *et al*., 1993; Han *et al*., 1999). In all cases, mixing sets additional requirements to the SSF system. First, the solid substrate should be able to withstand shear forces and should not have the tendency to aggregate to clumps as a result of mixing. Second, mixing could damage the fungus and thus affect its growth and metabolism, an effect that could also depend on the bioreactor scale.

Box 3: Orbiting-screw mixer versus scraped-drum mixer

The picture on the right shows an orbiting-screw mixer for pharmaceutical applications (www.hosokawamicron.com). The upper graph shows the temperature control achieved in a 50 L orbiting-screw mixer during solid-state fermentation using a double heating jacket and discontinuous mixing (Nagel and Rinzema, unpublished data). The lower graph shows a comparison between the cumulative CO_2 production in the orbiting-screw mixer and small (1.5 L) mixed bioreactor (scraped-drum reactor, Nagel *et al*., 2001b) for the cultivation of *Aspergillus niger* on moistened oat grains (Nagel and Rinzema, unpublished data). The orbiting-screw mixer contained initially 11 kg dry oats and the small mixed fermentor 0.142 kg dry oat. These preliminary results indicate that fungal growth can withstand the shear forces in such a bioreactor.

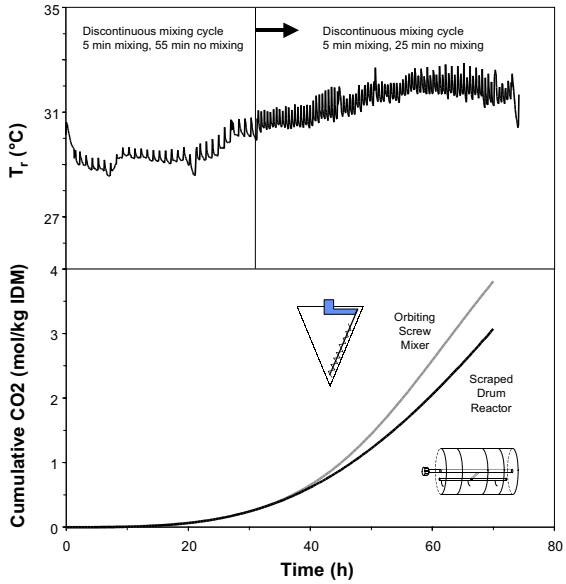

Orbiting-screw mixer, pharma design (Hosokawa micron B.V., by permission)

For certain substrates like grains, it has been shown that the fungus is protected by the seed coat (Nagel *et al*., 2001a; Oostra *et al*., 2000) in a continuously mixed 35-dm^3 paddle mixer. Similar preliminary studies in our laboratory revealed that respiration rates of *Aspergillus niger* on oat grains were similar in a 50-L orbiting-screw mixer and in a 1.5-L scraped-drum mixer (Box 3, unpublished data), which showed that scale-up of such a fermentation did not affect fungal growth.

At the moment the effect of mixing on SSF is not fully understood. Therefore, more research is needed to determine the optimum lay-out of the mixing device and frequency of mixing events in order not to disturb fungal growth while maintaining acceptable temperature and moisture-content control. Development of mechanistic models for the mixing process may help to understand the complex interactions in a mixed SSF system (Schutyser *et al*., 2001).

In summary, the solids mixers mentioned above have several advantages:

- They are designed according to the latest hygienic-design requirements with respect to cleaning and sterilization.
- They exert low shear forces on the solid substrate.
- The solid substrate can be pretreated (soaking, sterilization) and inoculated inside the solids mixer, in order to prevent contamination.
- Water can be added homogeneously during mixing for moisture-content control.
- Temperature control is improved by the external cooling jacket and mixing.

These solids mixers are expensive compared to equipment currently used for SSF, especially when all hygienic-design considerations are taken into account. They will probably only be economically feasible for the production of high-added-value products, like pharmaceuticals.

MOISTURE CONTROL IN PRACTICE

The impact of water activity (a_w) on the formation of products like aroma compounds, enzymes and toxines is widely recognised and optimum values for product formation usually differ from those for growth (Gervais, 1990; Gervais and Sarette, 1990; Gervais *et al*, 1988a). Large-scale bioreactors depend almost entirely on evaporative cooling for temperature control. As a result, bioreactor performance is limited by dehydration effects in many cases. However, very few studies describe the control of moisture content during SSF.

Research on the water balance during SSF has revealed three important aspects with respect to moisture-content control (Table 2). First, a clear distintinction should be made between water inside fungal cells and water present in the solid substrate outside fungal cells (extracellular water) (Oriol *et al.*, 1988; Larroche *et al*., 1992b). Second, the water present outside fungal cells determines the water activity experienced by the fungus itself, and is determined by an osmotic and a matrix potential (Gervais *et al*., 1988b; Oriol *et al*., 1988; Narahara *et al*., 1982).

The osmotic potential depends on the concentration of solutes like glucose and amino acids outside the fungal cells and the matrix potential depends on the extracellular water content and the desorption isotherm of the solid substrate. Third, dry solid substrate is converted into biomass, CO2 and H2O, and this dry matter loss directly influences the extracellular water content (Nagel et al., 2001b; Smits et al., 1998; Larroche et al., 1998).

The extracellular water content is important for process control. As the extracellular water content cannot be measured directly, a model is necessary to estimate the extracellular water content during cultivation (Nagel *et al*., 2001b). Control of the extracellular water content using a model that regulated the amount of added water was demonstrated for SSF in a 35-L continuously mixed bioreactor (Nagel *et al*., submitted 2001a). Control aimed at constant extracellular water content was shown to be superior to control aimed at constant overall water content of the fermented solids, which clearly demonstrated the need to distinguish between intracellular and extracellular water.

Table 2. Overview of the most important papers dealing with water activity and the quantification and understanding of the water and dry-matter balance during solid-state fermentation.

Reference	**Description**
Narahara *et al*. 1984	Integration of water balance with energy balance. Automatic control of moisture content in packed bed.
Oriol *et al*. 1988	The limitation of growth by water limitation was confirmed experimentally. Distinction intracellular and extracellular water.
Gervais *et al*. 1988a	Optimal a_w values for growth and spore formation were determined, which justified the regulation of water activity in SSF. Fungal growth was related to water activity of the solid substrate itself.
Gervais *et al*. 1988b	Demonstrated the significance of the effect of water activity on fungal growth while the effect of water content was not significant.
Barstow *et al*., 1988; Ryoo *et al*., 1990	Simultaneous temperature and moisture-content control during SSF.
Grajek, 1988	Demonstrates that water-sorption properties of the substrate changes during fermentation. Dry-matter changes and metabolic-water production were taken into account to estimate the cooling-air requirements.
Gervais, 1990, Gervais and Sarette, 1990	Water activity modifies the metabolic production of aromas.
Larroche *et al*. 1992b; Larroche and Gros 1992a	Water is a limiting factor in fungal development, which correlates with residual water in the substrate and water activity. Estimation of fungal water content.
Sargantanis *et al*., 1993	Dynamic-growth model based on material and energy balances, which included metabolic-water production, dry-weight loss and maintenance metabolism to predict biomass, moisture content, total dry matter and temperature.
Dorta *et al*. 1994	Metabolic-water production was estimated in SSF without forced aeration.
Larroche *et al*. 1998; Smits, 1998	Estimation of dry-matter losses during SSF.
Nagel *et al*. 2001b	Model that uses on-line fermentation data to predict the extracellular moisture content during SSF. Model distinguishes between intra -and extracellular water. Direct measurement of water content fungal biomass. Estimation of metabolic-water production.
Nagel *et al*., submitted 2001a	Simulataneous control of temperature and extracellular water content during SSF in a continuously mixed bioreactor through addition of water.
Nagel *et al*., submitted 2001b	Water and glucose gradients in the solid substrate measured with NMR imaging during SSF.

The desorption isotherm for many natural substrates is such that the matrix potential remains close to one if the water content of the substrate is above 0.5 kg/kg dry matter (DM) (Nagel *et al*., 2001a; Weber *et al*., 1999). This implies that the matrix potential usually remains fairly constant during SSF. It has been demonstrated, however, that the osmotic water potential does limit SSF (Narahara *et al*., 1982; Oriol *et al*., 1988; Nagel *et al*., 2001b). Unfortunately, an estimation of the osmotic water potential would require detailed information on the kinetics of starch hydrolysis and solute uptake, which is usually not available. Furthermore, measurements on particle level reveal that strong gradients may exist inside substrate particles (Box 4; Nagel *et al*., submitted 2001b), which implies that also transport phenomena have to be considered in estimating the osmotic potential experienced by the fungus growing near the particle surface.

In the latest decade, significant advances have been made in the understanding and quantification of the water and dry-matter balances during SSF, which makes the technology appropriate to be applied on a large scale. Although this is not often recognised, many applications are probably limited by water availability, and the application of improved control strategies will improve bioreactor performance and facilitate scale-up of solid-state fermentation.

CONCLUSION

The current situation with regard to scale-up and process control in SSF shows that significant advances have been made with respect to temperature control (Mitchell *et al*., 2000a; Sangsurasak and Mitchell, 1998). Furthermore, better understanding has been achieved concerning the water and dry-matter balances during SSF (Table 2). Although fungal growth is limited by water in many applications, no attempts have been made to control the moisture content in large-scale applications. The implementation of advanced moisture-control strategies is restrained because it has significant implications on the design and operation of the bioreactor. Advanced moisture-content control requires mixing of the solid substrate, which could have a

Box 4: Fungal growth on particle level: Glucose concentration gradients

Gradients inside substrate particles cannot be prevented in solid-state fermentation. These gradients can have a strong effect on the physiology of the microorganisms, but have hitherto received little attention in experimental studies. The figure below shows a gradient in glucose content after 64 hours cultivation of *Aspergillus oryzae* on membrane-covered wheat-dough slices calculated from ^{1}H-NMR images measured *in vivo* (Nagel *et al.*, submitted 2001b). Position 0 indicates the position of the membrane. Glucose concentrations just below the fungal mat remained low due to high glucose uptake rates, but deeper in the matrix glucose accumulated to very high levels, which causes a strong decrease in local water activity.

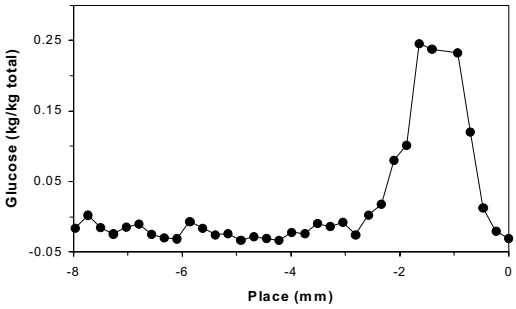

negative influence on fungal growth. It also requires addition of water, which increases the risk of contamination by bacteria. This will lead to higher bioreactor costs due to costly hygienic-design considerations. Therefore, we expect that advanced control strategies will be attractive for the production of high-added-value products like pharmaceuticals for which aseptic cultivation is mandatory. Commercially available solids mixers, which are already applied in the pharmaceutical industry, could be suitable bioreactors for the production of these molecules.

The production of low to medium-added-value products usually involves fungi that grow very fast and that can tolerate low water activities. Commercially available koji bioreactors could facilitate the scale-up for these applications, as temperature control is adequate. In addition, this bioreactor type prevents air channeling that limits the scale-up of many packed-bed bioreactors. However, many design details are not fully understood and research is needed to gain more insight in the currently used scale-up rules.

In summary, we conclude that scale-up of solid-state fermentation would be facilitated by the use of commercially available bioreactor concepts. More attention should be given to hygienic-design considerations when designing a solid-state bioreactor. Such a bioreactor can then be applied to any SSF-system and it allows the use of advanced moisture-control strategies and mixing, which both will improve the bioreactor performance.

REFERENCES

Acuña-Arguelles ME, Guttierrez-Rojas M, Viniegra-Gonzalez G, Favela-Torres E. 1995. Production and properties of three pectinolytic activities produced by *Aspergillus niger* in submerged and solid-state fermentation. Appl Microbiol Biotechnol 43: 808-814.

Aidoo, K.E., Hendry, R., Wood, B.J.B. 1984. Mechanized fermentation systems for the production of experimental soy sauce koji. J Food Technol 19: 389-398.

Anon. A first in enzyme technology. Agro Food Industry Hitech, March/April 1999, p. 45.

Bajracharya R, Mudgett RE. 1979. Solid-substrate fermentation of alfalfa for enhanced protein recovery. Biotechnol Bioeng 21: 551-560.

Bandelier S, Renaud R, Durand A. 1997. Production of gibberellic acid by fed-batch solid state fermentation in an aseptic pilot-scale reactor. Proc Biochem 32: 141-145.

Barstow LM, Dale BE, Tengerdy RP. 1988. Evaporative temperature and moisture control in solid substrate fermentation. Biotechnol Techn 2: 237-242.

Baxter CJ, Magan N, Lane B, Wildman HG. 1998. Influence of water activity and temperature on in vitro growth of surface cultures of a *Phoma* sp. and production of the pharmaceutical metabolites, squalestatins S1 and S2. Appl Microbiol Biotechnol 49: 328-332.

Castilho LR, Polato CMS, Baruque EA, Sant'Anna Jr. GL, Freire DMG. 2000. Economic analysis of lipase production by *Penicilium restrictum* in solid-state and submerged fermentations. Biochem Eng J 4: 239-247.

Chamielec Y, Renaud R, Maratray J, Almanza S, Diez M, Durand A. 1994. Pilot scale bioreactor for aseptic solid-state cultivation. Biotechnol Techn 8: 245-248.

Desgranges C, Vergoignan C, Lereec A, Riba G, Durand A. 1993. Use of Solid State Fermentation to Produce *Beauveria bassiana* for the Biological Control of European Corn Borer. Biotech Adv 11 (3): 577-587.

Dorta B, Bosch A, Arcas J, Ertola R. 1994. Water balance in solid-state fermentation without forced aeration. Enz Microbiol Technol 16: 562-65.

Durand A, Chereau D. 1988. A new pilot reactor for solid-state fermentation: application to the protein enrichment of sugarbeet pulp. Biotechnol Bioeng 31: 476-86.

Ellis SP, Gray KR, Biddlestone AJ. 1994. Mixing evaluation of a Z-blade mixer developed as a novel solid-state bioreactor. Food-Bioprod.Processing 72: 158-62.

Fernandez M, Perezcorrea JR, Solar I, Agosin E. 1996. Automation of a solid substrate cultivation pilot reactor. Bioproc Eng 16: 1-4.

Ferron G, Bonnarame P, Durand A. 1996. Prospects of the microbial production of food flavours. Trends Food Sci. Technol 7: 285-293.

Fukushima D. Industrialization of fermented soy sauce production centering around japanese shoyu. In: Steinkraus KH, editor. Industrialisation of fermented foods. 1989. Marcel Dekker Inc, New York.

Fung CJ, Mitchell DA. 1995. Baffles increase performance of solid-state fermentation in rotating drum bioreactors. Biotechnol Techn 9: 295-298.

Gervais P. 1990. Water activity: a fundamental parameter of aroma production by micro-organisms. Appl Microbiol Biotechnol 33: 72-75.

Gervais P, Molin P, Grajek W, Bensoussan M. 1988a. Influence of water activity of a solid substrate on the growth rate and sporogenesis of filamentous fungi. Biotechnol Bioeng 31: 457-463.

Gervais P, Sarrette M. 1990. Influence of age of mycelium and water activity of the medium on aroma production by *Trichoderma viride* grown on solid substrate. J Ferment Bioeng 69: 46-50.

Gervais P, Bensoussan M, Grajek, W. 1988b. Water activity and water content: comparative effects on the growth of *Penicillium roqueforti* on solid substrate. Appl Microbiol Biotechnol 27: 389-392.

Grajek W. 1988. Cooling aspects of solid-state cultures of mesophilic and thermophilic fungi. J Ferment Technol 66, 6: 675-79.

Han BZ, Kiers JL, Nout MJR. 1999. Solid-substrate fermentation of soybeans with *Rhizopus* spp.: comparison of discontinuous rotation with stationary bed fermentation. J Biosci Bioeng 88 (2): 205-209.

Hardin MT, Mitchell DA, Howes T. 2000. Approach to designing rotating drum bioreactors for solid-state fermentation on the basis of dimensionless design factors. Biotech Bioeng 67: 274-282.

Johns MR, Stuart DM .1991. Production of pigments by Monascus purpureus in solid culture. J Ind Microbiol 1: 23-28.

Kumar PKR, Lonsane BK. 1987. Extraction of gibberellic acid from dry mould bran produced under solid state fermentation. Proc Biochem 22: 139-143.

Larroche C, Gros JB. 1992a. Characterization of the growth and sporulation behavior of *Penicillium roquefortii* in solid-state fermentation by material and bioenergetic balances. Biotechnol Bioeng 39: 815-27.

Larroche C, Moksia J, Gros JB. 1998. A convenient method for initial dry weight determination in samples from solid-state cultivations. Proc Biochem 33: 447-451.

Larroche C, Theodore M, Gros JB. 1992b. Growth and sporulation behavior of *Penicillium roquefortii* in solid substrate fermentation: effect of the hydric parameters of the medium. Appl Microbiol Biotechnol 38: 183-187.

Lide DR. 1993. CRC Handbook of chemistry and physics. 74th edition. CRC Press Inc., Boca Raton.

Liu BL, Tzeng YM. 1999. Water content and water activity for the production of cyclodepsipeptides in solid-state fermentation by *Metarrhizium anisopliae*. Biotechnol Lett 21: 657-661.

Lonsane BK, Ghildyal NP, Budiatman S, Ramakrishna SV. 1985. Engineering aspects of solid-state fermentation. Enz Microbiol Technol 7: 258-265.

Lonsane BK, Saucedo-Castaneda G, Raimbault M, Roussos S, Viniegra-Gonzalez G, Ghildyal NP. 1992. Scale-up strategies for solid-state fermentation. Proc Biochem 27: 259-273.

Maldonado MC, de Saad AM. 1998. Production of pectinesterase and polygalacturonase by *Aspergillus niger* in submerged and solid-state systems. J Ind Microbiol Biotechnol 20: 34-38.

Maruyama JI, Ohnuma H, Yoshikawa A, Kadokura H, Nakajima H, Kitamoto K. 2000. Production and product quality assessment of human hepatitis B virus pre-S2 antigen in submerged and solid-state cultures of *Aspergillus oryzae.* J Ferment Bioeng 90: 118-120.

Merck, 1990. New 2-nonatrienyl-pyran-3-yl glycine ester. US Patent number US-4952604, Merck, USA.

Merck, 1991. New fungicide antibiotic isolated from *Fusarium* sp. fermentation broth. US patent number US-5008187, Merck, USA.

Mitchell DA, Krieger N, Stuart, DM, Pandey, A. 2000a. New developments in solid-state fermentation II. Rational approaches to the design, operation and scale-up of bioreactors. Proc Biochemistry 35: 1211-1225.

Mudgett RE. 1986. Solid-state fermentations. In: Manual of Industrial Microbiology and Biotechnology, ed. AL Demain and HA Solomon. American Society for Microbiology, Washington, D.C., pp. 66-83.

Nagel FJI, Tramper J, Bakker MSN and Rinzema A. 2001a. Temperature control in a continuously mixed bioreactor for solid-state fermentation. Biotechnol Bioeng 72: 219-230.

Nagel FJI, Tramper J, Bakker MSN and Rinzema A. 2001b. Model for on-line estimation of moisture content during solid-state fermentation. Biotechnol Bioeng 72: 231-243.

Nagel FJI, Tramper J, Bakker MSN and Rinzema A. submitted a. Simultaneous control of temperature and moisture content in a mist bioreactor for solid-state fermentation. Accepted in Biotechnol Bioeng.

Nagel FJI, Van As H, Tramper J, Rinzema A. submitted a. Water and glucose gradients in the substrate measured with NMR imaging during solid-state fermentation with *Aspergillus oryzae.* Submitted to Biotechnol Bioeng.

Narahara H, Koyama Y, Yoshida T, Pichangkura S, Ueda R, Taguchi H. 1982. Growth and enzyme production in a solid state culture of *Aspergillus oryzae*. J Ferment Technol 60: 311-319.

Narahara H, Koyama Y, Yoshida T, Atthasampunna P. 1984. Control of water content in a solid-state culture of *Aspergillus oryzae*. J Ferment Technol 62: 453-459.

Ohno A, Ano T, Shoda M. 1995. Effect of temperature on production of lipopeptide antibiotics, iturin A and surfactin by a dual producer, *Bacillus subtilis* RB14, in solid-state fermentation Journal of Fermentation and Bioengineering 80: 517-519.

Oostra J, Tramper J, Rinzema A 2000. Model-based bioreactor selection for large-scale solid-state cultivation of *Coniothyrium minitans* spores on oats. Enz Microbiol Technol 27: 652-663

Oriol E, Raimbault M, Roussos S, Viniegra-Gonzales G. 1988. Water and water activity in the solid-state fermentation of cassava starch by *Aspergillus niger*. Appl Microbiol Biotechnol 27: 498-503.

O'Toole DK. 1997. The role of microorganisms in soy sauce production. In: Neidlemann SL, Laskin AI. editors. Advances in applied microbiology Vol. 45. Academic press, 1997.

Pandey A, Selvakumar P, Soccol CR, Nigam P. 1999. Solid state fermentation for the production of industrial enzymes. Current science 77: 149-162.

Pandey A, Soccol CR, Nigam P, Soccol VT, Vandenberghe LPS, Mohan R. 2000b. Biotechnological potential of agro-industrial residues II: Cassave bagasse. Bioresource Technology 74: 81-87.

Pandey A, Soccol CR, Nigam P, Soccol VT. 2000a. Biotechnological potential of agro-industrial residues I: Sugarcane bagasse. Bioresource Technology 74: 69-80.

Pandey A. 1991. Aspects of fermentor design for solid-state fermentations. Proc Biochem 26: 355-361.

Pandey A. 1992. Recent process developments in solid-state fermentations. Proc Biochem 27: 109-117.

Pandey A, Soccol CR, Mitchell DA. 2000c. New developments in solid state fermentation: I-bioprocesses and products. Proc Biochem 35: 1153-1169.

Robinson T, Singh D, Nigam P. 2001. Solid-state fermentation: a promising microbial technology for secondary metabolite production. Appl Microbiol Biotechnol 55: 284-289.

Roels JA. 1983. Energetics and kinetics in biotechnology. Elsevier Biomedical Press, Amsterdam.

Ryoo D, Murphy VG, Karim MN, Tengerdy RP. 1991. Evaporative temperature and moisture control in a rocking reactor for solid substrate fermentation. Biotechnol Techn 5: 19-24.

Sadhukhan AK, Murthy MVR, Kumar RA, Mohan EVS, Vandana G, Bhar C, Rao KV. 1999. Optimization of mycophenolic acid production in solid-state fermentation using response surface methodology. J Ind Microbiol Biotechnol 22: 33-38.

Sangsurasak P, Mitchell DA. 1998. Validation of a model describing two-dimensional heat transfer during solid-state fermentation in packed bed bioreactors. Biotechnol Bioeng 60: 739-749.

Sargantanis J, Karim MN, Murphy VG, Ryoo D, Tengerdy RP. 1993. Effect of Operating Conditions on Solid-Substrate Fermentation. Biotechnol Bioeng 42: 149-158.

Sekar C, Balaraman K. 1998. Optimization studies on the production of cyclosporin A by solid-state fermentation. Bioproc Eng 18: 293-296.

Shurtleff W, Aoyagi A. 1980. Miso production. The book of miso: volume 2. 2nd edition. The soyfoods center. Lafayette, USA.

Silman RW. 1980. Enzyme formation during solid-substrate fermentation in rotating vessels. Biotechnol Bioeng 22: 411-420.

Smits JP, Rinzema A, Tramper J, van Sonsbeek HM, Hage JC, Kaynak A, Knol W. 1998. The influence of temperature on kinetics in solid-state fermentation. Enz Microbiol Technol 22: 50-57.

Solis-Pereira S, Favela-Torres E, Viniegra-Gonzalez G, Gutierrez-Rojas M 1993. Effects of different carbon sources on the synthesis of pectinase by *Aspergillus niger* in submerged and solid-state fermentations. Appl Microbiol Biotechnol 39: 36-41.

Steinkraus KH, editor. Industrialisation of fermented foods. 1989. Marcel Dekker Inc, New York.

Stuart DM, Mitchell DA, Johns MR, Litster JD. 1999. Solid-state fermentation in rotating drum bioreactors: Operating variables affect performance through their effects on transport phenomena. Biotechnol Bioeng 63: 383-391.

Terui G, Shibasaki I, Mochizuki T. 1958. Industrial culture of koji with through-flow system of aeration (II). Improved method. J Ferment Technol. 36: 109-116.

Tsuchiya K, Nagashima T, Yamamoto Y, Gomi K, Kitamoto K, Kumagai C. 1994. High level secretion of calf chymosin using a glucoamylase-prochymosin fusiongene in *Aspergillus oryzae*. Biosci Biotechnol Biochem 58: 895-99.

Van 't Riet K, Tramper J. 1991. Basic Bioreactor Design. Marcel Dekker. New York.

Venkateswarlu G, Krishna PSM, Pandey A, Rao LV. 2000. Evaluation of *Amycolatopsis mediterranei* VA18 for production of rifamycin-B. Process Biochem 36: 305-309.

Weber FJ, Tramper J, Rinzema A. 1999. A Simplified Material and Energy Balance Approach for Process Development and Scale-Up of *Coniothyrium minitans*. Conidia Production by Solid-State Cultivation in a Packed-Bed Reactor. Biotech Bioeng 65: 447-458.

Weber FJ, Oostra J, Tramper J, Rinzema A. 2002. Validation of a model for process development and scale-up of packed-bed solid-state fermenters. Biotechnol Bioeng, in press.

Wood BJB. editor. 1998. Microbiology of Fermented Foods. 2nd edition Volume 1&2 Blackie Academic & Professional, London.

Xu Y. 1990. Advances in the soy sauce industry in China. Journal of fermentation and bioengineering. 70: 434-439.

Xue M, Liu D, Zhang H, Qi H, Lei Z. 1992. A pilot process of solid-state fermentation from sugarbeet pulp for the production of microbial protein. J Ferment Bioeng 73: 203-205.

Yokotsuka T. 1986. Soy sauce biochemistry. In: Advances in Food Research 30 195-329.

Yokotsuka, T. 1985. Traditional Fermented Soybean Foods. In: Moo-Young M, Blanch HW, Drew S and Wang DIC. Ed. Comprehensive biotechnology, Vol. 3, The practice of biotechnology: current commodity products. Pergamon Press, pp. 395-427.

Summary

Solid-state fermentation (SSF), *i.e.* cultivation of micro-organisms on moist solid substrates in the absence of free-flowing water, is an alternative for submerged fermentation (SmF) for the production of biotechnological products. In recent years, research on SSF has led to a wide range of applications on lab scale, and comparative studies between SmF and SSF claim higher yields and other advantages for products made by SSF. In spite of these examples the commercial application of SSF processes in Western countries remains unusual mainly due to problems associated with scale-up. This thesis aims at solving one the most important scale-up problems, which is the simultaneous control of temperature and moisture content in a large-scale bioreactor.

A general introduction to SSF application and scale-up problems is given in Chapter 1. At first a model system was chosen to study scale-up problems using an agar matrix as solid support in which a defined medium was dissolved. *Rhizopus oligosporus* was chosen as a model organism with known physiology and kinetic parameters. Chapter 2 describes the improvements made to this model system. Control of pH was improved using a citric acid buffer that controlled the pH within acceptable limits. Addition of tryptone to a standard mineral medium increased the maximum specific growth rate and significantly shortened the lag phase.

The chosen model system was, however, not very practical for research on SSF. The effect of dehydration on fungal growth could not be studied on agar beads, due to the high moisture content. *R. oligosporus* had the disadvantage of converting glucose anaerobically, which would hamper predictions for biomass and heat production. Therefore, we decided to switch to a different SSF system in which *Aspergillus oryzae* was cultivated on moist wheat grains.

The use of mixed bioreactors for SSF was considered the first step in solving scale-up problems with respect to temperature and moisture-content control. Although mixing of the solid substrate offers many advantages, the question remains if these would outweigh possible disadvantages like effects of shear on growth. In Chapter 3, temperature control was studied in a continuously mixed bioreactor in which *A. oryzae* was cultivated on whole wheat kernels. Continuous mixing improved temperature control and prevented inhomogeneities in the bed. Respiration rates found in this system were comparable to those in small, isothermal, unmixed beds, which showed

that continuous mixing did not cause serious damage to the fungus or the wheat kernels. Continuous mixing improved heat transport to the bioreactor wall, which reduced the need for evaporative cooling and thus may help to prevent the desiccation problems that hamper large-scale SSF. However, scale-up calculations for the mixed bioreactor indicated that wall cooling will become insufficient at a scale of 2 m^3 for a rapidly growing fungus like *A. oryzae*. Consequently, evaporative cooling will remain important in large-scale mixed systems. Experiments showed that water addition is necessary when evaporative cooling is applied, to maintain a sufficiently high water activity of the solid substrate. For large-scale bioreactor design this implies: (1) the necessity for simultaneous control of temperature and moisture content and (2) the need for agitation devices in SSF systems.

Evaporative cooling is very important for large-scale bioreactors. However, it seriously dehydrates the solid substrate and will limit fungal growth. Water has to be added during fermentation to control the moisture content. The question is: "How much water should be added during fermentation for optimal growth?" Chapter 4 describes a model, which estimates the extracellular (nonfungal) and overall water contents of wheat grains during solid-state fermentation (SSF). Model parameters were determined using an experimental membrane-based model system, which mimicked the growth of *A. oryzae* on the wheat grains and permitted direct measurement of the fungal biomass dry weight and wet weight. The model can be used to calculate the water addition that is required to control the extracellular water content in a mixed solid-state bioreactor.

Chapter 5 integrates the work done on temperature control (Chapter 3) and the model to control the moisture content (Chapter 4) into a control strategy for simultaneous control of the temperature and moisture content during SSF in a continuously mixed paddle bioreactor. Evaporative cooling with varying air flow rate was applied to control the temperature of the solid substrate. The extracellular water content was controlled by adding a fine mist of water droplets onto the mixed solid substrate, using the model from Chapter 4 to calculate the required addition based on on-line measurements. Temperature and extracellular water content were successfully controlled, which resulted in an improved biomass production compared to similar fermentations with temperature control only. No negative effects of water addition were observed with regard to biomass production. Control aimed at constant

extracellular water content was shown to be superior to control aimed at constant overall water content of the fermented solids.

Chapter 6 describes the use of ^{1}H-NMR imaging as a powerful technique to study solid-state fermentation at particle level. Gradients inside substrate particles cannot be prevented in solid-state fermentation. We report gradients in moisture and glucose content during cultivation of *A. oryzae* on membrane-covered wheat-dough slices, which were calculated from ^{1}H-NMR images measured *in vivo*. We found that moisture gradients in the solid substrate remain small when evaporation is minimized. This is corroborated by predictions of a diffusion model. In contrast, strong glucose gradients developed. Glucose concentrations just below the fungal mat remained low due to high glucose uptake rates, but deeper in the matrix glucose accumulated to very high levels. Integration of the glucose profile gave an average concentration close to the measured average content. Based on published data, we expect that the glucose levels in the matrix cause a strong decrease in water activity. The results demonstrate that NMR can play an important role in quantitative analysis of water and glucose gradients at the particle level during solid-state fermentation, which is needed to improve our understanding of the response of fungi to this non-conventional fermentation environment.

Finally, the last chapter gives an overview of recent advances in process control in large-scale SSF systems. In addition, two commercially available bioreactors are discussed with respect to process control: the koji bioreactor and alternative bioreactors based on industrial solid mixers, which both can facilitate the scale-up of SSF.

The koji bioreactor is a promising bioreactor concept for the production of low added-value products for the food and feed industries. This bioreactor design provides a solution to prevent air channeling, caused by shrinkage and breakage of the bed, which currently limits the use of packed beds on a large scale.

It has been demonstrated in literature that an increasing number of pharmaceuticals can be produced using SSF. Bioreactors for the production of pharmaceuticals should comply with current FDA and GMP guidelines. Commercially available solids mixers that are already used in the pharmaceutical industry may facilitate the scale-up of pharmaceutical products.

Samenvatting

Vaste-stoffermentatie, d.w.z. het kweken van micro-organismen op vochtig vast substraat in de afwezigheid van vrijstromend water, is een alternatief voor vloeistoffermentatie voor de productie van biotechnologische producten. In de afgelopen jaren heeft onderzoek naar vaste-stoffermentatie geleid tot de ontwikkeling van verschillende toepassingen op labschaal. Vergelijkend onderzoek heeft aangetoond dat met vaste-stoffermentatie betere opbrengsten worden behaald dan met vloeistoffermentatie. Desondanks wordt vaste-stoffermentatie niet vaak commercieel toegepast in Westerse landen, voornamelijk vanwege problemen met schaalvergroting. Het hier beschreven onderzoek is gericht op het oplossen van een van de voornaamste opschalingsproblemen: het simultaan beheersen van temperatuur en vochtgehalte in een grootschalige bioreactor.

Hoofdstuk 1 is een algemene inleiding, waarin per type industrie wordt aangegeven op welke manier vaste-stoffermentatie kan worden toegepast. Verder wordt in algemene zin ingegaan op opschalingsproblemen die zich voordoen bij deze technologie.

Bij de start van dit onderzoek hadden we een modelsysteem gekozen om opschalingsproblemen te bestuderen, bestaande uit een agarmatrix als vast dragermateriaal met daarin opgelost een gedefinieerd medium. *Rhizopus oligosporus* was gekozen als modelorganisme, omdat de fysiologie en kinetische parameters van deze schimmel bekend waren. Hoofdstuk 2 beschrijft de verbeteringen aan het modelsysteem. Door gebruik te maken van een citraatbuffer kon de pH binnen acceptabele grenzen gehouden worden. De toevoeging van trypton aan het medium verhoogde de maximale specifieke groeisnelheid en verkortte de lagfase vergeleken met een standaardmedium.

Het gekozen modelsysteem bleek echter niet erg bruikbaar te zijn voor onderzoek naar vaste-stoffermentatie. Door het hoge vochtgehalte van de agarmatrix was het niet mogelijk het effect van uitdroging te bestuderen. Verder kon *R. oligosporus* anaëroob glucose omzetten, wat het voorspellen van biomassa- en warmteproductie moeilijker maakte. Er werd daarom besloten om een ander modelsysteem te kiezen, te weten *Aspergillus oryzae* gekweekt op vochtige tarwekorrels. *A. oryzae* is net als *R. oligosporus* een schimmel die veel in industriële vaste-stoffermentaties wordt gebruikt.

Mengen van het vaste substraat in een bioreactor is een eerste stap om problemen met beheersing van temperatuur en vochtgehalte op te lossen. Hoewel het mengen van het vaste substraat veel voordelen biedt, is onduidelijk of deze opwegen tegen mogelijke nadelen zoals beschadiging van de schimmel. In hoofdstuk 3 wordt onderzoek beschreven naar temperatuurbeheersing in een continu gemengde bioreactor waarin *A. oryzae* werd gekweekt op tarwe. De temperatuur werd beter beheerst door het continue mengen en inhomogeniteiten in het tarwebed werden op deze manier vermeden. De ademhalingssnelheid van de schimmel in deze bioreactor was vergelijkbaar met die in kleine, isotherme en niet-gemengde bedden, wat duidelijk aantoont dat mengen geen onherstelbare schade toebracht aan de schimmel of de tarwe. Warmtetransport naar de gekoelde reactorwand werd verbeterd door het mengen, waardoor minder verdampingskoeling nodig was. Op deze manier konden uitdrogingsverschijnselen die normaal gesproken het opschalen van vaste-stoffermentatie belemmeren, worden vermeden in een fermentor met 35 liter inhoud. Echter, er werd berekend dat in bioreactoren vanaf 2 m^3 wandkoeling ontoereikend is voor het kweken van een snelgroeiende schimmel zoals *A. oryzae*. Daarom zal verdampingskoeling altijd belangrijk zijn voor voldoende warmteafvoer in grootschalige vaste-stoffermentatie. Om een voldoende hoge wateractiviteit in het vaste substraat te handhaven als verdampingskoeling wordt toegepast, is het toevoegen van water noodzakelijk. Samenvattend betekent dit voor grootschalige vaste-stofermentatie bioreactoren dat (1) het vochtgehalte en de temperatuur simultaan beheerst moeten worden en (2) dat er gemengd moet worden.

Verdampingskoeling is erg belangrijk in grootschalige vaste-stof fermentoren. Het vaste substraat droogt daardoor echter uit, wat uiteindelijk de groei van de schimmel beperkt. Om het vochtgehalte op peil te houden, zal water toegevoegd moeten worden gedurende de fermentatie. De vraag is echter: hoeveel water moet er toegevoegd worden om het vochtgehalte te beheersen? Hoofdstuk 4 beschrijft een model dat een schatting maakt van het extracellulaire (buiten de schimmel) en het totale watergehalte van tarwekorrels tijdens vaste-stoffermentatie. De modelparameters zijn bepaald met een modelsysteem waarin *A. oryzae* op een membraan op tarwedeeg werd gekweekt. Met behulp van het membraan kon het vochtgehalte en het gewicht van de schimmel biomassa direct bepaald worden. Het model kan worden toegepast om de hoeveelheid

water te berekenen die nodig is om het extracellulaire watergehalte te beheersen in een gemengde bioreactor.

Hoofdstuk 5 integreert het werk dat gedaan is aan temperatuurbeheersing (Hoofdstuk 3) en vochtgehaltebeheersing (Hoofdstuk 4), zodat de temperatuur en vochtgehalte simultaan beheerst kunnen worden in een gemengde bioreactor. De temperatuur werd beheerst met verdampingskoeling, waarbij het luchtdebiet werd aangepast aan de warmteproductie. Het extracellulaire vochtgehalte werd beheerst door een mist van fijne waterdruppels over het vaste substraat te sproeien. Het model uit hoofdstuk 4 werd toegepast om de hoeveelheid water te berekenen uit metingen in het systeem. De temperatuur en het extracellulaire watergehalte werden met succes beheerst, wat resulteerde in een verhoogde biomassaproductie vergeleken met een fermentatie waarbij alleen de temperatuur werd beheerst. Er werden geen negatieve effecten van het toevoegen van water op de biomassavorming waargenomen. Het beheersen van het extracellulaire vochtgehalte gaf een betere schimmelgroei dan het beheersen van het totale vochtgehalte van het gefermenteerde substraat.

Hoofdstuk 6 beschrijft het gebruik van ^{1}H-NMR-imaging technieken om vaste-stoffermentatie op deeltjesniveau te bestuderen. Op deeltjesniveau ontstaan gradiënten in het vaste substraatdeeltje als gevolg van de fermentatie, die niet te voorkomen zijn. Gradiënten in glucoseconcentratie en vochtgehalte zijn berekend uit NMR-scans die werden opgenomen tijdens de groei van *A. oryzae* op een membraan-tarwedeeg systeem. Het bleek dat vochtgehaltegradiënten in het vaste substraat vrij gering waren, doordat nauwelijks waterverdamping plaatsvond. Glucoseconcentraties net onder het oppervlak van het membraan bleven laag, maar dieper in het vaste substraat ontwikkelden zich sterke gradiënten, wat plaatselijk leidde tot hoge glucoseconcentraties. De gemiddelde glucoseconcentratie berekend d.m.v. integratie van het glucoseprofiel kwam overeen met de gemeten glucoseconcentratie in het deeg. We verwachten dat de hoge glucoseconcentratie in het deeg een sterke daling van de wateractiviteit veroorzaakt. De resultaten van dit onderzoek geven aan dat NMR-technieken een belangrijke bijdrage kunnen leveren aan het kwantitatief analyseren van glucose- en vochtprofielen op deeltjesniveau tijdens vaste-stoffermentatie. De techniek is belangrijk voor een beter begrip van het gedrag van schimmels in deze niet-conventionele fermentatiemedia.

Het laatste hoofdstuk geeft een overzicht van de ontwikkelingen op het gebied van procesbeheersing in grootschalige fermentaties. Er worden twee commercieel verkrijgbare bioreactoren beschreven: de koji-bioreactor en bioreactoren gebaseerd op industriële mengers. Beide bioreactoren kunnen een belangrijke bijdrage leveren aan het opschalen van vaste-stoffermentatie.
De koji-bioreactor is een veelbelovend bioreactorconcept voor het produceren van producten met een lage toegevoegde waarde in de voedingsmiddelen- en veevoederindustrie. Het bioreactorontwerp voorkomt kanaalvorming in het gepakte bed, veroorzaakt door krimp en scheuren in het gepakte bed, wat momenteel de toepassing van gepakte bedden op grote schaal beperkt.
In de literatuur wordt steeds meer melding gemaakt van medicijnen die geproduceerd kunnen worden met vaste-stoffermentatie. Bioreactoren voor de productie van deze medicijnen moeten voldoen aan de huidige FDA- en GMP-richtlijnen. Commerciële vaste-stofmengers, die momenteel al worden toegepast in de farmaceutische industrie, kunnen worden aangepast zodat ze gebruikt kunnen worden als vaste-stoffermentor, wat de opschaling van deze processen zal vergemakkelijken.

Nawoord

Zes jaar en zes maanden heeft het geduurd vanaf het moment van aanstelling tot het inleveren van de lezersversie bij de promotiecommissie. Dan realiseer je je dat niet zozeer het einddoel maar de weg ernaar toe belangrijk voor je is geweest. Een lange weg voor een relatief bescheiden bijdrage aan de wetenschap, maar boordevol met uiteenlopende ervaringen. Een mooie periode om aan terug te denken waarbij veel mensen betrokken zijn geweest die ik graag wil bedanken.

Allereerst mijn directe begeleider en co-promotor Arjen Rinzema. Ik heb zeer prettig met je samengewerkt en daarbij was er altijd ruimte voor humor. Je wist feilloos aan te geven waar de zwakke plekken in een artikel zaten, en zonder jou zouden de artikelen nooit dit niveau hebben bereikt. Hans, je wist altijd precies op tijd mij een hart onder de riem te steken met een paar zinnetjes op de voorkant van de manuscripten. Ik ben blij dat ik op jouw aanraden het werk bij NMR heb doorgezet, wat nu een mooi artikel geworden is.

Naast dit project waren er nog verschillende andere projecten op het gebied van vaste stoffermentatie waarbij ik met name Frans en Jaap wil bedanken. Frans, ik denk dat jouw ervaring een aantal inzichten heeft gebracht die zeker ook dit onderzoek in een stroomversnelling hebben gebracht. Daarnaast wil ik je bedanken voor het corrigeren van een aantal manuscripten. Jaap, als mede SSF-er visten we, in het begin, soms in dezelfde vijver, maar al snel hadden we een goede samenwerking waar we de vruchten konden plukken van elkaars ervaringen. Ik wil je bedanken voor de prettige samenwerking en het feit dat ik altijd mijn verhaal bij je kwijt kon. Naast het onderzoek staan mij de Loburg bezoekjes nog vers in het geheugen en natuurlijk het wielrennen dwars door de Veluwe heen. Een speciaal woord van dank is weggelegd voor Marjolein Bakker die als analist werkzaam was en de meeste data voor dit proefschrift verzameld heeft. Je was erg zelfstandig en betrouwbaar en ik vond het prettig om met je samen te werken.

Henk, met plezier heb ik met je samengewerkt bij de Vakgroep Moleculaire Fysica. Nadat we het juiste modelsysteem hadden gevonden ging het onderzoek voorspoedig wat resulteerde in unieke resultaten. Bedankt dat je me de principes van NMR images wilde bijbrengen en je bijdrage aan de discussies.

Verder wil ik een aantal studenten bedanken die middels een stage of afstudeervak een belangrijke bijdrage geleverd hebben aan dit onderzoek, te weten: Floris Popma, Bas Tomassen, Paul Veldhuijsen, Conceicao de Almeida, Elizabeth White, Gerrit Westhoff, Johan Blonk, Anneke Abrahamse en Anita Dekker.

De werkplaats en de afdeling electronica hebben een belangrijke rol gespeeld in dit onderzoek. Vaak kon ik mijn opdrachten voortijdig aanleveren, maar vaak waren het toch vele tussendoorklusjes waarbij ik snel geholpen werd, waar ik iedereen zeer dankbaar voor ben en in het bijzonder Evert, Andre, Mees en Reinoud. Tevens gaat mijn dank uit naar de medewerkers van de Mediaservice, bibliotheek, chemicaliënmagazijn en glasblazer voor de vakkundige ondersteuning.

Een prettige werksfeer is van groot belang voor het doen van onderzoek. De sfeer bij proceskunde is altijd zeer plezierig. Ondanks de grote doorloop van studenten en AIO's zorgen de vele activiteiten rondon het werk ervoor dat iedereen zich er snel thuisvoelt. Bij deze bedank ik de gehele sectie proceskunde voor de plezierige tijd die ik bij jullie heb gehad.

Tevens wil ik de begeleidingscommissie bedanken die als kritisch klankbord fungeerde voor dit promotieonderzoek, te weten: Hein Stam (Quest international); Peter van der Wel (Hosokawa micron B.V.); Marco Giuseppin en Jan Ouwehand (Unilever); Pim Knol (TNO Voeding); Gert Groot en Jan Hunik (DSM), en Willem Ravenberg en Rick van der Pas (Kopper B.V.).

Vader en moeder, jullie hebben het promotieonderzoek altijd met veel belangstelling gevolgd en waren dan ook mijn grootste fans. Ik wil jullie bedanken voor de steun die jullie mij gegeven hebben in deze periode. Geertje, bedankt voor het verzorgen van de layout van dit proefschrift. Daarnaast is je steun en aanmoediging erg belangrijk geweest voor mij en ik vond het heel prettig om samen met jou (soms tot diep in de nacht) de laatste loodjes af te leggen.

Frank-Jan Nagel

Curriculum vitae

Franciscus Johannus Ignatius (Frank-Jan) Nagel werd geboren op 20 februari 1971 in Best. In 1989 behaalde hij het VWO-B diploma aan het Mgr. Zwijssencollege te Veghel. In datzelfde jaar startte hij zijn studie Moleculaire Wetenschappen aan de Landbouwuniversiteit Wageningen. Na het behalen van het propadeutisch examen in 1990 veranderde hij van studie en begon hij aan de studie Bioprocestechnologie, eveneens aan de Landbouwuniversiteit Wageningen.

In maart 1995 rondde hij zijn studie Bioprocestechnologie af met een afstudeerscriptie Proceskunde. Tijdens deze studie liep hij stage bij het Instituut voor Biotechnologie aan de Technische Universiteit in Graz.

Vanaf maart 1995 tot maart 1999 was hij als AIO verbonden aan de sectie Proceskunde van de Landbouwuniversiteit Wageningen en verrichte hij het onderzoek wat leidde tot dit proefschrift. Van maart 1999 tot mei 1999 verrichte hij onderwijstaken aan de sectie Proceskunde voor het vak Overdrachtsprocessen.

Vanaf oktober 1999 is hij in dienst van Unilever Research, in de unit Biotechnologie/Fermented Foods te Vlaardingen.

The studies described in this thesis were part of the research program of the Dutch Graduate School on Process Technology (OSPT).

Cover front: *Aspergillus oryzae* grown on a moistened wheat grain
Cover back: 35-L horizontal paddle mixer with wheat grains
(photos by Ton Feijen, Mediaservice Wageningen Universiteit)